Title
A study of miR-15/16 in T cell biology

Permalink
https://escholarship.org/uc/item/8xb9v153

Author
Gagnon, John David

Publication Date
2018

Peer reviewed|Thesis/dissertation

A study of miR-15/16 in T cell biology

by
John Gagnon

DISSERTATION
Submitted in partial satisfaction of the requirements for degree of
DOCTOR OF PHILOSOPHY

in

Biomedical Sciences

in the

GRADUATE DIVISION
of the
UNIVERSITY OF CALIFORNIA, SAN FRANCISCO

Approved:

DocuSigned by:

Alexander Marson
7F25CDCE383C4A8...

Alexander Marson
_____
Chair

DocuSigned by:

Arthur Weiss
DocuSigned by:4F5...

Arthur Weiss
_____

Jason Cyster
DocuSigned by:40D...

Jason Cyster
_____

K. Mark Ansel
BC645044B450408...

K. Mark Ansel
_____

_____
Committee Members

To my wife, Christina, who has been my emotional rock and a constant source of

support, encouragement, motivation, and love.

ACKNOWLEDGMENT

Next, I want to thank my thesis committee, Alex Marson, Art Weiss, and Jason Cyster. They are incredibly talented scientists and provided invaluable advice and feedback throughout my PhD. You have each made a great deal of time for me out of your busy schedules to discuss science, provide mentorship, and offer career advice. Thank you for your acceptance and words of encouragement in my decision to pursue a career in industry. I could not have asked for a better committee.

Over the course of my time in the Ansel lab, my project took some unexpected turns into the realm of $CD8^+$ T cell biology. Having never worked with these cells before, I was initially overwhelmed with the amount of knowledge and background I felt I was missing. It also became rapidly apparent that in order to make the most meaningful progress in this project, I was going to have to work with some initially daunting pathogens. Rather than attempting to go it alone, I sought out collaborators and found a great deal of help within the UCSF community. I must first thank Hesham Shehata and Shomi Sanjabi for a great deal of help with listeria experiments. I would also like to thank Mehrdad Matloubian, Brian Laidlaw, Pam Odorizzi, and Rachel Rutishauser for their help with getting LCMV experiments off the ground and for their helpful insights in the interpretation of our results. I also thank Dimitre Simeonov and Zhongmei Li of the Marson lab for their help in generating the Malat1 knock-in mouse. I still can't believe how effortless you both made something so complicated.

In addition to scientific collaborators, there were countless others at UCSF for whom I am eternally grateful. I want to thank Demian Sainz, Ned Molyneaux, Amanda Andonian, Monique Piazza, Nate Jew, Lisa Magargal, Fleur Reynolds, Annie Chan, Mary Siti, and everyone else in the BMS office and SABRE Center. You have all

provided so much help and support to me over the years and I am so appreciative of everything that you have done.

Moving to San Francisco to start my PhD was exciting for my wife and I but also a little scary. Neither of us had ever lived more than an hour from where we grew up so the idea of leaving behind our friends and family to live somewhere neither of us knew anyone was going to take some getting used to. Fortunately, we made some incredible friends over the last four years in San Francisco. Thank you so much, to my friends from UCSF and otherwise for all of your support. I've had such great times with all of you and am so grateful for your friendship. We've accumulated some great hobbies and traditions throughout my time here and I look forward to sharing in future adventures.

One of the most difficult aspects of moving to San Francisco was the amazing group of friends and family that we left behind. Thank you to all of my friends back East. You know who you are, and you know how much I love you. I'm so thankful to have remained so close even though we live across the country. To my mother-in-law, Pat and father-in-law, Jim, thank you so much for everything you have done for Christina and me. You have been so amazingly supportive of everything we do and I'm so grateful to have you in my life. To all of my aunts and uncles on both sides, I can't explain how grateful I am for the love and support you provided since day 1. Also, my cousins who I grew up with and who helped shape the person that I am today. A special thank you to my Great Great Uncle Tom and my Great Uncle Geno, my Mémé, Carol, my Papa, Ed, my Nana, Barbara, and my late grandfather, Al. You have all been hugely positive influences on my life and I love you dearly.

A study of miR-15/16 in T cell biology

John D. Gagnon

Abstract

Coordinate control of T cell proliferation, survival, and differentiation are essential for host protection from pathogens and cancer. Long-lived memory cells, whose precursors are formed during the initial immunological insult, provide protection from future encounters and their generation is the goal of many vaccination strategies. On the other hand, regulatory T cells play a critical role in the resolution of immune responses through an arsenal of anti-inflammatory molecules.

microRNAs are key nodes in regulatory networks that shape effective T cell responses through the fine-tuning of thousands of genes. Here, using new compound conditional mutant mice to eliminate miR-15/16 family miRNAs in T cells, I demonstrated that miR-15/16 restrict T cell cycle, survival, and memory T cell differentiation. High throughput sequencing of RNA isolated by cross-linking immunoprecipitation of AGO2 combined with gene expression analysis in miR-15/16 deficient T cells indicate that these effects are mediated through the direct inhibition of an extensive network of known and novel target genes within pathways critical to cell cycle, survival, and memory. Stability and miR-15/16 occupancy of the long non-coding RNA, Malat1, suggest that it may act as a sponge for miR-15/16, thus aiding in memory cell differentiation.

Regulatory T cells (Tregs) aid in the resolution of immune responses as well as protection from autoimmune disease. Through the characterization of miR-15/16 deficient $CD4^+$ T cells I uncovered a role for these microRNAs in the thymic

development and peripheral maintenance of Treg cells. Tregs deficient in miR-15/16 displayed reduced expression of markers associated with stability and suppressive capacity.

This body of work highlights the important role that miRNAs play in shaping the global gene expression program that is required for T cell cycle, survival, and the proper formation of memory cells as well as the development of appropriate populations of regulatory T cells. Additionally, I have developed an application, plotGrouper, for the graphing and statistical analysis of raw data; especially those associated with flow cytometry.

Chapter 2 is reprinted largely as appears in:

Gagnon JD., Kageyama R., Shehata HM., Fassett MH., Mar D., Litterman AJ., Odorizzi P., Simeonov D., Laidlaw BJ., Panduro M., Patel S., Jeker LT., Feeney ME., McManus MT., Marson A., Matloubian M., Sanjabi S., Ansel KM. miR-15/16 restrain cell cycle, survival, and memory T cell differentiation. CellReports. doi:http://dx.doi.org/10.2139/ssrn.3280244.

Table of Contents

List of Figures

List of Tables

Chapter 1: microRNA-mediated control of CD8+ T cell responses

Introduction

The vertebrate immune system is a truly remarkable thing. A combination of broad pattern recognition and astonishing molecular specificity among innate and adaptive immune cells, respectively, provides protection from omnipresent and ever-changing pathological insults. From viruses to bacteria to eukaryotes to cancer, the diversity and abundance of potential threats that we are constantly encountering is a testament to our immune systems protective capacity.

Essential to effective immunological protection is the ability to distinguish self from non-self. CD8$^+$ T cells are a subset of the adaptive immune system with an exceptional ability to recognize and kill cells exhibiting foreignness in a highly specific manner. Upon encountering their cognate antigen, naïve CD8$^+$ T cells can adopt a diverse multitude of behaviors depending on the context of their activation. The factors that govern these cellular fates include the presence of co-stimulatory molecules, the abundance of peptide-major histocompatibility complex (pMHC), T cell receptor (TCR) affinity for pMHC, the local cytokine milieu, as well as cell-intrinsic factors.

Among the cell-intrinsic factors that contribute to cellular states are microRNAs (miRNAs). miRNAs are short ~21-24 nucleotide non-coding RNAs that post-transcriptionally regulate their target genes. miRNAs are transcribed via RNA polymerase II as long primary transcripts (pri-miRNA) containing a hairpin structure proximal to the mature miRNA sequence. Once transcribed, pri-miRNAs are cropped by the micro-processor consisting of DiGeorge syndrome chromosomal region 8 (DGCR8) and Drosha into a precursor miRNA (pre-miRNA). Upon cropping, pre-miRNAs are exported from the nucleus via exportin 5 where they become accessible to the RNase

III-type endonuclease Dicer, which cleaves pre-miRNAs at their hairpin, thereby generating a duplex of a mature miRNA and a carrier strand. Finally, argonaute family proteins (AGO1-4) load mature miRNAs and form the RNA-induced silencing complex (RISC), which mediates miRNA effector function via Watson-Crick base pairing to the 3'UTRs of their target genes. In this manner, miRNAs facilitate translational repression as well as deadenylation and degradation of their target RNAs.

Adding to the complexity of miRNA regulation, the expression of miRNAs, their target genes, and the machinery required for miRNA function varies dramatically between cell types and differentiation states. Furthermore, the degree of complementarity between miRNA and target RNA can influence the sensitivity of the target to the miRNA. Therefore, the role of a particular miRNA in one cell type can, in theory, be dramatically different than its role in another. Depending on the expression level of a particular miRNA and a target RNA, the miRNA may exert little to no effect on protein abundance, tune the target protein to appropriate levels, or switch the abundance of the protein from effective levels to ineffective levels for the given protein's function (Bartel and Chen, 2004). In their elegant review, Ebert and Sharp describe the role of miRNAs in conferring robustness to biological processes (Ebert and Sharp, 2012). Herein they speculate that miRNAs act as a buffer for transcriptional expression that can be leaky and occur in bursts, which results in transcriptional stochasticity and noise (Raj et al., 2006; Blake et al., 2006). More recently, through the use of a single-cell reporter assay and mathematical modeling, others have confirmed this broad role of miRNAs in reducing the noise of weakly expressed genes while surprisingly increasing the noise of highly expressed genes (Schmiedel et al., 2015).

Thus far, we have only discussed miRNAs in the isolation of single miRNA-mRNA interactions. Individual miRNA-mRNA interactions can be sufficient to lead to profound phenotypes (Teng et al., 2008; Dorsett et al., 2008; Lu et al., 2015). However, even in these few reported instances where this has been rigorously tested, the observed effects of disrupting interaction with a single target did not account for the full effect of the removal of the miRNA. Exemplifying the broad nature of miRNA targeting, based on highly conserved miRNA seed-matches within 3'UTRs, miRNAs potentially can target over 60 percent of all RefSeq annotated genes (Friedman et al., 2009). Further, in mice, expanding this list to all 3'UTR seed-matches, regardless of conservation, reveals over 98 percent of all RefSeq annotated genes as putative targets based on a minimum of a 7mer seed-match (Figure 1A).

Importantly, a single miRNA can influence the expression of tens to thousands of individual target RNAs and a single RNA can be targeted by numerous miRNAs. The complex interactions of miRNAs regulating many targets within a given pathway are critical for the observed effects of miRNAs on cell behavior since individual miRNA-target interactions often lead to less than twofold changes in expression (Figure 1B). Recently, through the use of AGO2 high-throughput sequencing of RNAs isolated by crosslinking immunoprecipitation (AHC) (Chi et al., 2009) and differential AHC – in which AHC data from cells sufficient or deficient for a particular miRNA are compared (Loeb et al., 2012a) – it has become apparent that seed-match based methods of identifying target genes are likely underestimating the extent of targeting.

In this review, I will focus on the regulatory mechanisms that govern CD8$^+$ T cell fate and function within immune responses, with a strong emphasis on the role of

miRNAs in controlling or modulating these mechanisms. Additionally, I will provide commentary on emergent principles of miRNA regulation.

miRNA regulation of CD8+ T cell function

miRNAs are required for the normal development of both CD4^{+} and CD8^{+} T cells in the thymus (Muljo et al., 2005). Developmentally, CD8^{+} T cells appear to be more sensitive to miRNA deficiency, exhibiting a twofold reduction in the thymus and a fourfold reduction on average in the spleen. The absence of all Dicer-dependent miRNAs appears to be detrimental to T cell development. However, studies investigating individual miRNAs have uncovered diverse roles. Deletion of miR-15/16, for instance, enhances both CD4^{+} and CD8^{+} T cell accumulation in the thymus and secondary lymphoid organs (Gagnon et al., 2018).

In response to activation by their cognate antigen, CD8^{+} T cells adopt gene expression profiles conducive to rapid proliferation and effector function. While many of these changes occur at the transcriptional level owing to the activities of a multitude of transcription factors, as much as 50 percent of these changes are mediated post-transcriptionally (Cheadle et al., 2005). miRNAs also exhibit profound changes in abundance in response to T cell activation owing, at least in part, to the rapid turnover of miRNA processing machinery and Argonaute proteins (Bronevetsky and Ansel, 2013; Bronevetsky et al., 2013). miR-16, miR-142-3p, miR-150, miR-142-5p, miR-15b, and let-7f are the most abundantly expressed miRNAs in naïve CD8 T cells and all of these miRNAs are down-regulated with *in vitro* activation (Wu et al., 2007). Globally, the majority of miRNAs are immediately down-regulated in response to T cell activation

(Bronevetsky et al., 2013). However, some, such as miR-155, are increased in abundance.

Essential to an effective cytotoxic T cell response is the proliferation and accumulation of sufficient quantities of antigen-specific cells capable of killing infected cells and cancer. CD8^{+} T cells lacking miR-155, which is induced upon T cell activation, fail to appropriately expand in response to LCMV infection (Lind et al., 2013). In fact, in the absence of miR-155, there is a tenfold reduction in antigen-specific CD8^{+} T cell accumulation (Gracias et al., 2013) and this appears to be driven by miR-155 effects on both proliferation and survival (Dudda et al., 2013). Members of the miR-17~92 cluster of miRNAs are up-regulated in response to CD8^{+} T cell activation *in vivo* (Wu et al., 2012; Khan et al., 2013). Consistent with previous reports describing lymphoproliferative disease resulting from over-expression of the miR-17~92 cluster (Xiao et al., 2008), the proliferative capacity of antigen-specific CD8^{+} T cells is diminished in the absence of miR-17~92 (Khan et al., 2013). miR-17~92 has been demonstrated to directly target the tumor suppressor phosphatase and tensin homolog (PTEN) and the pro-apoptotic protein Bim, providing at least two targets with shared functionality by which miR-17~92 may act. miR-15/16 has been shown to directly target a network of cell cycle and survival associated genes including cyclin E1 (Ccne1) and B-cell lymphoma 2 (Bcl2) (Cimmino et al., 2005; Ofir et al., 2011; Gagnon et al., 2018). Consistent with these observations, deletion of miR-15/16 results in increased proliferative capacity and survival among antigen-specific CD8^{+} T cells (Yang et al., 2017; Gagnon et al., 2018).

Highlighting the importance of miRNAs in CD8^{+} T cell effector function, Dicer deficient CD8^{+} T cells exhibit increased production of perforin, granzyme B, and

interferon gamma (IFNy) (Trifari et al., 2013). Through the use of retroviral over-expression of pri-miRs, Trifari et. al. demonstrated that miR-139-3p can lead to a down-regulation in perforin and eomesodermin (Eomes) protein levels while miR-150 regulated CD25. Similarly, miR-29 is down-regulated in response to T cell activation by nuclear factor kappa-light-chain-enhancer of activated B cells (NF-kB) and is capable of directly regulating the expression of IFNy (Ma et al., 2011). On the other hand, miR-155 deficiency among CD8$^+$ T cells results in reduced cytotoxicity (Lind et al., 2013) and reduced effector cytokine production (Gracias et al., 2013) while overexpression results in increased degranulation (Hope et al., 2017). In addition to its role in effector function, miR-155 enhances the responsiveness of CD8$^+$ T cells to the homeostatic cytokines, IL-7 and IL-15 (Ji et al., 2015) as well as IL-2 (Dudda et al., 2013). Suppressor of cytokine signaling 1 (*Socs1*) knockdown rescues the decreased IL-2 responsiveness of miR-155 deficient T cells. Additionally, *Socs1* knockdown in CD8$^+$ T cells phenocopies the tumor protective effect of miR-155 over-expression. However, while miR-155 plays a critical role in the responsiveness of CD8$^+$ T cells in both acute and chronic infection models, *Socs1* repression by miR-155 is only sufficient to mediate a measurable change in response on its own in chronic models (Lu et al., 2015). In addition to *Socs1*, miR-155 have been reported to directly target *Ship1* and *Ptpn2*, two other negative regulators of *Akt* and signal transducer and activator of transcription 5 (*Stat5*) signaling, suggesting that the pleiotropic effects of this miRNA are likely mediated through the targeting of networks of genes rather than solely through their effects on an individual target.

Programming CD8+ T cell memory

In response to infection or cancer, antigen-specific CD8+ T cells may take on the properties of terminally differentiated effector (TE) cells, necessary for controlling the infection, or those of memory precursor (MP) cells capable of persisting long after antigen clearance to provide protection from future encounters. TE and MP populations can be distinguished early on post-infection (p.i.) based on their surface expression of killer cell lectin like receptor G1 (KLRG1) (Joshi et al., 2007) or CD127 (Kaech et al., 2003), respectively.

A single naïve CD8$^+$ T cell has the potential to give rise to both TE and MP cells based on independent approaches using transfer of single cells by limiting dilutions (Stemberger et al., 2007) and through barcoding approaches, which allow for the discrimination of cellular origin (Gerlach et al., 2010; 2013). Furthermore, studies employing microscopy-based approaches have demonstrated that asymmetric cell division can give rise to both MP and TE populations, providing a plausible mechanism by which a single cell could give rise to both fates (Chang et al., 2007; Ciocca et al., 2012; Pollizzi et al., 2016). However, on an individual cell basis, there is also a great deal of heterogeneity among T cells with respect to proliferative capacity, cytokine production, and the expression of the phenotypic markers, KLRG1 and CD127, which can be intrinsically biased by the TCR (Plumlee et al., 2013).

While no single master transcription factor has been found to regulate the differentiation of TE and MP cells, many contributing factors have been identified. Positive regulators of MP cell differentiation include Eomes (Banerjee et al., 2010), Tcf1 (Zhou et al., 2010), Id3 (Yang et al., 2011), Bcl-6 (Cui et al., 2011), Stat3 (Cui et al.,

2011), Foxo1 (Hess Michelini et al., 2013; Kim et al., 2013), and Bach2 (Roychoudhuri et al., 2016). Those found to bias cells towards TE fate include Tbet (Joshi et al., 2007; Intlekofer et al., 2007), Blimp-1 (Kallies et al., 2009; Rutishauser et al., 2009), Id2 (Yang et al., 2011; Hu and Chen, 2013; Masson et al., 2013), and Stat4 (Mollo et al., 2014). Given that most of these lineage-biasing transcription factors only differ by around twofold in their expression between TE and MP populations, it is likely that the fate of an activated CD8$^+$ T cell is driven by complex networks of genes and a great deal of importance must be attributed to genetic regulatory regions (Chang et al., 2014).

Among memory CD8$^+$ T cells, there is a great deal of heterogeneity. Central memory (Tcm) cells, marked by high expression of CD127, CD62L, CD27, CXCR3, and CCR7, are more proliferative in response to re-challenge and exhibit polyfunctionality with respect to effector molecule secretion. Tcm cells produce high levels interleukin (IL)-2, IFNy, and TNF but tend to secrete lower levels of granzyme B. Due to their expression of CD62L, CXCR3, and CCR7, Tcm cells circulate through secondary lymphoid organs (SLOs) and have an enhanced probability of encountering antigen presenting cells (APCs) displaying their cognate antigen. CD27 is member of the tumor necrosis factor receptor superfamily and acts as a co-stimulatory molecule on Tcm cells but is absent among TE populations (Hintzen et al., 1993). Additionally, these Tcm cells provide superior anti-tumor immunity (Klebanoff et al., 2005; Enamorado et al., 2017) and protection against re-infection with virus (Wherry et al., 2003; Hikono et al., 2007).

On the other hand, effector memory (Tem) populations express high levels of CD127 but their expression of CD62L, CXCR3, CD27, and CCR7 is low to none. Within the spleen, they are biased towards red pulp localization and often express chemotactic

9

and adhesion molecules that allow for entry into peripheral, non-lymphoid tissues while excluding them from SLOs. Functionally, Tem cells have enhanced killing capacity due to high expression of the inflammatory cytokines IFNy and TNF, as well as the cytotoxic molecules, perforin and granzyme.

miRNA regulation of CD8+ T cell memory

Defining the roles of miRNAs in TE and MP regulation is an active area of research. Various miRNAs have been described as promoting TE or MP differentiation, proliferation, and survival. For instance, miR-29 has been shown to reduce KLRG1+ TE cell differentiation while boosting MP cells, at least in part through the direct targeting of the master transcription factors, *Tbx21* and *Eomes* (Steiner et al., 2011). Interestingly, while there is a 7mer-m8 miR-15/16 seed-match within *Tbx21* adjacent to that of miR-29, miR-15/16 restrict, rather than enhance, MP differentiation through the targeting of a sizable network of memory cell associated genes (Gagnon et al., 2018).

While CD127 expression is required for the long-term survival of memory cells, over-expression of CD127 is insufficient to force memory cell differentiation (Williams and Bevan, 2007; Hand et al., 2007). However, IL-7 availability can limit memory cell formation (Nanjappa et al., 2008). In TE cells, CD127 is maintained at low levels via GFI-1 mediated silencing and can be reactivated in MP cells via GABP-alpha-mediated acetylation of the CD127 promoter (Florent Carrette, 2012).

Consistent with the role of IL-7 in memory cell survival, miR-15/16, which directly target and down-regulate CD127 expression, restrict the accumulation of MP cells (Gagnon et al., 2018). Given the role of miRNAs in enforcing the silencing of genes with

low or leaky transcription (e.g. miR-29 regulation of Eomes (Bellare and Ganem, 2009; Steiner et al., 2011)), miR-15/16 may serve to provide robustness to the restriction of CD127 expression among TE cells. However, the effects of miR-15/16 appear to be at least partially mediated through restricting the early differentiation of MP cells suggesting that other targets are likely highly relevant (Gagnon et al., 2018). Given the effects of miR-155 on increasing the sensitivity of CD8^{+} T cells to the common gamma chain cytokines, IL-7, IL-15, and IL-2 (Dudda et al., 2013; Ji et al., 2015), one might predict miR-155 to be a positive regulator of MP accumulation. In fact, miR-155 is down-regulated in response to *in vitro* culture of CD8^{+} T cells with IL-15 and deletion of miR-155 boosts the frequency of CD127^{+} CD62L^{+} IL-2 producing MP cells in response to infection with murid herpesvirus (Tsai et al., 2013).

Conversely, in response to infection with LCMV, the absence of miR-155 disrupts both MP and TE populations and over-expression of miR-155 enhances accumulation of effector memory (Tem) cells (Hope et al., 2017). Similar findings on CD8^{+} T cell accumulation and effector function were observed by other groups, however, attribution of the direct targets involved varies. Direct target, *Ship1*, was implicated for its role in the negative regulation of AKT phosphorylation (Lind et al., 2013) as well as TBET levels (Hope et al., 2017). However, other work has established that miR-155 likely acts through the down-regulation of networks of synergistic target genes since disruption of individual targets *Ikbke*, *Bach1*, *Socs1*, and *Ship1* were insufficient to recapitulate the effects of miR-155 (Gracias et al., 2013).

Recently, the transcription factors ZEB1 and ZEB2 have been reported to play reciprocal roles in the promotion of MP and TE cell differentiation (Guan et al., 2018).

Surprisingly, although the miR-200 family of miRNAs have been shown to negatively regulate both *Zeb1* and *Zeb2* in the context of epithelial differentiation (Brabletz and Brabletz, 2010), through the use of AGO antibodies Guan et al. demonstrate that only *Zeb1* was efficiently targeted by miR-200 family members. Consistent with these findings, miR-200 was essential for normal memory CD8^{+} T cell differentiation. This study highlights the importance not only of empirical capture and identification of targets using AGO antibodies, but also the importance of cellular context to miRNA-target interactions.

In addition to transcriptional regulators, metabolism plays a critical role in the proliferation and differentiation of CD8^{+} T cells. Inhibition of mTOR, for example, is sufficient to enhance memory cell persistence through the switch from glycolysis to fatty acid metabolism (Pearce et al., 2009; Araki et al., 2009) as well as through the regulation of Tbet and Eomes (Rao et al., 2010). Over-expression of the miR-17~92 cluster enhances TE differentiation while miR-17~92 deficient CD8^{+} T cells are biased towards a MP phenotype (Khan et al., 2013). Gain or loss of miR-17~92 expression mediated reciprocal effects on the known miR-17~92 target, *Pten*, and the PI3K-AKT-mTOR signaling axis. While these results are consistent with direct targeting of *Pten* by miR-17~92, they do not rule out other players. In fact, consistent with the regulation of a network of pathway-associated genes, additional negative regulators of mTOR (e.g., *Pdcd1*, *Btla*, and *Fcgr2b)*, have previously been demonstrated to be down-regulated by miR-17~92, although direct targeting was not confirmed (Wu et al., 2012). At least for *Btla*, however, AHC data confirms AGO2 occupancy at a 3'UTR seed-match for miR-17 and warrants further investigation as a direct target (Gagnon et al., 2018). Identification

of targets alone, however, is insufficient to ascribe function as mir-15/16 have been demonstrated to regulate both mTOR and Rictor (Singh et al., 2015a; Yang et al., 2017), yet miR-15/16 restrict rather than enhance memory cell differentiation. Again, miR-15/16 serve to highlight the importance of evaluating the networks of genes a miRNA regulates as opposed to attributing too much importance to an individual target.

Similar to miR-17~92, the over-expression of miR-143 boosts memory cell differentiation while miR-143 inhibition reduces memory based on expression of CD127, CD27, and CD28 in human CD8$^+$ T cells (Zhang et al., 2018). In this study, the authors attribute the effects of miR-143 to Glut-1, which was directly regulated by miR-143 and the effect of whose knockdown was consistent with the phenotypes observed in response to miR-143 over-expression. In addition to Glut-1, Zhang et al. identify the glycolysis enzyme, HK2, as being down-regulated upon miR-143 over-expression consistent with previous reports of direct targeting by miR-143 (Peschiaroli et al., 2013). The identification of these two targets is yet another example of a miRNA regulating multiple genes within a given pathway (i.e., glycolytic metabolism) and further supports the model of coordinated network regulation by miRNAs.

A linear transition of CD8$^+$ T cells from naïve to Tem to Tcm based on sorted transfer models of CD62L^{hi} and CD62L^{lo} populations of antigen-specific CD8$^+$ T cells is also well supported (Wherry et al., 2003). Methylation profiling of naïve, TE and MP CD8$^+$ T cell populations has revealed a role for demethylation of naïve-associated markers early after activation to be critical to memory cell differentiation (Youngblood et al., 2017). Furthermore, KLRG1$^+$ CD127$^+$ Tem cells can lose KLRG1 expression and seed Tcm cell compartments in a *Bach2*-dependent manner (Herndler-Brandstetter et

al., 2018). This suggests that conversion from Tem cells to Tcm cells does occur but does not rule out the possibility that early fate decisions can lead to differentiation to these cell fates.

The roles of miRNAs in these transitions between memory cell states currently remains poorly understood, however, while over-expression of miR-150 decreases CD127^{+} CXCR3^{+} Tcm populations, subsequent reduced expression at later timepoints leads to an increase in Tcm cells (Chen et al., 2017). c-Myb and miR-150 were reciprocally expressed in these cells and over-expression of c-Myb was sufficient to partially rescue some of the memory cell defects associated with miR-150 over-expression. In a back-to-back publication, another group also linked miR-150 with restraining memory CD8^{+} T cell differentiation but attributed the effects to *Foxo1*, which is a direct target of miR-150 and sufficient to drive memory cell differentiation through TCF1 (Ban et al., 2017). Furthermore, miR-150 has previously been implicated in directly targeting a number of other relevant genes including *Trp53*, *Cd25*, and *Slc2a1*. Together, these diverse targets and convergent phenotypes highlight the general mechanism by which miRNAs exert their effects through the regulation of networks of genes.

miRNA regulation of CD8+ T cell exhaustion

Effective memory generation requires the clearance of the pathogen or tumor. In the presence of chronic stimulation due to persistent antigen exposure, CD8^{+} T cells up-regulate expression of exhaustion-associated inhibitory receptors including PD1, CTLA4, LAG3, TIM3, BTLA, CD160, 2B4, and TIGIT, leading to reduced proliferation

capacity, effector function, and survival (Wherry, 2011; Wherry and Kurachi, 2015).

Understanding the drivers and maintainers of exhaustion is especially pressing in the

context of tumor immunology. Over the two past decades, it has become evident that

the reversal of T cell exhaustion can unleash existing tumor-specific cytotoxic T cells to

attack and kill cancerous cells (Leach et al., 1996). Strikingly, the blockade of these

receptors can reverse exhaustion leading to a productive immune response (Blackburn

et al., 2009). However, PD-L1 blockade only temporarily reinvigorates exhausted CD8^{+}

T cells if the causative antigen is not cleared, indicating that targeting these surface

receptors alone may be insufficient for many immunotherapies (Pauken et al., 2016).

While no master regulator of exhaustion has been identified, a growing number

of transcription factors have been implicated in exhaustion including TBET, EOMES,

SPRY2, BLIMP1, VHL, FOXO1, FOXP1, IRF4, BATF, and NFATc1 (Wherry and

Kurachi, 2015; Man et al., 2017). Interestingly, many of these transcription factors are

also critical to functional effector and memory CD8^{+} T cells suggesting a complexity to

the drivers of exhaustion that remains to be fully understood. In fact, while IRF4 and

BATF are essential for CD8^{+} T cell effector function during infection with LCMV

(Grusdat et al., 2014), in conjunction with NFATc1, they can lead to the elevated

expression of the inhibitory receptor, PD1, while simultaneously repressing the memory-

associated transcription factor, TCF1, thereby promoting exhaustion while inhibiting

memory formation (Man et al., 2017).

A number of miRNAs have been identified to play a role in CD8^{+} T cell

exhaustion. In response to chronic infection with LCMV clone 13, miR-31 deficient CD8^{+}

T cells express reduced levels of exhaustion-associated markers, higher expression of

markers of effector, and increased polyfunctionality (Moffett et al., 2017). Furthermore, mice lacking miR-31 expression among T cells were protected from the wasting associated with chronic infection and had reduced viral titers. In addition to transcriptional regulators, type I IFNs can induce the expression of PD1 on primary T cells suggesting a role in promoting exhaustion (Terawaki et al., 2011). Moffett et al. demonstrate that knockdown of miR-31 target, *Ppp6c*, could drive increased sensitivity to type I IFNs, however, it is unclear how relevant this individual target is to the observed phenotypes on exhaustion.

In addition to miR-31, recently, miR-155 has been linked with enhancing the persistence of exhausted CD8^{+} T cells during chronic infection (Stelekati et al., 2018). Using a combination of differential expression, TargetScan prediction, and pathway analysis, Stelekati et al. identify *Fosl2* as a direct target capable of reversing many of the effects of miR-155 over-expression. Unlike memory cells, exhausted CD8^{+} T cells do not require the homeostatic cytokines IL-7 and IL-15 to persist and instead rely on constant exposure to their cognate antigen (Shin et al., 2007). These findings suggest that effects of miR-155 on sensitizing CD8^{+} T cells to common gamma chain cytokines is unlikely to be relevant to the increased persistence of miR-155 over-expressing exhausted T cells. Uncoupling persistence from effector function, miR-155 over-expression leads to increased expression of inhibitory receptors and a cytokine/cytotoxic potential consistent with terminal exhaustion. Given previous reports linking miR-155 with decreasing the sensitivity of CD8^{+} T cells to type I IFN signaling, this is also unlikely to play a role in the observed phenotype on exhaustion. These reports highlight the context specific effects miRNAs can have.

Discussion

miRNAs are important regulators of a diverse array of biological processes. Both miRNAs and seed-matches within their target genes are often highly conserved, emphasizing their importance. The role of miRNAs on individual targets in many contexts appears to be to serve as a buffer for reducing noise among leaky genes while increasing noise among highly expressed genes. These effects of individual miRNA-target interactions can have profound impacts on cellular behavior, however, mounting evidence suggests that in many – perhaps most – contexts miRNAs exert their effects through the targeting and fine tuning of networks of genes within pathways in a context-specific manner.

Gaining a complete picture of miRNA function is a daunting task. However, emerging technologies, such as AHC and differential AHC make it possible to map the footprint of miRNAs globally. Through continuing to leverage transcriptome-wide mapping of miRNA-AGO RNP binding via AHC and differential AHC as well as complementary techniques such as differential expression analysis and seed-match conservation, we will gain a more complete understanding of how miRNAs function. This is likely a more robust means of identifying true targets over dual-luciferase assays of cherry-picked putative targets, which, even under ideal conditions within the cell type of interest, can be misleading.

Figure 1: miRNAs target broad, overlapping networks of target genes to elicit phenotypes

(A) Characterization of RefSeq annotated genes with the potential for targeting by miRNAs based on TargetScan prediction algorithm or 3'UTR seed-match. **(B)** Schematic of how individual miRNAs can regulate networks of genes shared between pathways and individual mRNAs can be regulated by multiple miRNAs.

miRNAs target broad, overlapping networks of target genes to elicit phenotypes

A

None (372)

3'UTR Seed-match
(7691)

Targetscan
Predicted
(12477)

B

microRNA Family

Target Genes

Phenotype

X

Y

Clonal expansion

Survival

Memory cell differentiation

Metabolism

Apoptosis

TCR signaling

Terminal effector cell differentiation

Cytokine sensitivity
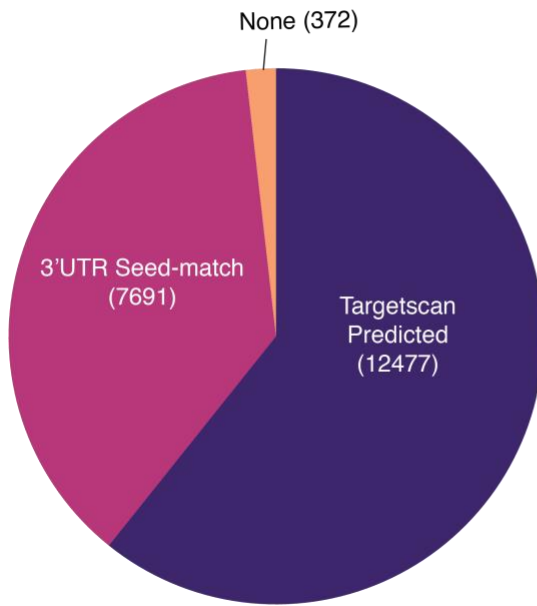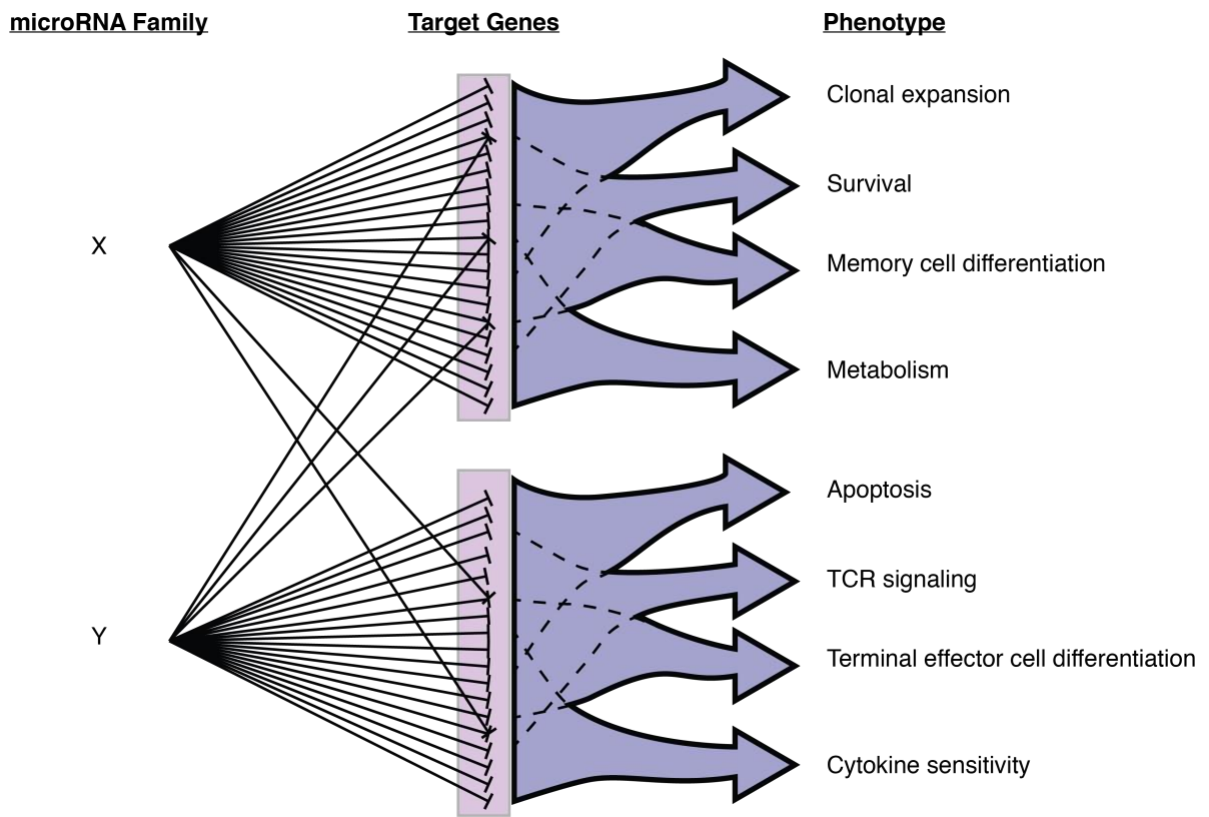
Chapter 2: miR-15/16 restrain cell cycle, survival, and memory T cell differentiation

Introduction

Regulation of T cell proliferation, survival, and differentiation is vital for effective immunity. In response to immunological challenge, naive antigen-specific T cells expand rapidly and undergo massive gene expression changes. As much as 50 percent of these changes are mediated post-transcriptionally (Cheadle et al., 2005). As early as the first division, responding CD8^{+} T cells acquire sustained gene expression programs that lead to their differentiation into appropriately proportionate populations of terminal effector (TE) and memory precursor (MP) cells identified by expression of killer cell lectin-like receptor subfamily G member 1 (KLRG1) and IL-7 receptor alpha (*Il7r*/CD127), respectively (Kaech et al., 2002; 2003; Sarkar et al., 2008; Kakaradov et al., 2017). Effector T cells are important for pathogen or tumor clearance. MP cells form a long-lived pool of memory cells capable of rapidly responding to subsequent encounters with the same antigen.

microRNAs (miRNAs) are short non-coding RNAs that mediate post-transcriptional regulation, predominantly via Watson-Crick base pairing to 3' untranslated regions (UTRs) of target mRNAs (Agarwal et al., 2015). miRNAs play key roles in the differentiation and functional characteristics of memory T cells (Steiner et al., 2011; Khan et al., 2013; Baumjohann and Ansel, 2013; Pua et al., 2016; Moffett et al., 2017; Ban et al., 2017; Chen et al., 2017; Wells et al., 2017; Guan et al., 2018). While the effects of miRNAs on the down-regulation of individual targets are often less than two-fold, through coordinated tuning of gene networks, their overall biological effects can be profound.

The miR-15/16 family of miRNAs function as tumor suppressors. Deletions of the *Dleu2/Mirc30* locus, which encodes miR-15a and miR-16-1, occur in more than 50% of human CLL cases (Calin et al., 2002), and targeted deletion of these miRNAs in mice induces a CLL-like indolent B lymphocyte proliferative disease (Klein et al., 2010). miR-15/16 restrict the proliferation of B cells through the direct targeting of numerous cell cycle and survival-associated genes including *Ccnd1*, *Ccne1*, *Cdk6,* and *Bcl2* (Liu et al., 2008). In addition to *Mirc30*, T cells strongly express *Mirc10* and its two mature miRNA products, miR-15b and miR-16-2. Patients with T cell lymphoblastic lymphoma/leukemia (T-LBL/ALL) exhibiting lower than median expression levels of miR-16 exhibit a worse prognosis suggesting a similar role for miR-15/16 in T cells (Xi et al., 2013). miR-15/16 has also been implicated in T cells anergy, regulatory T cell (Treg) induction, Treg/Th17 balance, and tumor-infiltrating T cell activation (Marcais et al., 2014; Singh et al., 2015b; Wu et al., 2016; Yang et al., 2017). However, the requirements for miR-15/16 in T cell development, proliferation, survival, and differentiation remain unknown.

To this end, we generated mice with conditional inactivation of both *miR-15a/16-1/Mirc30* and *miR-15b/16-2/Mirc10* in T cells (*miR-15/16$^{\Delta/\Delta}$*). miR-15/16 restricted T cell proliferation, limited T cell survival *ex vivo*, and directly targeted numerous cell cycle and survival-associated genes. Deletion of miR-15/16 in T cells did not result in overt lymphoproliferative disease. Instead, *miR-15/16$^{\Delta/\Delta}$* mice selectively accumulated memory T cells, and miR-15/16 restricted the differentiation of MP cells in response to lymphocytic choriomeningitis virus (LCMV). Rather than working through any one critical target, miR-15/16 physically interacted with and repressed the expression of a surprisingly broad network of memory-associated genes.

Materials and Methods

Mice

Mice generated from Mirc10[tm1Mtm] ES cells (Park et al., 2012)} were crossed with *Rosa26-Flp* mice (GT(ROSA)26Sor[tm1(FLP1)Dym]; 009086, Jackson Laboratory) to delete the selection cassette, yielding a loxP-flanked allele. "*miR-15/16^{fl/fl}*" animals were generated by crossing the resulting *miR-15b/16-2^{fl/fl}* animals with *miR-15a/16-1^{fl/fl}* (Mirc30[tm1.1Rdf]) animals (Klein et al., 2010). "*miR-15/16^{Δ/Δ}*" animals were generated by further crossing *miR-15/16^{fl/fl}* animals with *CD4-Cre* mice (Tg(CD4-cre)1Cwi; 4196, Taconic) (Sawada et al., 1994). For hematopoietic chimeras, B6-Ly5.1/Cr (CD45.1+; Charles River) mice were lethally irradiated (2x550 rad), reconstituted with 5x10^6 bone marrow cells, and analyzed 8-10 weeks later. Male and female age and sex matched mice were used between 5 to 12 weeks of age. All mice were housed and bred in specific pathogen-free conditions in the Animal Barrier Facility at the University of California, San Francisco. Animal experiments were approved by the Institutional Animal Care and Use Committee of the University of California, San Francisco.

in vitro cultures

CD4^+ T cells from the spleen and lymph nodes of mice were enriched and cultured as previously described (Pua et al., 2016). Cells were stimulated *in vitro* with biotinylated anti-CD3 (clone 2C11, 1μg/ml) and anti-CD28 (clone 37.51, 0.5μg/ml) on plates coated with NeutrAvidin (5μg/ml, Thermo Fischer Scientific), then rested with 20 units/ml recombinant IL-2 (National Cancer Institute) for an additional 2 days. RNA was extracted and quantified for miRNA qPCR as previously described (Pua et al., 2016).

Flow Cytometry

Cells were harvested from thymus, spleen, and lymph nodes by mashing through 70µM filters. Splenic and blood RBCs were lysed with ACK buffer. Single cell suspensions were prepared in PBS 2% FCS and stained with reagents (Supplementary Table 1) for analysis on an LSRFortessa (Becton Dickenson). For transcription factor stains, cells were fixed and permeabilized using the Foxp3 Transcription Factor Staining Buffer Set (eBioscience). For cytokine stains, cells were fixed for 8 min at room temperature with 4% paraformaldehyde, and permeabilized with 0.5% saponin buffer. Data were analyzed with FlowJo.

LCMV responses

Animals were infected intraperitoneally with $2x10^5$ plaque forming units (p.f.u.) LCMV Armstrong or LCMV clone 13. Mice were bled retroorbitally with heparinized 75mm hematocrit tubes (Drummond) or sacrificed for spleen harvesting. Splenocytes were restimulated *in vitro* with 2µg/ml GP33-41 (KAVYNFATM) or GP276-286 (SGVENPGGYCL) for 5 hours in the presence of brefeldin A. For EdU labeling, 1mg EdU was injected retroorbitally 16 hours before sacrifice and detected using the Click-iT EdU flow cytometry assay kit (Thermo Fisher Scientific). For measurement of viral titers, a quantitative PCR method was used as previously described (McCausland and Crotty, 2008)

AGO2 HITS-CLIP

Libraries were constructed as previously described (Loeb et al., 2012a), with the following modifications. To eliminate nuclei, SDS was excluded from the lysis buffer and physical lysis was not performed with a needle. SDS was included before adding the lysate to anti-AGO2 coated beads. AGO2 immunoprecipitation was performed using a monoclonal antibody (Wako; clone 2D4). To increase resolution and precision, we used a 10% TBE gel (BioRad) for extracting final PCR products. 10% PEG was added to 3' and 5' linker ligation steps to improve ligation efficiency. A randomized dinucleotide was added to the 3' linker to reduce ligation bias. Maximum read depths across mature miRNAs and miRNA targets were generated using the samtools package (Li et al., 2009). Bedfiles used for mapping to transcriptomic regions were acquired from the UCSC table browser using the mm10 reference genome.

RNA sequencing

$1x10^6$ CD4$^+$ T cells cultured as described above were lysed in Trizol (Life Technologies) and RNA isolated using miRNeasy Micro Kit (QIAGEN) with on-column DNase digestion. cDNA was synthesized using the TruSeq PolyA library kit. Single-end 50 base-pair RNA sequencing was performed on the Illumina HiSeq 4000. Alignment was performed using STAR_2.4.2a (Dobin et al., 2013) against the Ensembl Human GRCm38.78 alignment genome. Differential expression was tested using DESeq2 v1.14.0 (Love et al., 2014).

Listeria monocytogenes infection and determination of colony forming units

Mice 24 hours post receiving memory cells and naive control mice (no transfer) were infected with 1-2x105 c.f.u. of LM-GP33. Animals 30+ days post-infection (p.i.) with LCMV Armstrong and naive control mice (no prior infection with LCMV) were infected with 1-2x10^5 colony forming units (c.f.u.) of LM-GP33. Two days later, spleen and liver samples were harvested, and c.f.u. in these organs was calculated as previously described (Shehata et al., 2018). Data were normalized to the mean c.f.u of naive control mice. For transfer experiments, memory CD8+ T cells from animals that were immunized intraperitoneally (i.p.) with LCMV Armstrong (2x105 plaque forming units (p.f.u.)) were purified by magnetic bead sorting. The number of GP33-specific CD8+ T cells was pre-determined using flow cytometric staining and 8x104 GP33 specific memory cells were adoptively transferred independently into naive B6 recipients.

Luciferase Assays

Approximately 250,000 CD4$^+$ T cells were transfected on day 1 of culture with 1µg luciferase reporter constructs and/or 500nM miRIDIAN miRNA mimics (Dharmacon) using the Neon Transfection System (Thermo Fisher Scientific). Luciferase activity was measured 24 h after transfection with the Dual Luciferase Reporter Assay System (Promega) and a FLUOstar Optima plate-reader (BMG Labtech). The full-length *Il7r, Cd28, and Adrb2,* 3'UTRs were cloned into the psiCHECK-2 (Promega). Primers for cloning and site-directed-mutagenesis (SDM) are in Supplementary Table 2.

Quantitative PCR

CD4^{+} T cells were stimulated and rested as described above. Cells were subsequently re-stimulated using anti-CD3 (clone 2C11, 1µg/ml) and anti-CD28 (clone 37.51, 0, 0.02, 0.1 or 0.5µg/ml) for 6 hours at 37°C. Approximately 500,000 cells from each condition were lysed in Trizol (Life Technologies) and RNA isolated using miRNeasy Micro Kit (QIAGEN) with on-column DNase digestion. cDNA was synthesized using SuperScript III (Invitrogen). Quantitative PCR was performed using a RealPlex[2] thermocycler (Eppendorf). Primers used are listed in Supplementary Table 3.

Statistics and Data Analysis

Excel, GraphPad Prism, and R were used for data analysis. Bar graphs were generated using the Bioconductor package, plotGrouper (Gagnon, 2018). For all figures, bar graphs display mean $\pm$ s.d. and each point represents an individual mouse unless otherwise stated. *$P<0.05$, **$P<0.01$, ***$P<0.001$, and ****$P<0.0001$ for significance. All data were assumed to be normally distributed unless otherwise stated.

Data Sharing Statement

The RNA-seq data reported in this paper are archived at the NCBI Gene Expression Omnibus database (accession no. GSE111568).

Results

miR-15/16 are dynamically regulated during T cell responses

Activated T cells rapidly reset their mature miRNA repertoire through increased turnover of the miRNA-induced silencing complex (miRISC) and transcriptional regulation of miRNA precursors (Bronevetsky et al., 2013). To determine the kinetics of miR-15/16 expression in response to activation, we performed qPCR on CD4+ T cells over the course of four days post-in vitro stimulation (Figure 1A). Consistent with this prior report, miR-15a, miR-15b, and miR-16 were substantially down-regulated over a 4-day course of CD4$^+$ T cell activation in vitro (Figure 1A). miR-155 (up-regulated), miR-103/107 (transiently down-regulated), and miR-150 (down-regulated) also behaved as expected.

To assess expression kinetics of these miRNAs in a physiologically relevant context, we re-analyzed published data from CD8$^+$ TE and MP cells sorted from LCMV infected mice (Khan et al., 2013). miR-15/16 were down-regulated in both TE and MP cells (Figure 1B). In MP cells, miR-15b and miR-16 down-regulation was sustained for at least 30 days p.i., placing these miRNAs among the most down-regulated during memory T cell formation. miR-15a expression recovered to naïve T cell levels by 30 days p.i. in MP cells (Figure 1B). However, miR-15a accounts for <10% of the total miR-15/16 family miRNAs in resting CD4$^+$ T cells (Figure 1C). These results suggest that limiting the expression of miR-15/16 may be an important component of the gene expression program initiated by T cell activation and sustained among memory CD8$^+$ T cells.

T cell-specific inactivation of both miR-15/16 gene loci

miR-15/16 clusters occur in two genomic locations. The *miR-15a/16-1* cluster (*Mirc30*) resides intronic to the long non-coding RNA, *Dleu2*, on chromosome 14 in mice (13 in humans), and *miR-15b/16-2* (*Mirc10*) resides intronic to *Smc4* on chromosome 3 within the genomes of mice and humans. Previous studies of these miRNAs have been restricted to genetic ablation of either one of these clusters independently, overexpression, or transient inhibition. However, cells with CD4-Cre-mediated deletion of either one of these clusters independently (*miR-15a/16-1*$^{\Delta/\Delta}$ or *miR-15b/16-2*$^{\Delta/\Delta}$ T cells) retained high levels of miR-16 expression, whereas removal of both clusters (*miR-15/16*$^{\Delta/\Delta}$) effectively abrogated miR-15 and miR-16 expression (Figure 1C). Thus, this study represents the first investigation of the effects of the complete and specific removal of miR-15/16 in any cell type to date.

T cell-specific deletion of both miR-15/16 clusters revealed subtle effects on T cell accumulation in primary and secondary lymphoid tissues without affecting total cellularity (Supplementary Figure 1A-C). These effects were cell-intrinsic, as they were also observed among *miR-15/16*$^{\Delta/\Delta}$ T cells within mixed bone marrow (BM) chimeric mice (Supplementary Figure 1D). Mice with B cell-specific deletion of miR-15a/16-1 develop a delayed clonal lymphocytosis (Klein et al., 2010). To investigate the possibility that T cell-specific deletion of miR-15/16 could result in a delayed onset lymphocytosis, *miR-15/16*$^{\Delta/\Delta}$ animals were examined after aging over 1.5 years. Analysis of these animals revealed no apparent lymphoproliferative disease, lymphoma or leukemia. In fact, rather than an exacerbation of the lymphoaccumulative phenotype, we instead observed a reduction in the magnitude (Supplementary Figure 1E). These

findings demonstrate that miR-15/16 restrict the accumulation of T cells in specific-pathogen-free animals but have no apparent role in the prevention of T cell lymphoproliferative disease in mice.

miR-15/16 bind and regulate a large network of direct target RNAs in T cells

To investigate the global gene expression differences between miR-15/16fl/fl and *miR-15/16$^{\Delta/\Delta}$* T cells, we performed RNA-seq on CD4+ T cells stimulated in vitro for 3 days and rested for 2 days in the presence of IL-2. RNA-seq comparison of *miR-15/16$^{fl/fl}$* and *miR-15/16$^{\Delta/\Delta}$* T cells showed that genes predicted to be targeted by miR-15/16 by TargetScan 7.1 (Agarwal et al., 2015) were more likely to be up-regulated in *miR-15/16$^{\Delta/\Delta}$* T cells compared to all expressed genes lacking a miR-15/16 seed-match in their 3'UTR (Figure 2A). The full set of genes with 3'UTR seed-matches was also enriched for up-regulation in *miR-15/16$^{\Delta/\Delta}$* cells. This set contains 3 times as many putative target genes as the restricted TargetScan subset (3281 vs. 944), but also many more false-positive targets.

miRNAs mediate their effects on gene expression through binding with Argonaute (AGO) proteins within the RISC complex. To further enrich for genes directly targeted in T cells, we performed <u>A</u>GO2 <u>h</u>igh-throughput sequencing of RNAs isolated by <u>c</u>rosslinking immunoprecipitation (AHC) to globally map AGO2-miRNA complex binding to target RNAs (Chi et al., 2009). Consistent with efficient AGO2 pull-down, mature miRNAs accounted for 37% of all AHC reads (Supplementary Figure 2A), and among these, miR-15/16 was the third most abundant family (Figure 2B, top). Non-miRNA AHC relative coverage was highly enriched at TargetScan predicted miRNA

binding sites, and again miR-15/16 seed-matches were the third most abundant (Figure 2B, bottom). Indeed, there was a significant correlation between the density of AHC reads mapping to all miRNAs and their corresponding seed-matches (Supplementary Figure 2B).

Restricting the list of putative miR-15/16 targets to the 1280 genes with 3'UTR seed-matches corresponding with AHC read depth $\geq$ 5 enriched for genes up-regulated in *miR-15/16$^{\Delta/\Delta}$* cells equally as well as TargetScan (Figure 2A). Supporting the validity of this approach and the large number of detected direct miR-15/16 target mRNAs expressed in T cells, differentially expressed genes ($P \leq 0.05$) up-regulated in *miR-15/16$^{\Delta/\Delta}$* cells were frequently occupied by AGO2 at miR-15/16 seed-matches as compared with genes down-regulated in *miR-15/16$^{\Delta/\Delta}$* cells (Figure 2C). Furthermore, up-regulated genes with 3'UTR seed-matches (n = 680) had significantly greater AHC read depth than down-regulated genes with 3'UTR seed-matches (n = 195) (Figure 2D top). Previous work leveraging AHC suggested that miRNAs can bind elsewhere in the transcriptome, but they exert their effects on gene expression largely through targeting 3'UTRs (Loeb et al., 2012b). Bolstering those claims, up-regulated genes in *miR-15/16$^{\Delta/\Delta}$* cells containing 5'UTR or coding sequence (CDS) but not 3'UTR seed-matches had no enrichment for AGO2 binding compared with down-regulated genes (Figure 2D bottom). Together, these data indicate that miR-15/16 directly bind a large network of target genes in T cells.

miR-15/16 directly target cell cycle-associated genes and restrict accumulation of
antigen-specific T cells in response to LCMV infection

Consistent with our findings that miR-15/16 restrict T cell accumulation, gene-set-enrichment analysis (GSEA) identified KEGG Cell Cycle as a major signature of gene expression in *miR-15/16^{Δ/Δ}* cells (Figure 3A). Strikingly, all differentially expressed genes ($P \le 0.05$) within the KEGG Cell Cycle gene set containing miR-15/16 seed-matches were up-regulated in *miR-15/16^{Δ/Δ}* cells (Figure 3B). All but 3 of these genes had considerable AHC reads at miR-15/16 seed-matches suggesting that they were directly targeted by miR-15/16.

Based on these gene expression profiles and given our findings that miR-15/16 were down-regulated in response to T cell activation as well as their effects on baseline T cell accumulation in vivo, we hypothesized that these miRNAs may play a role in restricting T cell proliferation in response to antigenic stimulation. Furthermore, since miR-15/16 expression returned to baseline among TE cells around the time of the contraction phase in response to LCMV clearance (Figure 1B), and given previous reports linking miR-15/16 to known regulators of cell survival including Bcl2 (Klein et al., 2010) we hypothesized that these miRNAs may also play a role in the contraction of TE cells post-viral clearance.

To test whether miR-15/16 restrict the T cell response to antigen stimulation, we infected *miR-15/16^{fl/fl}* and *miR-15/16^{Δ/Δ}* mice with LCMV. Cycling CD8^+ and CD4^+ T cells were measured by EdU incorporation 8 days p.i. Compared to *miR-15/16^{fl/fl}* mice, *miR-15/16^{Δ/Δ}* mice had significantly more proliferating CD8^+ and CD4^+ T cells (Figure 3C,D). Additionally, *miR-15/16^{Δ/Δ}* mice had increased frequencies and absolute numbers of

cells specific for LCMV immunodominant epitopes (GP33 and GP276) both at the peak

of the response and long after viral clearance (Figure 3E,F). Accumulation of antigen-

specific cells in *miR-15/16$^{Δ/Δ}$* mice was cell-intrinsic as it also occurred in mixed bone

marrow chimeric mice (Figure 3G). T cells lacking either miR-15a/16-1 or miR-15b/16-2

alone did not exhibit increased proliferation or accumulation of LCMV-specific T cells

(Supplementary Figure 3A-D).

These experiments demonstrate that both miR-15/16 clusters act to restrict the

accumulation of antigen-specific T cells in response to LCMV infection and suggest that

at least part of this effect can be accounted for by decreased proliferation. Further, the

effects of miR-15/16 on the accumulation of CD4$^+$ and CD8$^+$ T cells are likely mediated

by direct binding and post-transcriptional regulation of a network of cell cycle-associated

genes.

miR-15/16 restrict the formation of CD8$^+$ memory cells

We hypothesized that the increased accumulation of antigen-specific T cells in

LCMV-infected *miR-15/16$^{Δ/Δ}$* mice would be accounted for by increased expansion and

survival of virus-specific effector T cells. Surprisingly, however, the absolute number of

antigen-specific KLRG1$^+$ effector cells was unchanged in *miR-15/16$^{Δ/Δ}$* mice (Figure 4A-

C). Instead, the percentage and absolute number of KLRG1$^-$ and CD127$^+$ memory cells

increased by more than 50%. This effect was apparent as early as 8 days p.i. and

stabilized by 15 days p.i. (Figure 4D). Both miR-15/16 clusters contributed to this effect,

since single conditional knockout animals displayed only modest changes in these

populations (Supplementary Figure 4A,B).

Previous studies investigating memory cell subsets in response to infection have yielded a number of markers that distinguish effector and long-lived memory compartments (Kaech et al., 2002; Wherry et al., 2003; Baars et al., 2005; Hikono et al., 2007; Hu et al., 2011; Olson et al., 2013). *miR-15/16$^{\Delta/\Delta}$* mice generated higher frequencies and absolute numbers of antigen-specific CD8$^+$ T cells with long-lived memory surface phenotypes including high expression of CD127, CXCR3 and CD27, and low or absent KLRG1 (Figure 4A-E). In contrast, effector cells marked as KLRG1$^+$, CD127$^-$, CXCR3$^-$, CD27$^-$ were present at reduced frequency but equivalent absolute numbers (Figure 4F). Mixed bone marrow chimera experiments demonstrated that these effects were cell-intrinsic (Figure 4G).

Consistent with miR-15/16 regulating memory T cell accumulation broadly, the absolute number of CD44^{hi} memory cells was increased among both CD4$^+$ and CD8$^+$ T cells within the spleens and iLNs of unchallenged *miR-15/16$^{\Delta/\Delta}$* mice (Supplementary Figure 4C,D). The frequencies of CD25$^+$ T cells were not increased among CD44^{hi} populations (Supplementary Figure 4E). These findings suggest that miR-15/16 specifically restrict the accumulation of long-lived memory cells in unchallenged animals and in response to infection with LCMV but not at the expense of the effector cell compartment.

miR-15/16 restrict memory CD8$^+$ T cell differentiation

We investigated the possibility that memory CD8$^+$ T cells preferentially accumulate in miR-15/16 deficient mice due to MP-specific effects on cell survival or proliferation. Overnight *ex vivo* culture of splenocytes from mice 8 days p.i. with LCMV

revealed a significant increase in viable and early apoptotic cells with a corresponding

decrease in dead cells among miR-15/16 deficient virus-specific CD8$^+$ T cells within

both MP and TE populations (Figure 5A,B). The cell cycle effects of miR-15/16 were

also apparent in both MP and TE cells, as measured by *in vivo* EdU incorporation 8

days p.i. with LCMV. Either miR-15b/16-2 or miR-15a/16-1 were sufficient to restrict cell

survival and proliferation of both MP and TE populations (Supplementary Figure 5A-C).

These results support a model wherein miR-15/16 preferentially restrict memory CD8$^+$ T

cell accumulation through effects on differentiation. Further supporting this hypothesis,

miR-15/16$^{Δ/Δ}$ CD8$^+$ T cells were less likely to express the TE marker KLRG1 as early as

5 days p.i. with LCMV (Figure 5D).

miR-15/16$^{Δ/Δ}$ memory CD8$^+$ T cells exhibit functional hallmarks of long-lived

memory cells

We further characterized the quality of *miR-15/16$^{Δ/Δ}$* memory CD8$^+$ T cell

responses to antigen re-challenge and secondary infection. First, we pulsed

splenocytes from LCMV-infected mice with GP33 or GP276 ex vivo. Consistent with the

increases in antigen-specific cells detected by tetramer staining, greater frequencies

and absolute numbers of CD8$^+$ T cells from *miR-15/16$^{Δ/Δ}$* mice produced the effector

cytokines TNF and IFNγ 8 days p.i. (Figure 6A,B), with a non-significant trend toward an

increase at day 30$^+$ p.i. (Figure 6C). To assess the effectiveness of miR-15/16 deficient

antigen-specific memory CD8$^+$ T cells *in vivo*, we re-challenged animals 30 days p.i.

with LCMV with *Listeria monocytogenes* expressing GP33 (LM-GP33). Equivalent

control of bacterial burden was observed in *miR-15/16$^{\Delta/\Delta}$* and *miR-15/16$^{fl/fl}$* mice (Figure 6D,E).

CD27- CD8+ long-lived effector T cells have increased killing capacity compared with CD27+ cells (Olson et al., 2013). Given our findings that *miR-15/16$^{\Delta/\Delta}$* mice exhibited decreased frequencies of CD27- cells, we predicted that on a cell to cell basis, *miR-15/16$^{\Delta/\Delta}$* memory CD8+ cells would perform worse in a model of acute re-challenge. Indeed, transfer of equal numbers of GP33-specific cells from LCMV-infected mice 30+ days p.i. resulted in reduced capacity of *miR-15/16$^{\Delta/\Delta}$* cells to control infection with recombinant Listeria monocytogenes expressing the LCMV peptide, GP33 (LM-GP33) (Figure 6F,G). These data suggest that miR-15/16 are dispensable for the establishment of a functionally protective CD8$^+$ memory compartment, though they are required for the generation of a normally proportioned TE:MP pool.

miR-15/16$^{\Delta/\Delta}$ animals are protected from chronic infection

Infection with LCMV containing a single amino acid change in the LCMV glycoprotein (LCMV clone 13) causes chronic infection and severe pathology in mice (Matloubian et al., 1990). Both CD4$^+$ and CD8$^+$ T cells have been demonstrated to play a role in the pathology of LCMV clone 13 infection. We hypothesized that control of proliferation and survival of CD4$^+$ and CD8$^+$ T cells by miR-15/16 may play a role in preventing excessive cellular accumulation to limit pathology during chronic infection.

To test this hypothesis, we infected *miR-15/16$^{fl/fl}$ and miR-15/16$^{\Delta/\Delta}$* animals with LCMV clone 13 and monitored their weight over the course of 24 days p.i. Surprisingly, rather than exacerbating the disease, *miR-15/16$^{\Delta/\Delta}$* animals were significantly protected

from wasting (Figure 7A). Furthermore, we observed a trend towards increased probability of survival for $miR-15/16^{\Delta/\Delta}$ animals (Figure 7B). To determine whether this was a result of early viral clearance, we examined viral titers 24 days p.i. While viral titers trended towards reduced levels in $miR-15/16^{\Delta/\Delta}$ spleens, the magnitude of difference was relatively subtle suggesting that viral load is unlikely to explain protection from wasting in $miR-15/16^{\Delta/\Delta}$ animals (Figure 7C).

miR-15/16 restrict CD8⁺ T cell accumulation and contribute to exhaustion during chronic infection

Chronic infection with LCMV clone 13 leads to sustained antigen exposure and eventually, T cell exhaustion, marked by a progressive loss of effector function and proliferative capacity (Wherry and Kurachi, 2015). Of particular note, memory CD8⁺ T cell differentiation is markedly inhibited by chronic antigen exposure (Wherry, 2011).

Based on the reduced wasting, improved survival, and trending reduced viral titers among $miR-15/16^{\Delta/\Delta}$ animals, we hypothesized that CD8⁺ T cells lacking miR-15/16 may be protected from exhaustion or biased towards a memory phenotype as was observed in acute infection. Analysis of LCMV-specific CD8⁺ T cells 14 days p.i. with LCMV clone 13 revealed trends towards increased cellularity (Figure 8A). By day 24 p.i., $miR-15/16^{\Delta/\Delta}$ animals had as high as 10-fold increased cellularity of antigen-specific CD8⁺ T cells suggesting that they had not become fully exhausted (Figure 8B).

To further investigate the possibility that $miR-15/16^{\Delta/\Delta}$ animals were protected from CD8⁺ T cell exhaustion, we measured expression of markers associated with unexhausted cells. Strikingly, $miR-15/16^{\Delta/\Delta}$ animals trended towards having increased

frequencies and absolute numbers of TCF1$^+$, CD127$^+$, and CD43$^-$ antigen-specific CD8$^+$

T cells as early as 14 days p.i. with significant increases in these populations by 24

days p.i. (Figure 8C-E). Furthermore, *miR-15/16$^{\Delta/\Delta}$* antigen-specific CD8$^+$ T cells had

reduced expression of the exhaustion marker PD-1 14 and 24 days p.i. (Figure 8F,G).

A network of memory-associated genes is regulated by miR-15/16

In order to shed light on the mechanistic targets of miR-15/16 that contribute to

memory CD8$^+$ T cell differentiation, we coupled our RNA-seq and AHC data with

existing data that defined a set of genes up-regulated in memory T cells following LCMV

infection (Kaech et al., 2002). Since long-lived memory CD4$^+$ and CD8$^+$ T cells share

more than 95% similarity in gene expression (Chang et al., 2014), we reasoned that

experiments conducted using CD4$^+$ T cells could provide valuable insights into miR-

15/16 regulation of CD8$^+$ T cells. Twenty-two memory-associated genes contained a

3'UTR seed-match and were differentially expressed in *miR-15/16$^{\Delta/\Delta}$* T cells ($P \le 0.1$).

Of these, 19 were up-regulated in *miR-15/16$^{\Delta/\Delta}$* cells (Figure 9A, left). AHC detected

AGO2 binding at miR-15/16 seed-match sites in most of these genes, further supporting

direct regulation by miR-15/16 (Figure 9A right). Among the genes up-regulated in *miR-*

15/16$^{\Delta/\Delta}$ T cells and containing AGO2 binding at miR-15/16 seed-match sites, *Adrb2*

(Slota et al., 2015), *Pim1* (Knudson et al., 2017), *Il7r* (Nanjappa et al., 2008), *Cd28*, and

Bcl2 (Kurtulus et al., 2011) have been extensively studied in the context of CD8$^+$

memory.

This approach identified numerous novel putative targets of miR-15/16 that may

contribute to memory cell differentiation. *Il7r* was of particular interest, as it has been

previously reported that addition of exogenous recombinant IL-7 can boost memory formation (Nanjappa et al., 2008). Surface CD127 protein abundance was elevated in naive *miR-15/16*$^{\Delta/\Delta}$ CD8$^+$ and CD4$^+$ T cells (Figure 9B). This effect was cell intrinsic as it was also observed in mixed BM chimeric mice (Figure 9C). Similar to the well characterized target of miR-15/16, *Ccnd2*, the *Il7r* 3'UTR contains multiple major AHC peaks corresponding to miR-15/16 seed-matches (Figure 9D). Dual luciferase assays in *miR-15/16*$^{\Delta/\Delta}$ cells transfected with control (CM) or miR-16 mimic validated the capacity of miR-16 to directly target the *Il7r* 3'UTR (Figure 9E). Site-directed mutagenesis of both miR-15/16 seed-match sites completely rescued luciferase expression to CM-treated levels proving that the effects of miR-15/16 on the *Il7r* 3'UTR are dependent upon these seed-matches (Figure 9E). These results provide strong evidence that *Il7r* is a bona fide target of miR-15/16.

AHC peaks also sharply coincided with miR-15/16 3'UTR seed-matches in many of these putative memory-associated targets (Supplementary Figure 6A), especially *Cd28* and *Adrb2* (Figure 9D). Dual luciferase assays confirmed these two additional novel targets, and mutating the miR-15/16 seed-matches within their 3'UTRs completely rescued luciferase expression to CM-treated levels (Figure 9E). While it is unlikely that any one of these targets could account for the effects of miR-15/16 on CD8$^+$ memory cell differentiation, regulation of this network of memory-associated genes provides a plausible mechanism by which miR-15/16 may regulate memory differentiation.

One well characterized driver of CD8$^+$ T cell memory differentiation is signal strength upon antigen encounter. CD4$^+$ and CD8$^+$ T cells are activated by a combination of three major signals: 1) TCR engagement with cognate peptide-MHC, 2) co-

stimulation (e.g., CD28), and 3) the inflammatory environment (e.g., cytokines, chemokines, growth factors). While it is unclear whether the precise mechanism is via frequency of interactions, duration of interactions, strength of interactions, or a combination of the three, it is clear that memory cell differentiation is driven by lower signaling states than effector cells (Kaech and Cui, 2012). To assess responsiveness of miR-15/16 deficient T cells to stimulation, we performed serial dilutions of anti-CD28 in the presence of anti-CD3 and measured expression of immediate early genes by qPCR. Out of the 6 immediate early genes measured, *Tnf*, *Irf4*, *Nr4a1*, and *Il2* displayed significantly lower induction for at least one concentration of anti-CD28 (Supplementary Figure 7A-F). These data demonstrate that miR-15/16 contribute to CD8^{+} T cell exhaustion.

Discussion

The experiments in this study demonstrated roles for miR-15/16 in the restriction of T cell cycle, survival, and CD8^{+} memory cell differentiation through the direct targeting of networks of genes associated with cell cycle, signaling, metabolism, and survival. Both the miR-15a/16-1 and miR-15b/16-2 clusters were sufficient to restrict cell cycle, survival, and CD8^{+} memory cell differentiation during the response to LCMV infection. Moreover, all four mature miRNAs from these clusters are downregulated during the response and both miR-15b and miR-16 remain low long after viral clearance. Given the importance of the quantity and quality of cells generated in response to an immunologic insult such as infection or cancer, our findings mark miR-15/16 as critical tuners of the cell-mediated adaptive immune response.

miRNAs exert their biological effects through multiple target genes (Pua et al., 2016), and our data indicate that miR-15/16 regulate a remarkably extensive target network. We combined biochemical and bioinformatic approaches to map AGO2 binding at thousands of miR-15/16 seed-match sequences in mRNAs and linked this with gene expression analysis in *miR-15/16*$^{\Delta/\Delta}$ T cells to identify a large network of high confidence direct miR-15/16 target genes that restrict cell cycle and CD8$^+$ long-lived memory T cell differentiation. This approach is best suited to highly expressed miRNAs like miR-15/16 since seed-match occupancy correlated robustly with miRNA AGO2 occupancy. Deletion of both the endogenous *Mirc30* (*miR-15a/16-1*) and *Mirc10* (*miR-15b/16-2*) clusters was also critical to unveiling this large set of target genes.

At the peak of infection with LCMV, antigen-specific CD8$^+$ T cells divide as rapidly as once every 2 hours (Yoon et al., 2010) and complete > 14 divisions in 7 days p.i. (Blattman et al., 2002). Even with this remarkably rapid rate of division, removal of miR-15/16 increased the accumulation of virus-specific cells, emphasizing the degree of control exerted by miR-15/16. Previous studies in CLL as well as malignant pleural mesothelioma demonstrated that miR-15/16 are frequently down-regulated or deleted and directly targets several cell cycle genes (Klein et al., 2010; Reid et al., 2013). Our findings expand this cell cycle target network and extend the influence of miR-15/16 to the control of antigen-driven T cell clonal selection.

Prior work in T cells has focused on the miR-15/16 targets Mtor and Rictor, which influence T cell anergy and exhaustion (Marcais et al., 2014; Yang et al., 2017). These target mRNAs were also occupied by AGO2 in T cells at their predicted miR/15-16 bindings sites, and up-regulated in *miR-15/16*$^{\Delta/\Delta}$ T cells. In addition, we detected a

network of memory-associated signaling molecules and receptors that influence T cell differentiation.

miR-150, which is also down-regulated in response to T cell activation (Figure 1A,B), also restricts memory cell development (Ban et al., 2017; Chen et al., 2017). However, unlike miR-150, miR-15/16 expression is maintained at reduced levels during the memory phase (Figure 1B) suggesting that targets of miR-15/16 may be critical to the maintenance of memory cells. In fact, a number of miR-15/16 targets including *Bcl2* (Kurtulus et al., 2011), *Pim1* (Knudson et al., 2017), *Il7r* (Kaech et al., 2003), and *Cd28* (Klein Geltink et al., 2017) have been linked with the maintenance and functional capacity of the memory CD8$^+$ T cell pool. Interestingly, *Il7r*/CD127 may represent not only a target of miR-15/16 but also part of a feed-forward negative regulator of miR-15/16 expression through STAT5, which is activated downstream of CD127 signaling and a direct transcriptional repressor of *miR-15b/16-2* (Li et al., 2010; Lindner et al., 2017). This feed-forward circuit may play important roles in other lymphocyte cell fate decisions. For example, miR-15 family activity was inversely correlated with IL-7 receptor surface expression in pre-B cells (Lindner et al., 2017).

D- and E-type cyclins activate cyclin-dependent kinases (CDKs) to regulate cell cycle in response to T cell activation. miR-15/16 directly target Ccnd1, Ccnd2, Ccnd3, Ccne1, and Cdk6 (Liu et al., 2008) (Figure 4 B). The CDK inhibitor, p27Kip1 (also known as CDKN1b), preferentially restricts CD8+ memory precursor cell proliferation resulting in the accumulation of memory CD8+ T cells in p27Kip1-/-} animals (Singh et al., 2010). Therefore miR-15/16 may act coordinately with p27Kip1 to fine tune CDK activation.

Interestingly, in addition to playing a robust role in restricting memory CD8$^+$ T cell differentiation, preliminary experiments suggest that miR-15/16 may play an even larger role in CD8$^+$ T cell exhaustion. Consistent with these results, a recent study demonstrated that systemic *miR-15a/16-1* deficiency lead to CD8$^+$ T cells that were less susceptible to exhaustion and were protected from death in a model of glioma (Yang et al., 2017). In this study, the authors attributed the effect to direct targeting of mTOR by *miR-15a/16-1*. However, these *in vivo* results are complicated by systemic knockout of *miR-15a/16-1*, which is known to play important roles in other cell types. Our present study demonstrates that T cell restricted deletion of miR-15/16 is sufficient to provide CD8$^+$ T cells from exhaustion in a model of chronic infection. Interestingly, in this model of chronic LCMV infection, *miR-15/16$^{\Delta/\Delta}$* animals were significantly protected from wasting, which is thought to be driven by a combination of CD4$^+$ and CD8$^+$ T cells. Given that the effect of miR-15/16 deficiency on viral titter was subtle, it is unlikely that this could account for the effects on wasting observed. Future work will address the role of miR-15/16 in chronic infection-induced wasting and it will be of great interest what the contribution is between CD4$^+$ vs CD8$^+$ T cells.

We conclude that miR-15/16 represents an important node in the coordinate regulation of cell proliferation, survival, and early differentiation of memory CD8$^+$ T cells. High precursor frequencies of long-lived memory cells reduce the proliferative burden required for response to secondary challenge, thereby preserving mitochondrial integrity and allowing for a more productive secondary response (Sheridan et al., 2014). Therefore, reducing of miR-15/16 expression might be beneficial in the context of vaccination and cancer immunotherapies where the capacity of memory CD8$^+$ to

expand and respond is critical for protection. Furthermore, the effects of miR-15/16 on CD8$^+$ T cell exhaustion add to the attractiveness of miR-15/16 as a therapeutic target. Future studies investigating the regulation of miR-15/16 in response to T cell stimulation as well as the maintenance of its suppression in memory CD8$^+$ T cells could identify up-stream drivers of memory formation and maintenance and provide potential therapeutic targets to modulate T cell memory.

Figure 1: miR-15/16 are dynamically regulated during T cell responses

(A) qPCR of miRNA expression within CD4$^+$ T cells in response to *in vitro* stimulation with anti-CD3 and anti-CD28 for 3 days followed by 1 day resting with IL-2 (n = 6 from 2 independent experiments). **(B)** Time course miRNA microarray of CD8$^+$ TE and MP cells after infection with LCMV (n = 3 from one experiment). **(C)** qPCR of miRNAs purified from naive CD4$^+$ T cells of the indicated genotypes (n = 3 from one experiment).

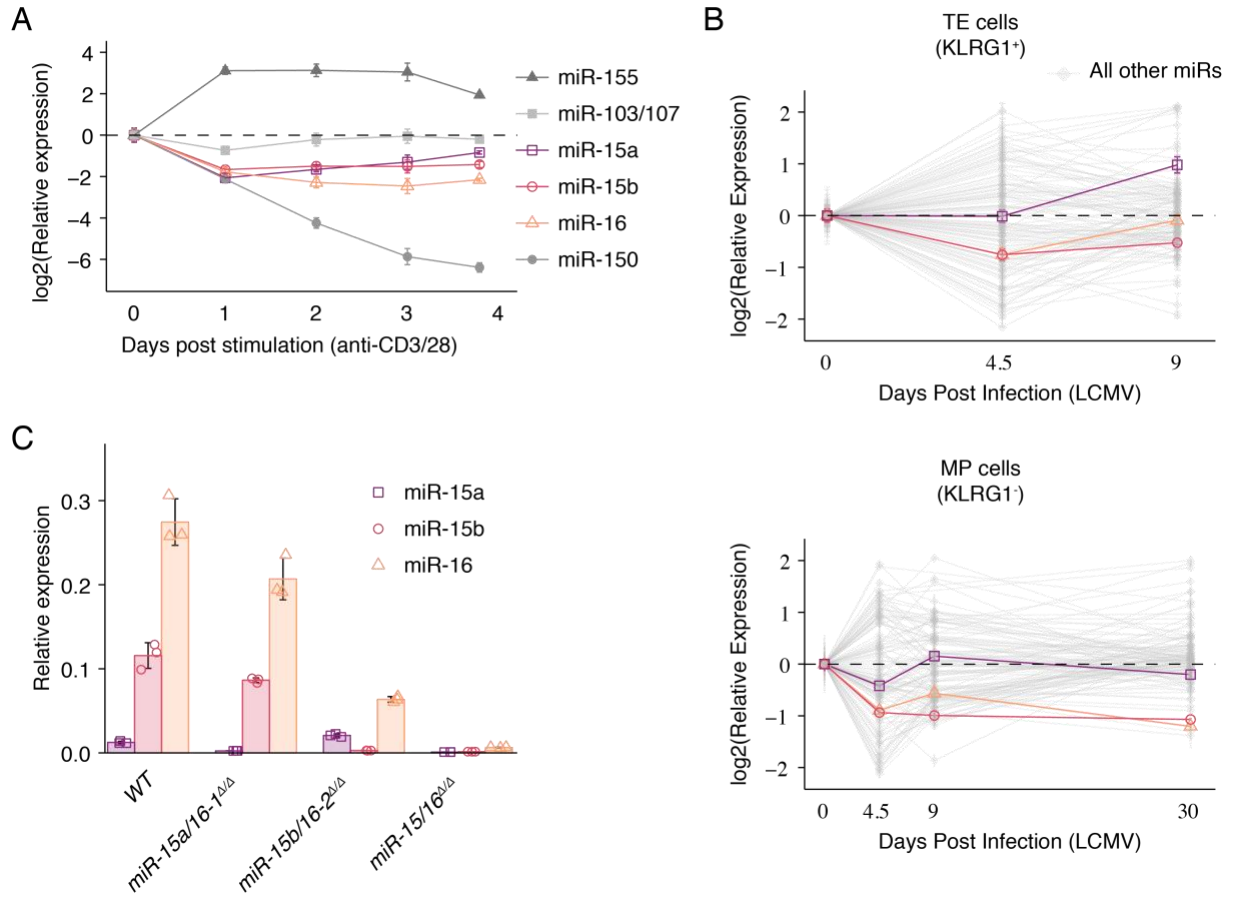# miR-15/16 are dynamically regulated during T cell responses

Figure 2: miR-15/16 bind and regulate a large network of direct target RNAs in T cells

(A) Cumulative density plot depicting global expression by RNA sequencing as a ratio of the fold-change between *miR-15/16*$^{\Delta/\Delta}$ (n = 5) and *miR-15/16fl/fl* (n = 4) resting CD4$^+$ T cells for all genes without a 7mer or 8mer miR-15/16 3'UTR seed-match (black), genes with a 7mer or 8mer miR-15/16 3'UTR seed-match (green), genes with a 7mer or 8mer miR-15/16 3'UTR seed-match and AHC read depth ≥5 (blue), and genes classified as targets of miR-15/16 by TargetScan 7.0 (red) (AHC reads represent the combined depth of n = 10 independent immunoprecipitations). **(B)** Relative abundance of miRNAs bound by AGO2 (top) and AHC coverage across transcriptomic locations relative to region length (bottom). **(C)** Heatmap of genes with a *P* value ≤ 0.05 plotted alongside a bar graph of AHC read depth at miR-15/16 seed matches for each gene they occur at. **(D)** Comparison of AHC reads between genes that are down-regulated and up-regulated (*P* ≤ 0.05) in *miR-15/16*$^{\Delta/\Delta}$ cells among genes with seed-matches in the 3'UTR (top) or 5'UTR/CDS (bottom) (Mann-Whitney U test).

miR-15/16 bind and regulate a large network of direct target RNAs in T cells

A

Cumulative Fraction vs log2(Fold-Change) ($miR-15/16^{\Delta/\Delta}$ vs $miR-15/16^{fl/fl}$)

- All genes (no 3'UTR seed-match)
- 3'UTR seed match
- AHC reads > 5
- Targetscan

D = 0.272 ; P < 2.2e−16
D = 0.379 ; P < 2.2e−16

3281
758
522
1579
422

B

miRNA AGO2 ocupancy

- miR−142−3p
- miR−21−5p
- miR−15−5p/16−5p
- let−7−5p
- miR−30−5p
- miR−17−5p
- miR−150−5p
- miR−29−3p
- miR−27−3p
- miR−26−5p
- Other miRNAs

miR-15/16

Relative coverage: 5' UTR, CDS, introns, 3' UTR, Targetscan seed matches

C

Row Z-score: −2, −1, 0, 1, 2

$\log_{10}$(AHC reads): 0, 1, 2, 3

$miR-15/16^{fl/fl}$ $miR-15/16^{\Delta/\Delta}$

D

Relative gene expression ($miR-15/16^{\Delta/\Delta}$ vs $miR-15/16^{fl/fl}$)

Fraction of genes (3'UTR seed-match)
- Downregulated n = 195
- Upregulated n = 680

P = 8.03e−15

Fraction of genes (5'UTR or CDS seed-match)
- Downregulated n = 308
- Upregulated n = 444
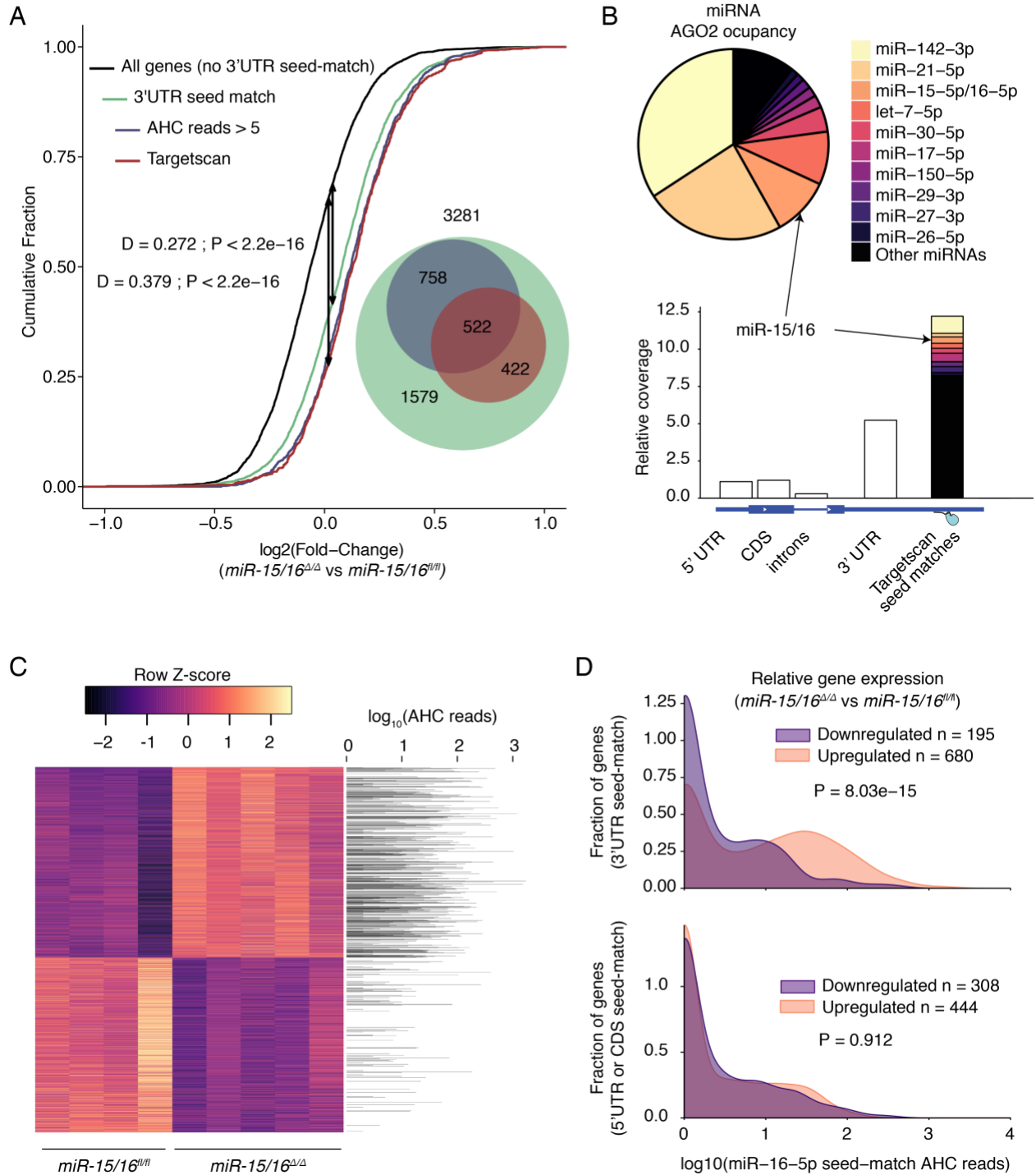
P = 0.912

log10(miR−16−5p seed−match AHC reads)

48

Figure 3: miR-15/16 directly target cell cycle-associated genes and restrict accumulation of antigen-specific T cells in response to LCMV infection

(A) Gene set enrichment analysis of all expressed genes (normalized read depth ≥ 5). Plotted are the enrichment curve for and positional location of each target in the KEGG Cell Cycle gene set arrayed in ranked order from most up-regulated to most down-regulated (left to right) in *miR-15/16$^{\Delta/\Delta}$* (Enrichment score (ES) = 0.4354147; nominal *P* value < 0.001; FDR q value = 0.088). **(B)** Heatmap of KEGG Cell Cycle genes with miR-15/16 seed matches in their 3'UTR plotted alongside a bar graph of AHC read depth at miR-15/16 seed matches for each gene they occur at. **(C)** Flow cytometry of EdU-labeled CD8$^+$ and CD4$^+$ T cells 8 days p.i.. **(D)** Quantification of frequencies (left) and absolute numbers (right) of EdU$^+$ CD8$^+$ and CD4$^+$ T cells 8 days p.i. with LCMV (n = 10 representative of 2 independent experiments, two-tailed t test) **(E)** Flow cytometry of antigen-specific T cells. **(F)** Quantification of frequencies (left) and absolute numbers (right) of antigen-specific CD8$^+$ T cells (n = 10 representative of 2 independent experiments, two-tailed t test)**. (G)** Quantification of frequencies of antigen-specific CD8$^+$ T cells in mixed bone marrow chimeras (n $\geq$8, representative of $\geq$3 independent experiments, two-tailed t test). *, P < 0.05; **, P < 0.01; ***, P < 0.001; ****, P < 0.0001.

miR-15/16 directly target cell cycle-associated genes and restrict accumulation of antigen-specific T cells in response to LCMV infection
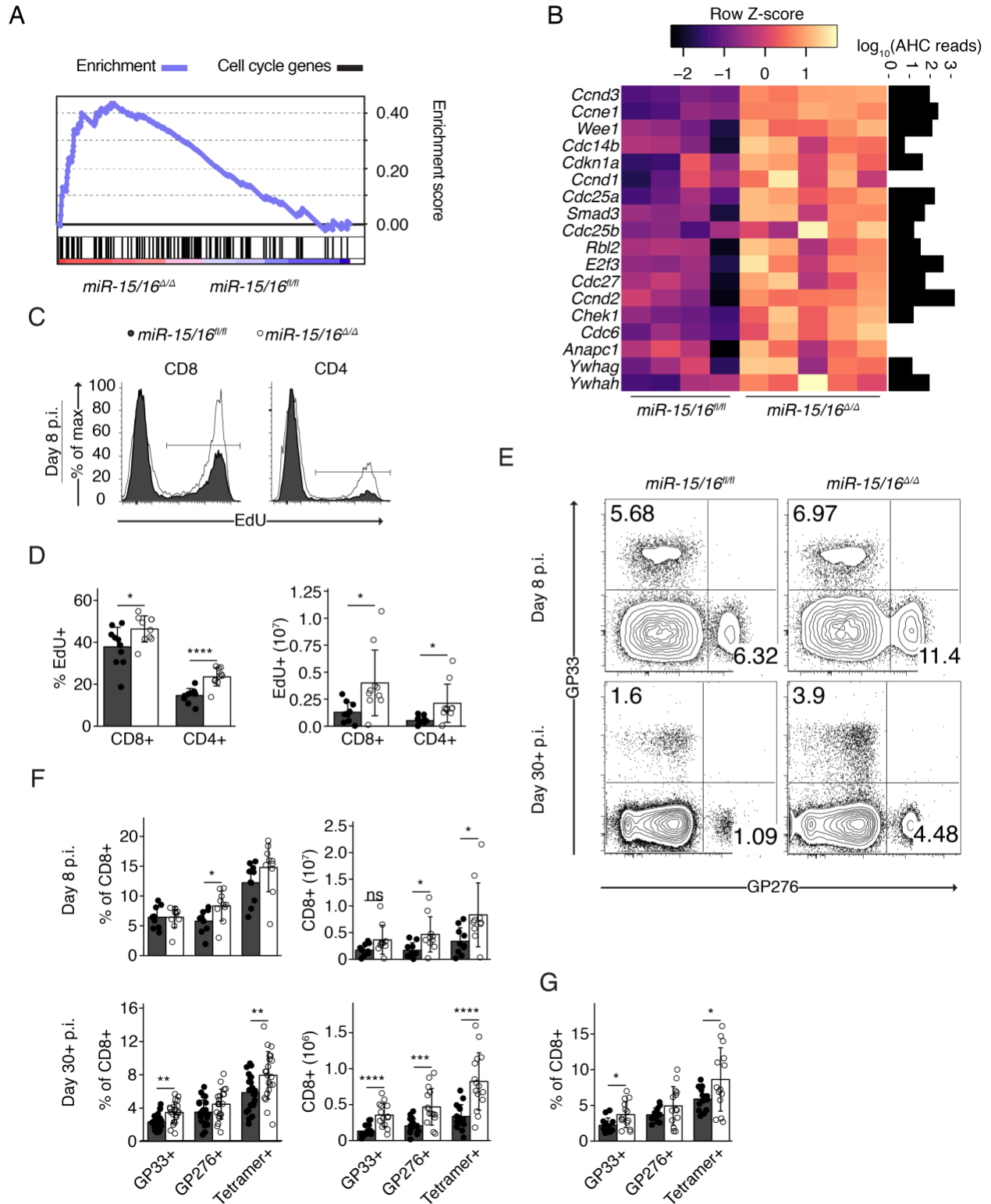
A

Enrichment — Cell cycle genes —

$miR\text{-}15/16^{\Delta/\Delta}$ $miR\text{-}15/16^{fl/fl}$

B

Row Z-score

$\log_{10}$(AHC reads)

Ccnd3, Ccne1, Wee1, Cdc14b, Cdkn1a, Ccnd1, Cdc25a, Smad3, Cdc25b, Rbl2, E2f3, Cdc27, Ccnd2, Chek1, Cdc6, Anapc1, Ywhag, Ywhah

$miR\text{-}15/16^{fl/fl}$ $miR\text{-}15/16^{\Delta/\Delta}$

C

● $miR\text{-}15/16^{fl/fl}$ ○ $miR\text{-}15/16^{\Delta/\Delta}$

Day 8 p.i. / % of max — CD8 / CD4 — EdU

D

E

$miR\text{-}15/16^{fl/fl}$ $miR\text{-}15/16^{\Delta/\Delta}$

Day 8 p.i. — 5.68 / 6.32 ; 6.97 / 11.4

Day 30+ p.i. — 1.6 / 1.09 ; 3.9 / 4.48

GP33 / GP276

F

G

50

Figure 4: miR-15/16 restrict the formation of CD8$^+$ memory cells

(A) Flow cytometry of tetramer$^+$ CD8$^+$ T cells from spleens harvested 8 days p.i. (top) or 30$^+$ days p.i. (bottom) with LCMV. **(B)** Quantification of frequencies of tetramer$^+$ CD8$^+$ T cells from spleens harvested 8 days p.i. (top) or 30$^+$ days p.i. (bottom) with LCMV (n $\geq$ 10 from at least 2 independent experiments, two-tailed t test). **(C)** Quantification of absolute numbers of tetramer$^+$ CD8$^+$ T cells from spleens harvested 8 days p.i. (top) or 30$^+$ days p.i. (bottom) with LCMV (n = 10 from 2 independent experiments, two-tailed t test). **(D)** Quantification of frequencies of tetramer$^+$ CD8$^+$ T cells from peripheral blood over the course of 30$^+$ days p.i. with LCMV (n $\geq$ 9 from at least 2 independent experiments, two-tailed t test). **(E,F)** Quantification of flow cytometry of LCMV-specific CD8$^+$ T cells 30$^+$ days p.i. (n $\geq$ 5 from $\geq$ 2 independent experiments, two-tailed t test). **(G)** Quantification of frequencies of tetramer$^+$ CD8$^+$ T cells from spleens of mixed bone marrow chimeric mice 30$^+$ days p.i. (n $\geq$ 8, representative of $\geq$ 3 independent experiments, two-tailed t test). **, P < 0.01; ***, P < 0.001; ****, P < 0.0001.

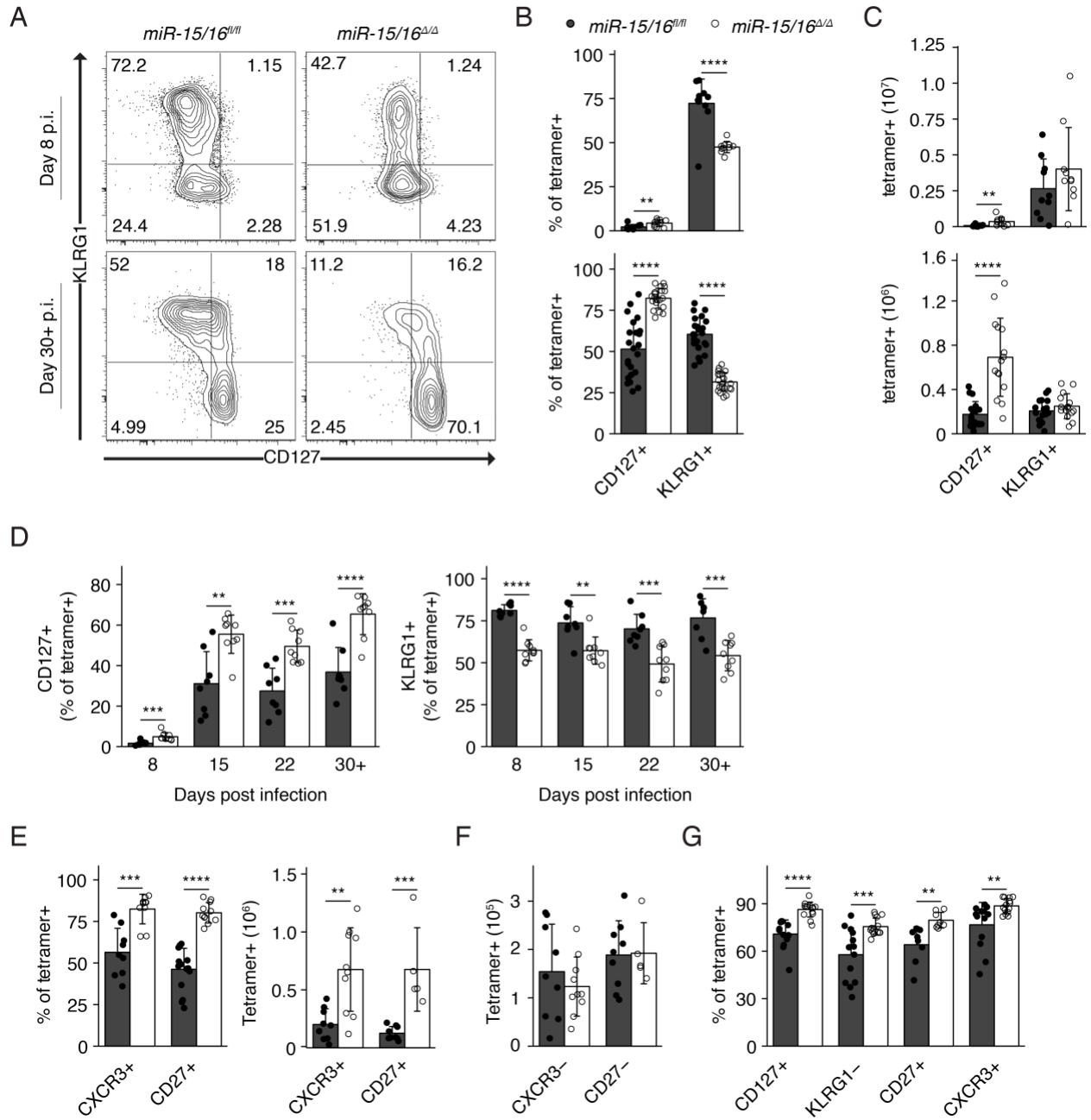# miR-15/16 restrict the formation of CD8+ memory cells

**Figure 5: miR-15/16 restrict memory CD8$^+$ T cell differentiation**

(**A**) Flow cytometry of GP33$^+$ CD8$^+$ T cells from spleens harvested 8 days p.i. with LCMV cultured overnight *in vitro* (n = 7 from 2 independent experiments). (**B**) Quantification of frequencies of Live/Dead$^-$ activated caspase-3$^-$ GP33$^+$ CD8$^+$ T cells from spleens harvested 8 days p.i. with LCMV cultured overnight *in vitro* (n = 7 from 2 independent experiments, two-tailed t test). (**C**) Quantification of frequencies of EdU$^+$ CD44$^+$ CD8$^+$ T cells from spleens harvested 8 days p.i. with LCMV (n = 7 from 2 independent experiments, two-tailed t test). (**D**) Quantification of frequencies of MP and TE populations among tetramer$^+$ CD8$^+$ T cells from spleens harvested 5 days p.i. with LCMV (n = 8 from 2 independent experiments) *, P < 0.05; **, P < 0.01; ***, P < 0.001.

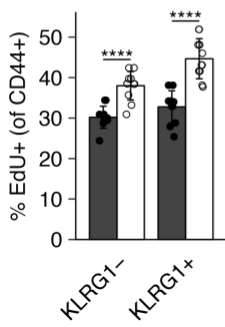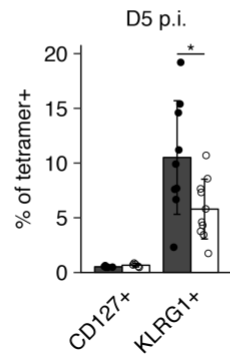# miR-15/16 restrict memory CD8+ T cell differentiation

A
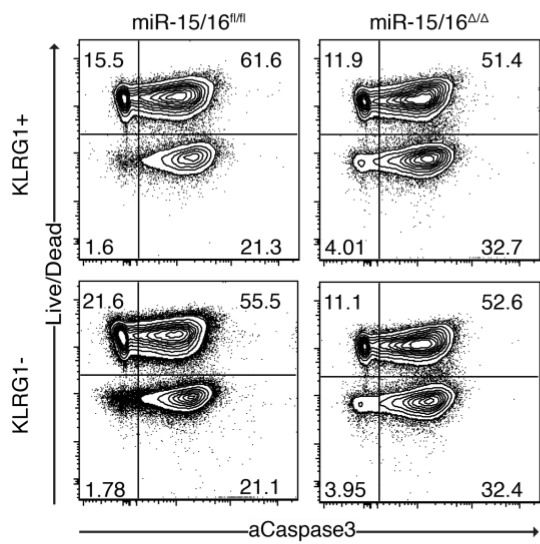
B
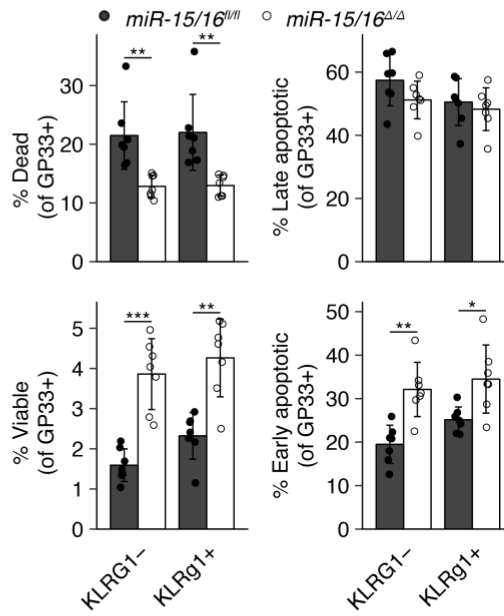
C

D

Figure 6 *miR-15/16^{Δ/Δ}* **memory CD8⁺ T cells exhibit functional hallmarks of long-lived memory cells**

(A) Flow cytometry of CD8⁺ T cells 8 days p.i. with LCMV responding to splenocytes pulsed with either GP33 (top) or GP276 (bottom). **(B)** Quantification of cytokine-producing CD8⁺ T cells re-stimulated *in vitro* with peptide-pulsed splenocytes 8 days p.i. (n = 5 representative of at least 2 independent experiments, two-tailed t test). **(C)** Quantification of cytokine-producing CD8⁺ T cells re-stimulated *in vitro* with peptide-pulsed splenocytes 30⁺ days p.i. (n $\geq$ 10 from $\geq$ 2 independent experiments, two-tailed t test). **(D)** Experimental outline of direct re-challenge model. **(E)** LM-GP33 colony forming units (c.f.u.) from spleen and liver of mice infected with LM-GP33 30+ days p.i. with LCMV and harvested 48 hours later normalized to the naive group of each respective experiment (n $\geq$ 9 of 2 independent experiments, two-tailed t test). *, P < 0.05; **, P < 0.01. **(F)** Experimental outline of adoptive transfer model. **(G)** LM-GP33 colony forming units (c.f.u.) from spleen and liver of mice that received 8x104 GP33-specific memory CD8+ T cells from miR-15/16fl/fl, or**.** *miR-15/16^{Δ/Δ}* or none (Naive) collected 48 hours p.i. with 1.5-2x105 c.f.u. LM-GP33 and normalized to the naive group of each respective experiment (n $\geq$ 10 of 2 independent experiments, two-tailed t test).

miR-15/16^(Δ/Δ) memory CD8+ T cells exhibit functional hallmarks of long-lived memory cells
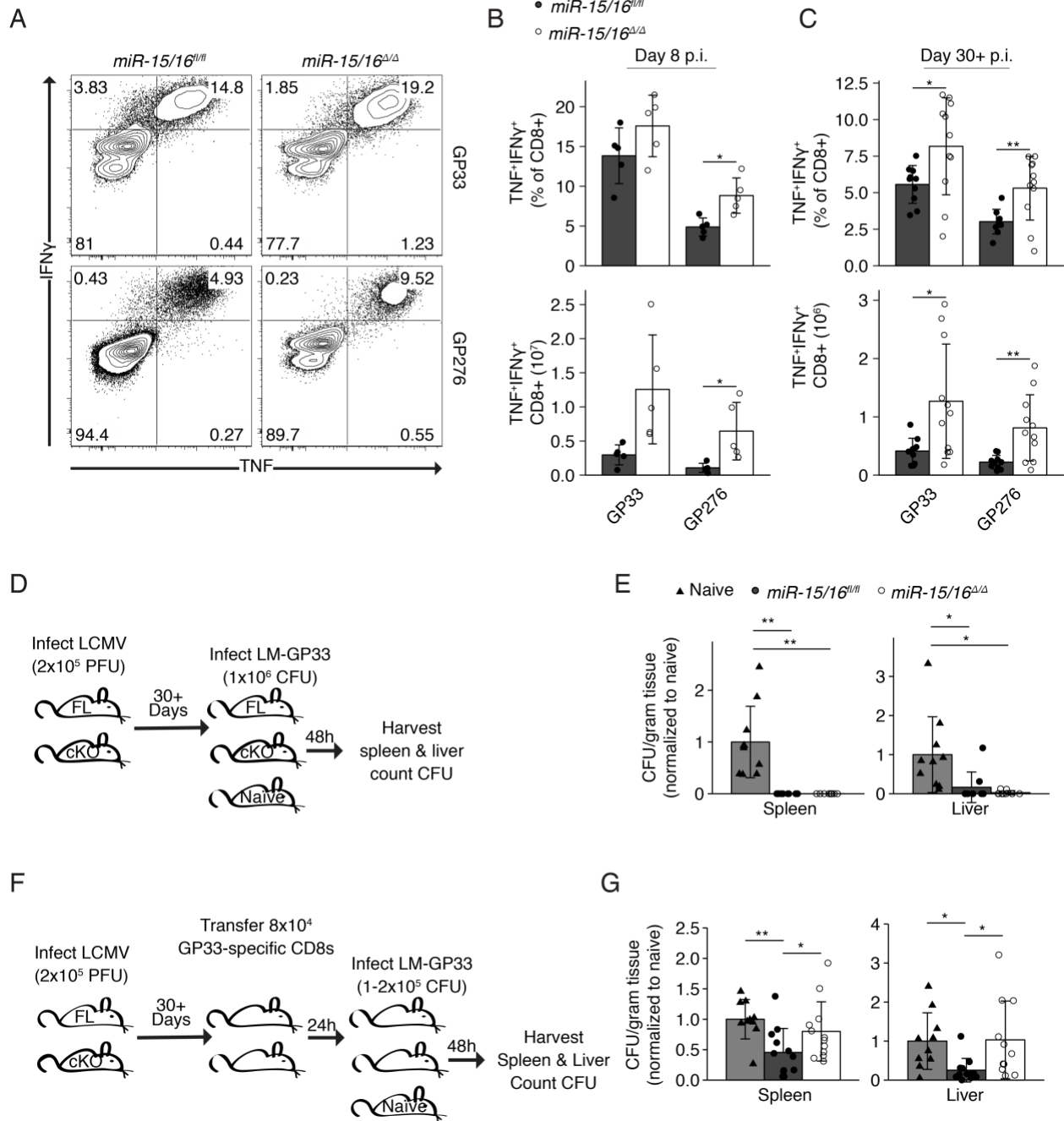
Figure 7: miR-15/16$^{\Delta/\Delta}$ animals are protected from chronic infection

(A) Quantification of mouse weights relative to day 0 post infection with LCMV clone 13 (n $\geq$ 5, from 2 independent experiments, two-tailed t test). **(B)** Kaplan-Meier curve summarizing percent survival over the course of 24 days p.i. with LCMV clone 13 (n $\geq$ 5, from 2 independent experiments, Mantel-Cox test). **(C)** Quantification of viral particles per gram of spleen tissue 24 days p.i. with LCMV clone 13 (n = 5, from 1 experiment). *, $P < 0.05$; **, $P < 0.01$; ***, $P < 0.001$.

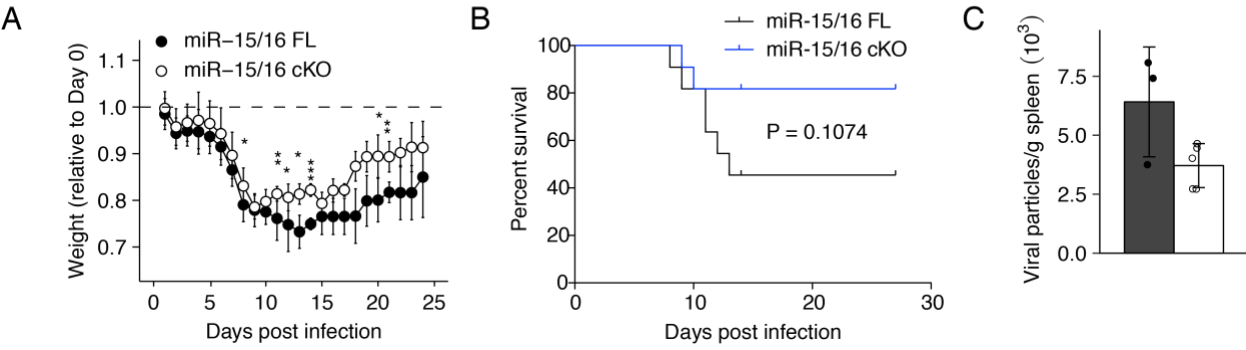# $miR\text{-}15/16^{\Delta/\Delta}$ animals are protected from chronic infection

Figure 8: miR-15/16 restrict CD8$^+$ T cell accumulation and contribute to exhaustion during chronic infection

(A,B) Quantification of frequencies and absolute numbers of CD8$^+$ T from spleens harvested 14 **(A)** or 24 **(B)** days p.i. with LCMV clone 13 (n $\geq$ 5 from 1 experiment each, two-tailed t test). **(C)** Flow cytometry of LCMV-specific CD8$^+$ T cells 24 days p.i. with LCMV clone 13. **(D,E)** Quantification of frequencies and absolute numbers of LCMV-specific CD8$^+$ T from spleens harvested 14 **(D)** or 24 **(E)** days p.i. with LCMV clone (n $\geq$ 5 from 1 experiment each, two-tailed t test). **(F,G)** Quantification of the MFI of LCMV-specific CD8$^+$ T cells 14 **(F)** or 24 **(G)** days p.i. with LCMV clone 13 (n $\geq$ 5 from 1 experiment each, two-tailed t test). *, P < 0.05; **, P < 0.01; ***, P < 0.001; ****, P < 0.0001.

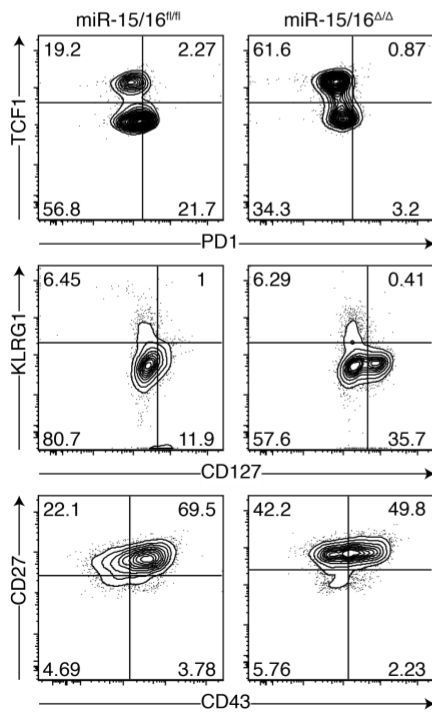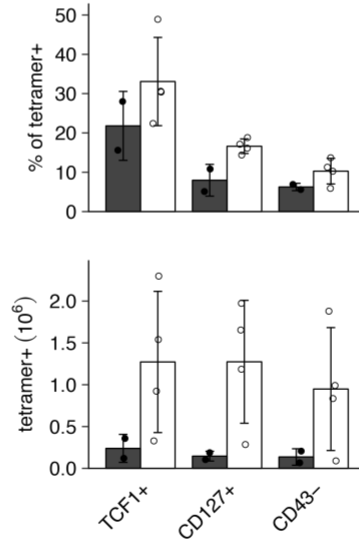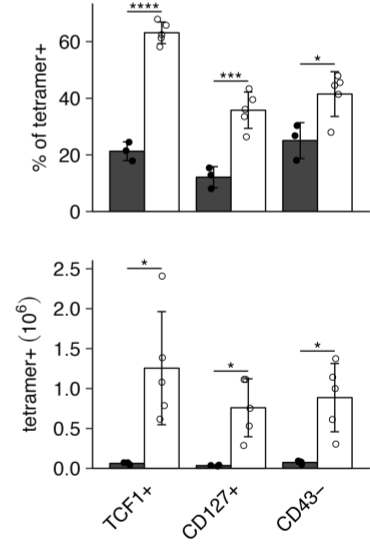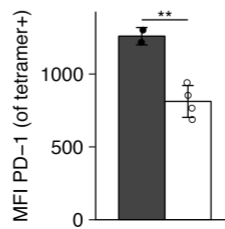# miR-15/16 restrict CD8+ T cell accumulation and contribute to exhaustion during chronic infection
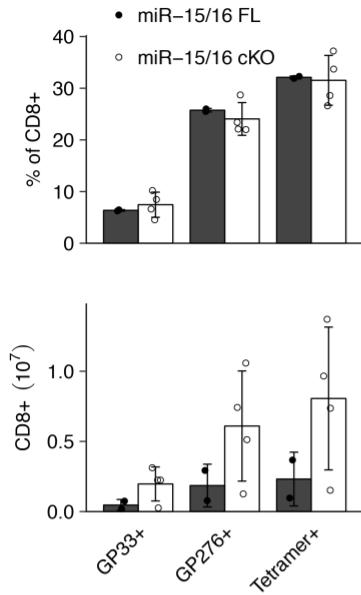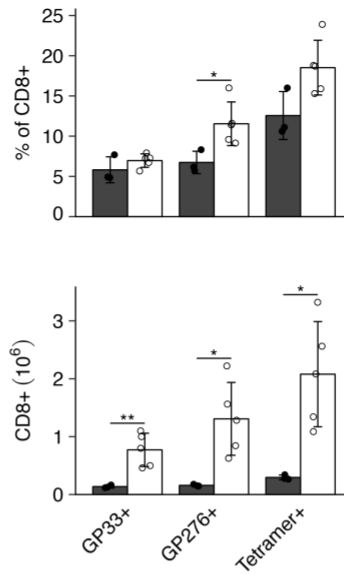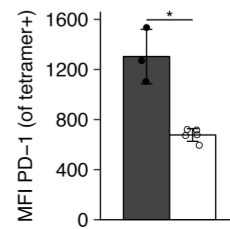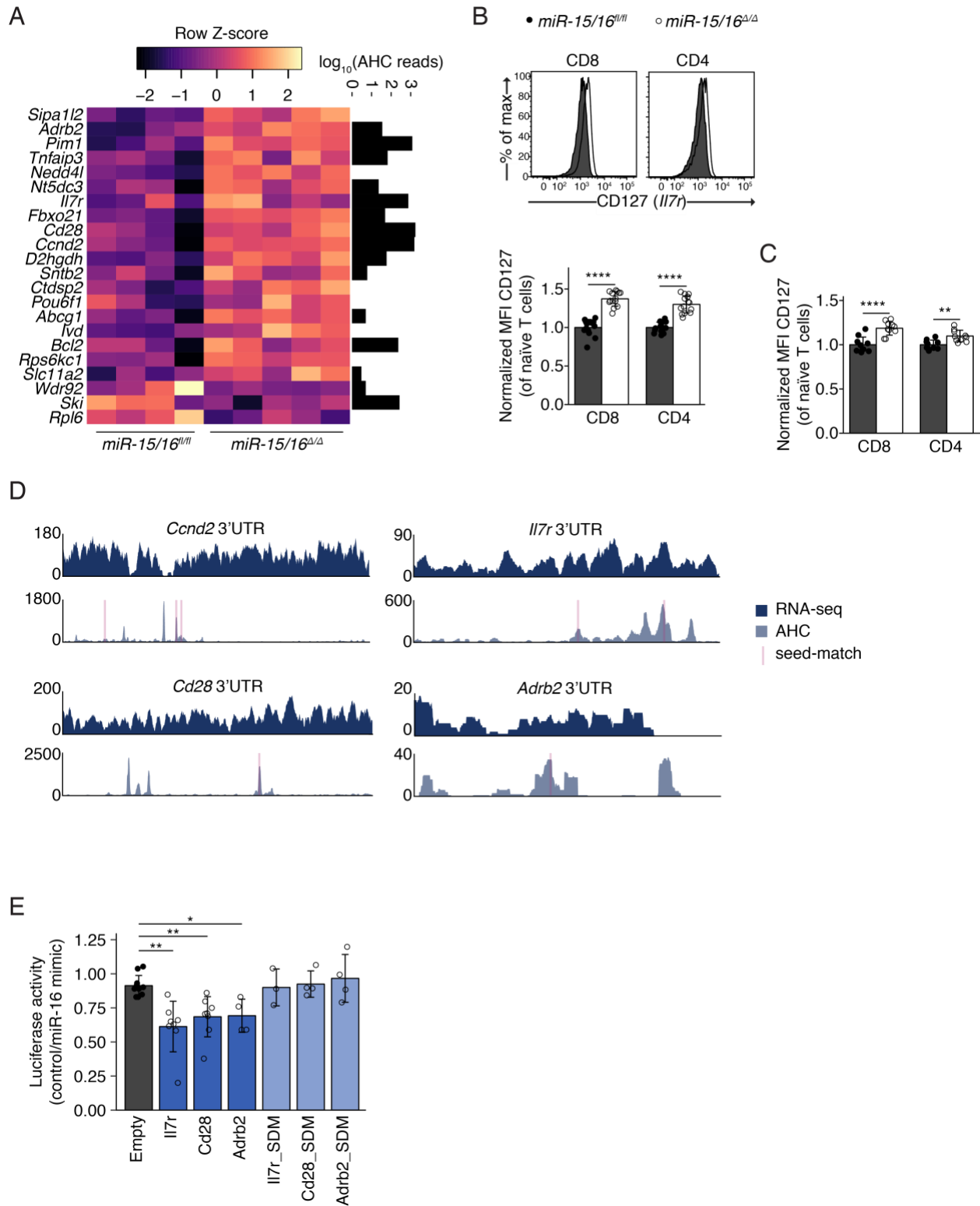
Figure 9: A network of miR-15/16 targets are up-regulated in memory cells

(A) Row z-score normalized expression of genes found to be up-regulated in memory cells compared to day 8 p.i. effector cells, differentially expressed in *miR-15/16$^{\Delta/\Delta}$* cells (*P*-value $\leq$ 0.1) and containing at least one miR-15/16 seed-match in their 3'UTR. Black bars indicate AHC reads at miR-15/16 seed-matches **(B)** Flow cytometry of CD127 on naive CD4$^+$ and CD8$^+$ T cells (n $\geq$ 14 from 3 independent experiments, two-tailed t test). **(C)** Flow cytometry of CD127 on naive CD4$^+$ and CD8$^+$ T cells from mixed bone marrow chimeric mice (n $\geq$ 9 from 2 independent experiments, two-tailed t test). **(D)** RNA-seq (top) and AHC (bottom) for the 3'UTRs of *Ccnd2*, *Il7r*, *Cd28*, and *Adrb2* with red shaded regions indicating the locations of miR-15/16 seed-matches. **(E)** Relative luciferase activity between empty vector, *Il7r* 3'UTR, *Cd28* 3'UTR, *Adrb2* 3'UTR and all three 3'UTRs with their respective miR-15/16 seed-matches scrambled (n $\geq$ 3 from at least 2 independent experiments, two-tailed t test). *, P < 0.05; **, P < 0.01; ***, P < 0.001; ****, P < 0.0001.

# A network of miR-15/16 targets are up-regulated in memory

A

Row Z-score

log_{10}(AHC reads)

B
● *miR-15/16^{fl/fl}*   ○ *miR-15/16^{Δ/Δ}*

C

D

Ccnd2 3'UTR

Il7r 3'UTR

Cd28 3'UTR

Adrb2 3'UTR

RNA-seq
AHC
seed-match

E

Supplementary Figure 1: miR-15/16 restrict CD4⁺ and CD8⁺ T cell accumulation in unchallenged animals

(A) Flow cytometry of CD4⁺ and CD8⁺ T cells in primary and secondary lymphoid tissues collected from *miR-15/16$^{fl/fl}$* and *miR-15/16$^{\Delta/\Delta}$* mice. **(B)** Quantification of frequencies and absolute numbers of CD4⁺ and CD8⁺ T cells in primary and secondary lymphoid tissues collected from *miR-15/16fl/fl* and *miR-15/16$^{\Delta/\Delta}$* mice (n = 10 from 2 independent experiments, two-tailed t test). **(C)** Quantification of absolute numbers of live cells within primary and secondary lymphoid tissues collected from *miR-15/16$^{fl/f}$* and *miR-15/16$^{\Delta/\Delta}$* mice (n ≥ 9 from 3 independent experiments, two-tailed t test). **(D)** Quantification of frequencies of CD4⁺ and CD8⁺ T cells in primary and secondary lymphoid tissues collected from *miR-15/16$^{fl/fl}$* and *miR-15/16$^{\Delta/\Delta}$* mixed bone marrow chimeric mice (n ≥ 10 from 3 independent experiments, two-tailed t test). **(E)** Quantification of frequencies and absolute numbers of CD4⁺ and CD8⁺ T cells in primary and secondary lymphoid tissues collected from *miR-15/16fl/fl* and *miR-15/16$^{\Delta/\Delta}$* mice 1.5 years of age (n ≥ 2 from 1 experiment, two-tailed t test). *, P < 0.05; **, P < 0.01; ***, P < 0.001; ****, P < 0.0001.

miR-15/16 restrict CD4+ and CD8+ T cell accumulation in unchallenged animals
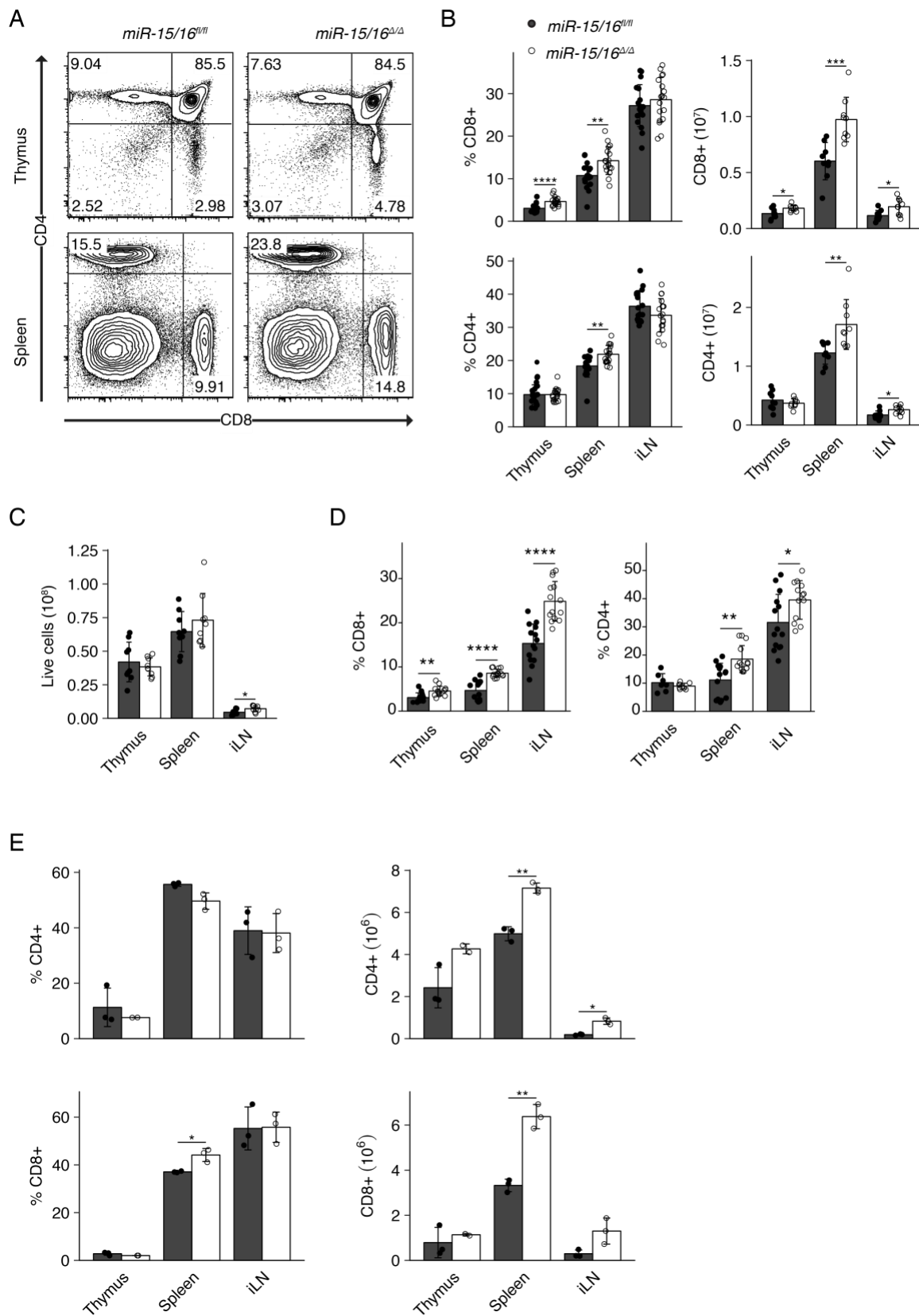
Supplementary Figure 2: miR-15/16 bind and regulate a large network of direct target RNAs in T cells

(A) Fraction of AHC reads mapping to genomic loci. **(B)** Correlation between AHC reads mapping to mature miRNAs and their respective TargetScan predicted seed-matches.

miR-15/16 bind and regulate a large network of direct target RNAs in T cells

A

B
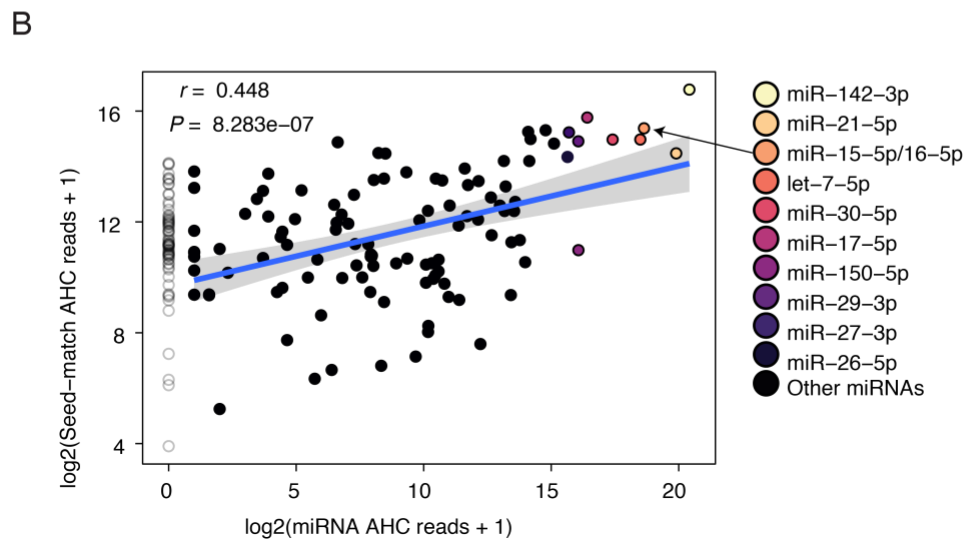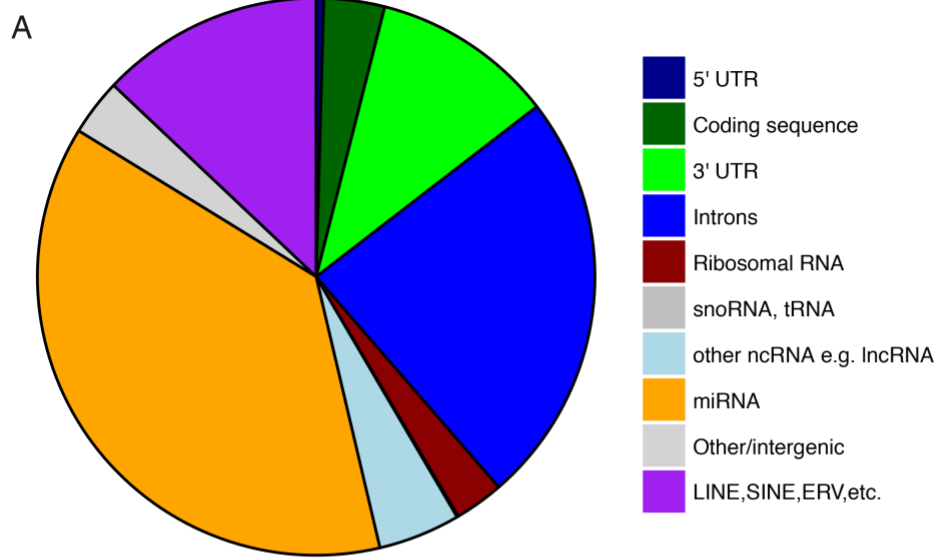
Supplementary Figure 3: miR-15a/16-1 and miR-15b/16-2 are sufficient to restrict the accumulation of antigen-specific T cells

(A,B) Frequencies of EdU$^+$ CD8$^+$ T cells 8 days p.i. with LCMV from single conditional knockout animals (n $\geq$ 6 of 2 independent experiments, two-tailed t test). **(C,D)** Frequencies and absolute numbers of antigen-specific CD8$^+$ T cells 8 days p.i. with LCMV from single conditional knockout animals (n $\geq$ 6 of 2 independent experiments, two-tailed t test).

miR-15a/16-1 and miR-15b/16-2 are sufficient to restrict the accumulation of antigen-specific T cells
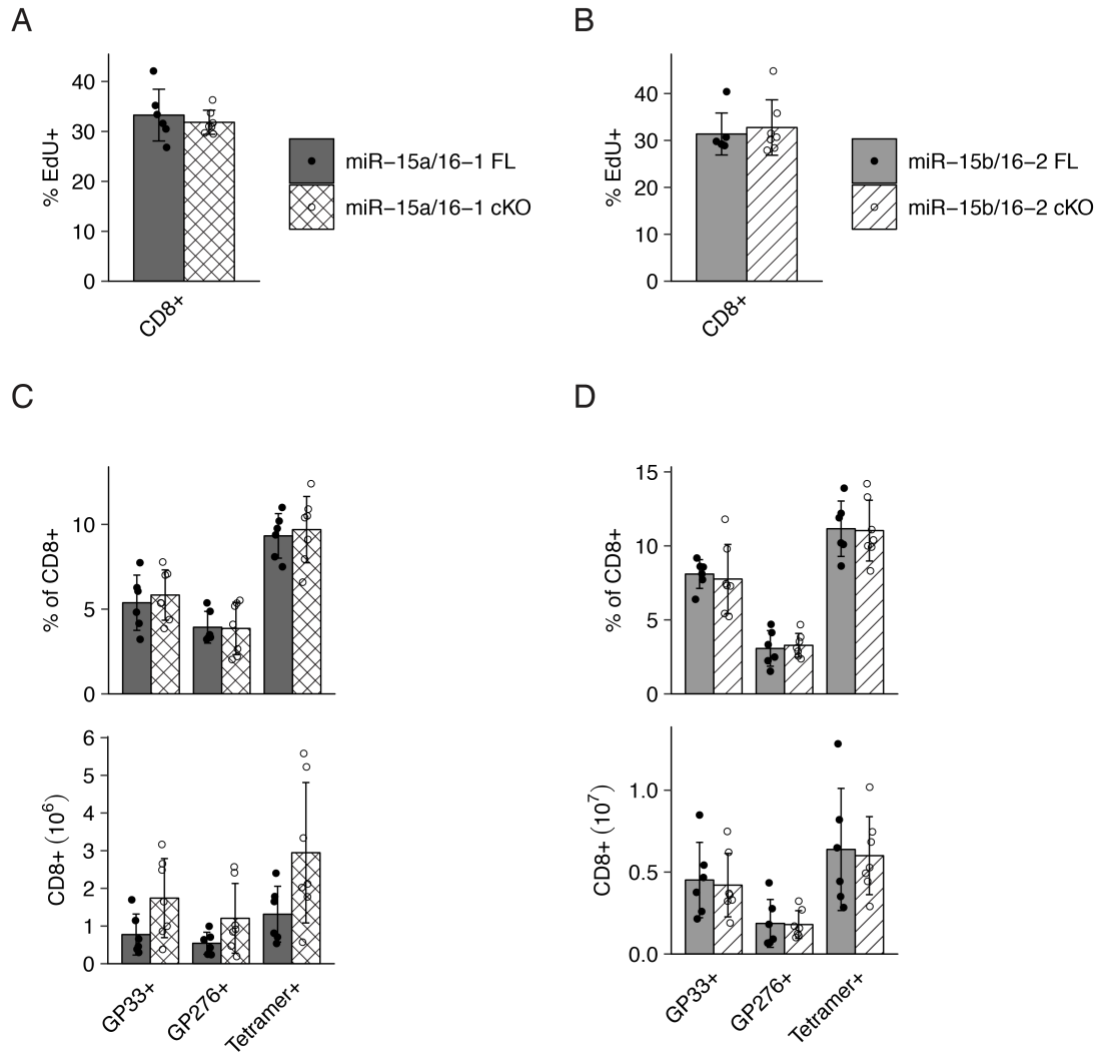
Supplementary Figure 4: miR-15a/16-1 and miR-15b/16-2 are sufficient to restrict the accumulation of long-lived memory cells and miR-15/16 restrict memory cell accumulation in unchallenged animals

(A,B) Frequencies and absolute numbers of antigen-specific CD8$^+$ T cells 8 days p.i. with LCMV from single conditional knockout animals (n $\geq$ 6 of 2 independent experiments, two-tailed t test). **(C)** Flow cytometry of CD44 expression among FOXP3$^-$CD4$^+$ and CD8$^+$ T cells within spleen and iLN collected from *miR-15/16$^{fl/fl}$* and *miR-15/16$^{\Delta/\Delta}$* mice. **(D)** Quantification of frequencies and absolute numbers of CD44$^+$ cells among FOXP3$^-$CD4$^+$ and CD8$^+$ T cells within spleen and iLN collected from *miR-15/16$^{fl/fl}$* and *miR-15/16$^{\Delta/\Delta}$* mice (n $\geq$ 9 from 3 independent experiments independent experiments, two-tailed t test). **(E)** Quantification of frequencies of CD25$^+$ cells among CD44^{hi} FOXP3$^-$CD4$^+$ and CD8$^+$ T cells within spleen and iLN collected from *miR-15/16$^{fl/fl}$* and *miR-15/16$^{\Delta/\Delta}$* mice (n $\geq$ 9 from 3 independent experiments, two-tailed t test). *, P < 0.05; **, P < 0.01; ****, P < 0.0001.

miR-15a/16-1 and miR-15b/16-2 are sufficient to restrict the accumulation of long-lived memory cells and miR-15/16 restrict memory cell accumulation in unchallenged animals

A

B

C

D

E
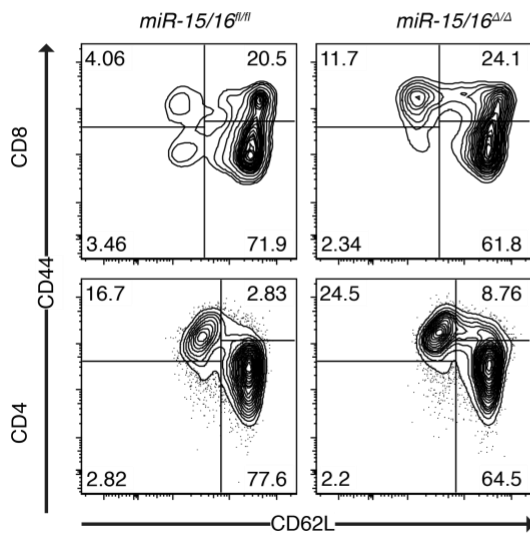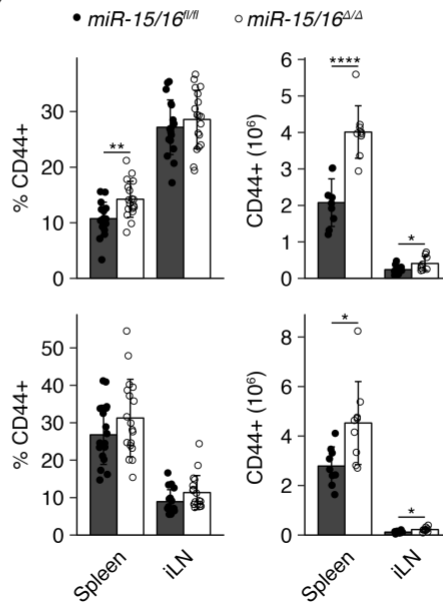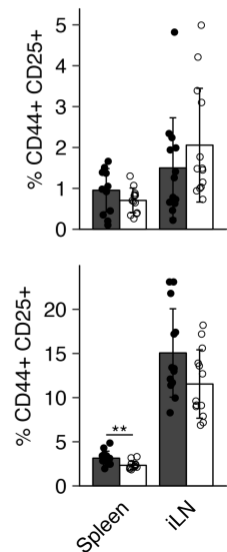
Supplementary Figure 5: miR-15a/16-1 and miR-15b/16-2 are sufficient to restrict survival of antigen-specific T cells

(A,B) Frequencies of viable (active Caspase3⁻ Live/Dead⁻), early apoptotic (active Caspase3⁺ Live/Dead⁻), late apoptotic (active Caspase3⁺ Live/Dead⁺), and dead (active Caspase3⁻ Live/Dead⁺), antigen-specific T cells 8 days p.i. with LCMV cultured overnight *in vitro* from single conditional knockout animals (n $\geq$ 6 of 2 independent experiments, two-tailed t test).

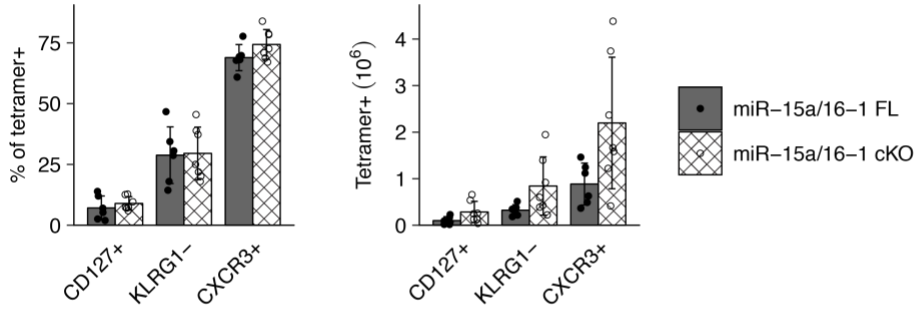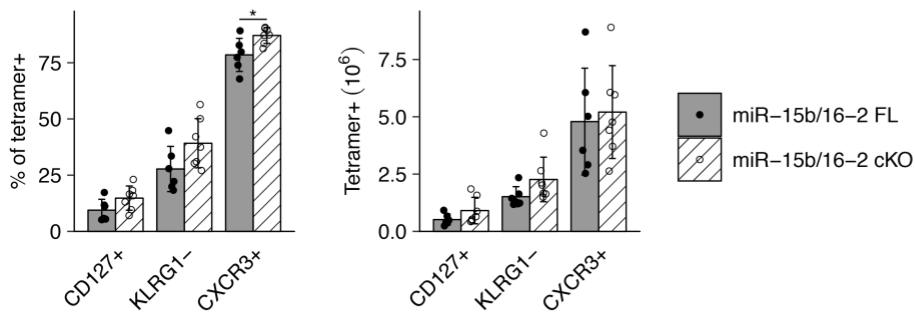# miR-15a/16-1 and miR-15b/16-2 are sufficient to restrict survival of antigen-specific T cells

A

B
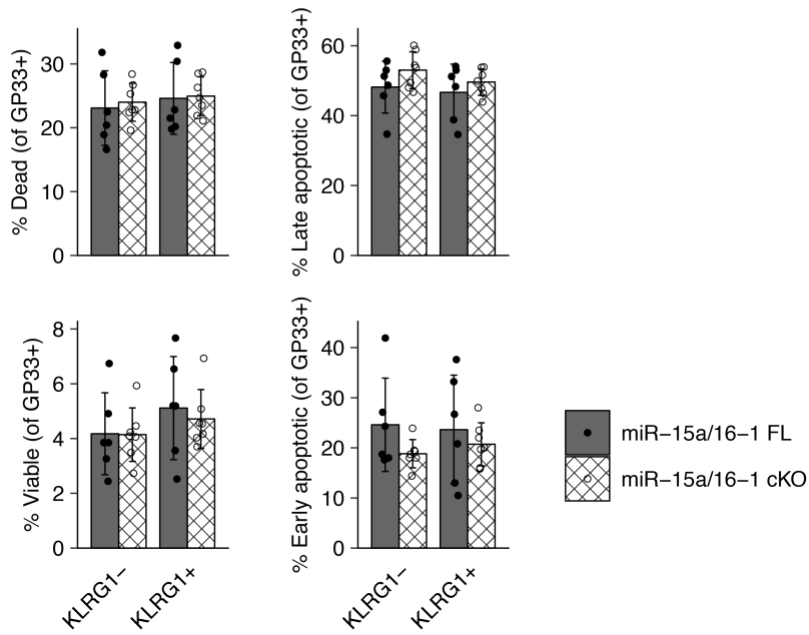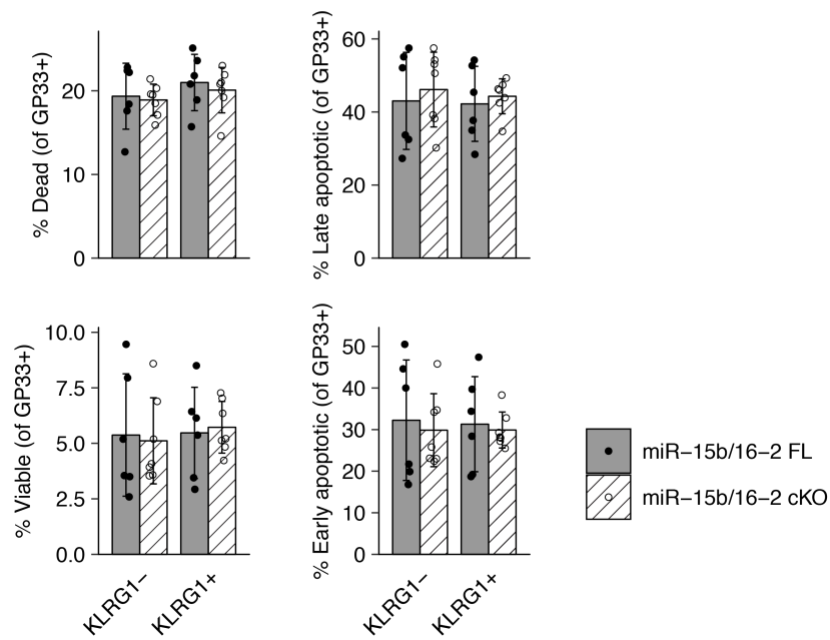
Supplementary Figure 6: A network of miR-15/16 targets are up-regulated in memory cells

(A) RNA-seq and AHC reads aligned to the 3'UTRs of memory-associated putative targets of miR-15/16 (red shaded regions indicate locations of miR-15/16 seed-matches).

A network of miR-15/16 targets are up-regulated in memory cells

A

RNA-seq ■   AHC ■   seed-match |

Abcg1 3'UTR	Ctdsp2 3'UTR	Rps6kc1 3'UTR
Adrb2 3'UTR	D2hgdh 3'UTR	Sipa1l2 3'UTR
Bcl2 3'UTR	Fbxo21 3'UTR	Ski 3'UTR
Ccnd2 3'UTR	Il7r 3'UTR	Slc11a2 3'UTR
Cd28 3'UTR	Ivd 3'UTR	Sntb2 3'UTR
Pim1 3'UTR	Nedd4l 3'UTR	Tnfaip3 3'UTR
Rpl6 3'UTR	Pou6f1 3'UTR	Wdr92 3'UTR

74
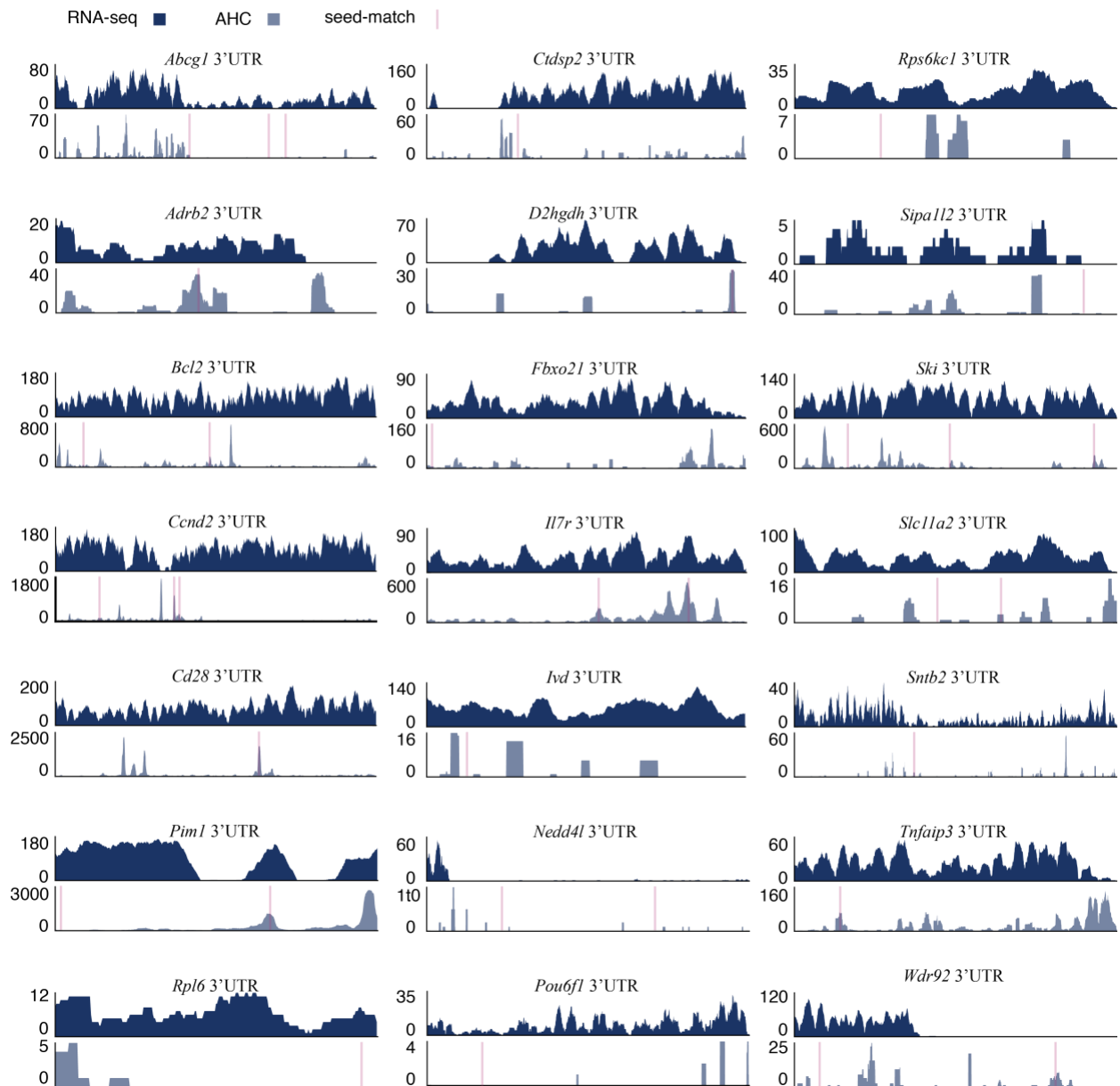
Supplementary Figure 7: miR-15/16 heightens the sensitivity of T cells to stimulation

(A-F) Quantitative PCR for immediate early genes 6 hours post stimulation of resting CD4$^+$ T cells with ant-CD3 and variable amounts of anti-CD28 (n $\geq$ 4 from 1 experiment, two-tailed t test). *, P < 0.05.

miR-15/16 heightens the sensitivity of T cells to stimulation
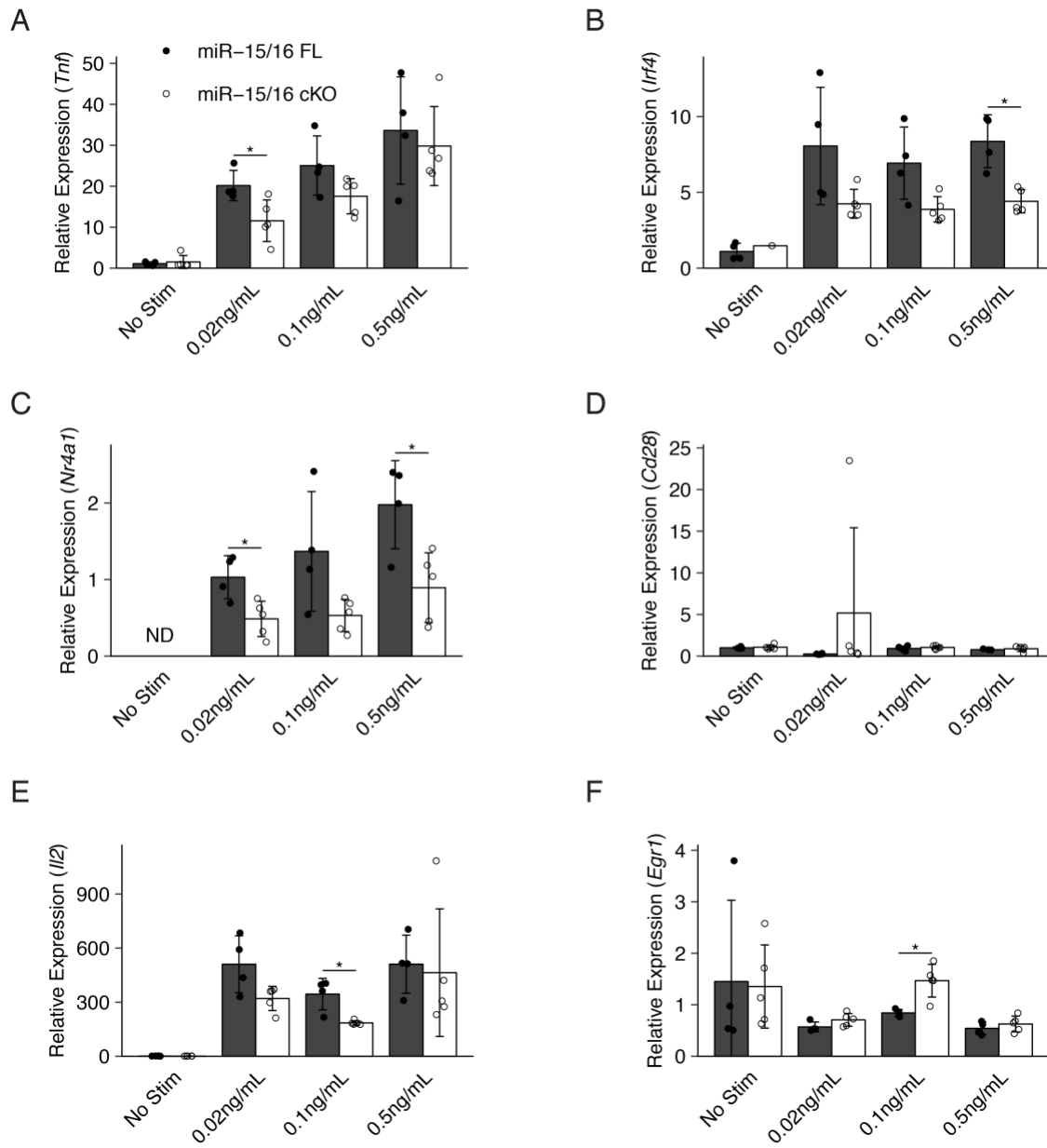
Supplementary Table 1: Reagents used

Reagent	Clone/Peptide
anti-CD3	145-2C11
anti-CD8a	53-6.7
anti-CD4	GK1.5
anti-Foxp3	FIK16s
anti-CXCR3	CXCR3-173
anti-CD127	A7R34
anti-CD62L	MEL-14
anti-CD45.1	A20
anti-CD45.2	104
anti-CD43	1B11
anti-KLRG1	MAFA
anti-CD44	IM7
anti-CD27	LG.7F9
anti-GR-1	RB6-8C5
anti-CD11b	M1/70
anti-activatedCaspase-3	C92-605
anti-CD19	1D3
anti-TNF	MP6-XT22
anti-IFNg	XMG1.2
anti-CD16/CD32	2.4G2
tetramerizedH-2DbGP33-41	KAVYNFATM
tetramerizedH-2DbGP276-286	SGVENPGGYCL

Supplementary Table 2: Luciferase primers used

Target	Primer	Sequence
Il7r 3'UTR	Fwd	CAGGCTCGAGATTATAAGAAAACCCTTCCATCGACAACC
Il7r 3'UTR	Rev	GATGCGGCCGCTTCCAGAAAATAGCGCATGCTTGTATTTG
Cd28 3'UTR	Fwd	TAGCTCGAGCAGGGACCCCTATCCAGAAG
Cd28 3'UTR	Rev	CTAGCGGCCGCAGTCAATGAATAAATATTTATTGCAGGCTAAGC
Adrb2 3'UTR	Fwd	CAGCTCGAGAGGCTTTCTACTCTCTAAGACCC
Adrb2 3'UTR	Rev	CAGGCGGCCGCCCACTCATCGGTCACGACAC
Il7r SDM	Fwd	GATAACCACAACAGTCCTGAATGCTTGATTATATTCTCAGG
Il7r SDM	Rev	CCTGAGAATATAATCAAGCATTCAGGACTGTTGTGGTTATC
Cd28 SDM	Fwd	GAAAACTATGTCACTTGTCCTGATTATTGTAAGAGTCTAAGAAC
Cd28 SDM	Rev	GAAAACTATGTCACTTGTCCTGATTATTGTAAGAGTCTAAGAAC
Adrb2 SDM	Fwd	GAATGATATATATTGTCCTGGGAAATCCATATCTAAAGGAGAGAG
Adrb2 SDM	Rev	CTCTCTCCTTTAGATATGGATTTCCCAGGACAATATATATCATTTC

Supplementary Table 3: mRNA primers used

Gene	Primer	Sequence
Egr1	Forward	TCGGCTCCTTTCCTCACTCA
Egr1	Reverse	CTCATAGGGTTGTTCGCTCGG
Irf4	Forward	TCCGACAGTGGTTGATCGAC
Irf4	Reverse	CCTCACGATTGTAGTCCTGCTT
Tnf	Forward	CCCTCACACTCAGATCATCTTCT
Tnf	Reverse	GCTACGACGTGGGCTACAG
Il2	Forward	TGAGCAGGATGGAGAATTACAGG
Il2	Reverse	GTCCAAGTTCATCTTCTAGGCAC
Nr4a1	Forward	TTGAGTTCGGCAAGCCTACC
Nr4a1	Reverse	GTGTACCCGTCCATGAAGGTG
Cd28	Forward	GTTCTTGGCTCTCAACTTCTTCT
Cd28	Reverse	TGAGGCTGACCTCGTTGCTAT

Acknowledgments

Authorship Contributions

J.D.G., R.K., and K.M.A. designed the research. J.D.G., R.K., H.M.S., M.S.F., P.O., D.M., D.S., B.J.L., M.PS., and S.P. performed the experiments. K.M.A., L.T.J., M.E.F., M.T.M., A.M., M.M., J.G.C., and S.S. supervised the research. J.D.G., R.K., A.J.L., performed the bioinformatic analysis under the advisement of K.M.A. and analyzed the results. J.D.G. and K.M.A wrote the manuscript. All authors read and approved the final version of this manuscript.

Conflict of Interest Disclosures

A.M. is a co-founder of Spotlight Therapeutics. A.M. serves as an advisor to Juno Therapeutics and PACT Pharma and the Marson laboratory has received sponsored research support from Juno Therapeutics, Epinomics and Sanofi.

Chapter 3: The long non-coding RNA Malat1 may serve as a sponge for miR-15/16

Summary:

The long non-coding RNA Malat1 is up-regulated among memory precursor cells and cells predicted to become memory precursors after a single division post-antigen encounter. The 8mer seed-match for miR-15/16 within Malat1 is the single most highly occupied miR-15/16 seed-match, however, despite the high degree of AGO2 occupancy, a dual-luciferase reporter containing a fragment of *Malat1* with the miR-15/16 seed-match was insensitive to miR-16-mediated repression. Furthermore, analysis of previously published data using *Malat1* anti-sense oligos or genetic knockout revealed a consistent pattern of down-regulation of genes predicted to be direct targets of miR-15/16. These results, combined, suggest that *Malat1* may behave as a sponge for miR-15/16, readily binding to mature microRNAs in complex with AGO2 but remaining stable. To investigate this, we generated *Malat1* mutant mice with a scrambled seed-match for miR-15/16.

Materials and Methods

Luciferase assay

Approximately 250,000 CD4$^+$ T cells were transfected on day 1 of culture with 1µg luciferase reporter constructs and/or 500nM miRIDIAN miRNA mimics (Dharmacon) using the Neon Transfection System (Thermo Fisher Scientific). Luciferase activity was measured 24 h after transfection with the Dual Luciferase Reporter Assay System (Promega) and a FLUOstar Optima plate-reader (BMG Labtech). A 1500 base pair fragment of *Malat1* was cloned into the psiCHECK-2 (Promega). Primers for cloning and site-directed-mutagenesis (SDM) are in Table 1.

Generation of transgenic animals with Cas9 RNP and HDR

13 C57BL/J (Jackson Laboratories) female mice 23 days of age were given pregnant mare's serum gonadotropin (PMSG) (2.5iu) to induce super ovulation. 24 hours later, the same animals were given human chorionic gonadotropin (hCG) (5iu). 19 hours after administration of hCG, 10 of the 13 females were identified as being plugged and zygotes/eggs were collected (recovered more than 120 zygotes/eggs from 20 oviducts observing expected thinning of zona pellucida). Cas9/guideRNA riboucleoproteins (RNPs) were generated as follows: 1) resuspend the HDR template (Table 2) at 100µM in Buffer (Buffer = 0.22µm filtered 10mM Tris, pH 7.4 + 150mM KCL). 2) resuspend the crRNA (Table 2) and tracrRNA (universal from IDT: Alt-R CRISPR-Cas9 tracrRNA) at 160µM in Buffer and allowed to equilibrate for 5 minutes at room temp. 3) mix 3µL of crRNA (160µM) and 3µL of tracrRNA (160µM) in a PCR tube to make the gRNA (80µM, 6µL) and incubated at 37°C for 10min. 4) add 6µL of Cas9 (40µM) to the 6µL of gRNA

to make a 2:1 ratio of gRNA:Cas9 RNP and incubated at 30°C for 10min. 5) add 4µL

(100µM) HDR template to the RNP for a final volume of 16µL and kept on ice.

Electroporate zygotes/eggs with BioRad GenePulser XL Square wave, 30V, 3ms, 2x,

with 100ms interval. On same day, generate pseudo-pregnant females by setting up

matings between CD1-Elite (SOPF, Charles River) female mice and vasectomized male

C57BL/6 mice. 24 hours later, check the survival and development of zygotes. Transfer

around 10-15 2-cell embryos to pseudo-pregnant females. 19 days later, 19 live pups

were born from 5 dams. All mice were housed and bred in specific pathogen-free

conditions in the Animal Barrier Facility at the University of California, San Francisco.

Animal experiments were approved by the Institutional Animal Care and Use Committee

of the University of California, San Francisco.

Results

Malat1 may act as a sponge for miR-15/16

One limitation of the use of TargetsScan (Loeb et al., 2012b) for the identification

of relevant microRNA target genes is that it is restricted to the 3'UTR. Through our work

in Chapter 1, we confirmed that AGO2 occupancy elsewhere in an mRNA transcript

(e.g., 5'UTR or CDS) does not globally correlate with differential gene expression in

$miR\text{-}15/16^{\Delta/\Delta}$ animals (Figure 2.2). However, the dynamics between microRNAs and

long non-coding RNAs is poorly understood. Through our comparison of AGO2

occupancy at miR-15/16 seed-matches and differential expression data, we observed

robust binding at a perfect 8mer seed-match for miR-15/16 within the long non-coding

RNA, _Malat1_ (Figure 1A,B). Strikingly, this single seed-match accounted for 4 percent of

all miR-15/16 seed-match-associated reads (Figure 1A).

Interestingly, although AGO2 robustly binds to this miR-15/16 seed-match,

differential expression data comparing $miR\text{-}15/16^{\Delta/\Delta}$ and $miR\text{-}15/16^{fl/fl}$ T cells revealed

no change in gene expression (Figure 1A). To better assess the sensitivity of _Malat1_ to

miR-15/16 targeting, we generated a dual luciferase reporter with a 1500 base pair

fragment of _Malat1_ containing the miR-15/16 seed-match. Consistent with the RNA-seq

data, the _Malat1_ fragment was insensitive to a miR-16 mimic (Figure 1C).

These data suggested to us that _Malat1_ may act as a sponge for miR-15/16 by

robustly binding with but remaining insensitive to AGO2-miR-15/16 complex. In order to

shed light on this possibility, we turned to previously published data on _Malat1_. We

hypothesized that if _Malat1_ was behaving as a sponge for miR-15/16, reduction or

deletion of _Malat1_ would result in increased miR-15/16 activity and therefore, down-

regulation of target genes. Consistent with our prediction, differential expression data from *Malat1* anti-sense oligo vs scramble oligo control treated cells exhibited a global repression of genes predicted to be targeted by miR-15/16 (Arun et al., 2016) (Figure 1D). Furthermore, in an independent experiment using *Malat1* knockout animals compared with wild-type controls, again, miR-15/16 predicted target genes were globally down-regulated (Nakagawa et al., 2012) (Figure 1E).

Generation of *Malat1* miR-15/16 seed-match scrambled mice

To investigate the biological significance of *Malat1* and miR-15/16 interaction, we generated transgenic animals with a disrupted miR-15/16 seed-match within the endogenous *Malat1* locus. Our approach was to design a 200 base pair DNA ultramer to serve as the homology directed repair (HDR) template. Within the center of the HDR template was the miR-15/16 seed-match which we rearranged 5 nucleotides to disrupt the seed-match without altering nucleotide content (Figure 2A). We designed a guide RNA that covered the miR-15/16 seed-match so that upon successful HDR with the template, Cas9 with the guide RNA would no longer be able to bind and cut (Figure 2A).

Discussion

The results of this study identify the long non-coding RNA, *Malat1,* as the single most highly occupied target of miR-15/16. Furthermore, despite robust binding, *Malat1* appears to be insensitive to miR-15/16. Through the re-analysis of previously published data, we demonstrate that reduction or loss of *Malat1* results in a global gene expression signature consistent with increased abundance of miR-15/16. We have

utilized Cas9 RNPs with an HDR template to generate knockin mice with a scrambled seed-match for miR-15/16 within the endogenous *Malat1* locus.

Through the use of this novel mouse, future studies will be able to address the contribution of the *Malat1* miR-15/16 seed-match to mouse biology. Of particular interest will be the contribution to CD8^{+} T cell memory. Prior work investigating gene expression profiles consistent between memory precursors and cells after a single division identified *Malat1* as one of only a handful of genes to be up-regulated (Kakaradov et al., 2017). Our own work reported in Chapter 1 identifies miR-15/16 as a negative regulator of CD8^{+} T cell memory differentiation. Therefore, it is possible that increased *Malat1* expression among cells destined to become memory precursors could serve as a sponge for the highly abundant miR-15/16 family of microRNAs and thereby effectively reduce its global efficacy.

Figure 1: *Malat1* may act as a sponge for miR-15/16

(A) Fold-change gene expression between *miR-15/16$^{\Delta/\Delta}$* and *miR-15/16$^{fl/fl}$* CD4$^+$ T cells and AHC read depth at miR-15/16 seed-matches within the 3'UTR of each gene. **(B)** RNA-seq and AHC read depth for *Malat1*. **(D,E)** Cumulative density plot depicting global expression by RNA sequencing as a ratio of the fold-change between *Malat1* anti-sense oligo vs scramble oligo treated MMTV (mouse mammary tumor virus)-PyMT mouse mammary carcinoma cells **(D)** or microarray fold-change between *Malat1* knockout and wild-type mouse embryonic fibroblasts **(E)** for all genes without a 7mer or 8mer miR-15/16 3'UTR seed-match (black), genes with a 7mer or 8mer miR-15/16 3'UTR seed-match (green), genes with a 7mer or 8mer miR-15/16 3'UTR seed-match and AHC read depth $\geq$5 (blue), and genes classified as targets of miR-15/16 by TargetScan 7.0 (red) (AHC reads represent the combined depth of n = 10 independent immunoprecipitations).

Malat1 may act as a sponge for miR-15/16

A
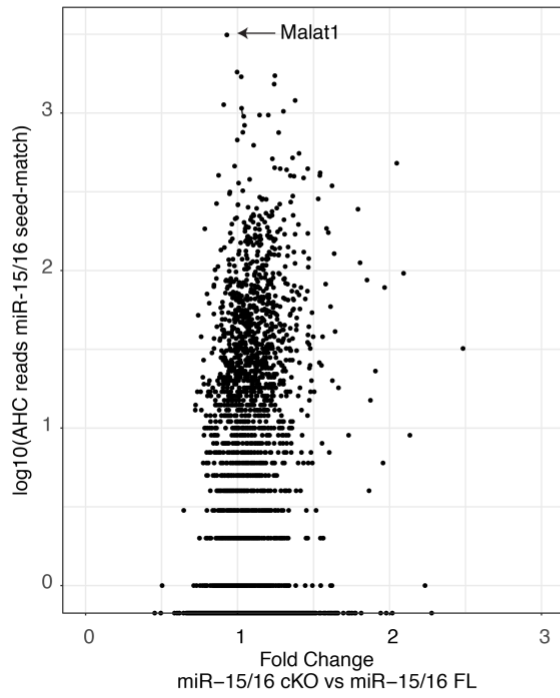
B
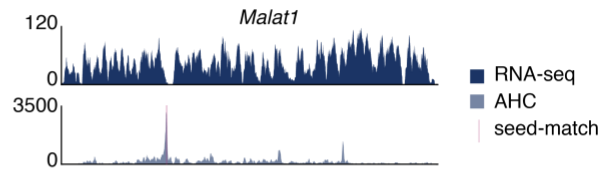
C
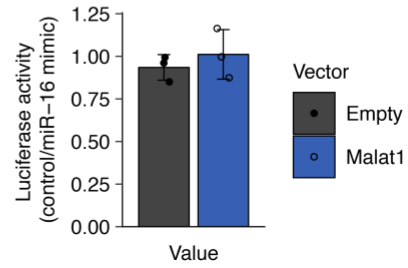
D
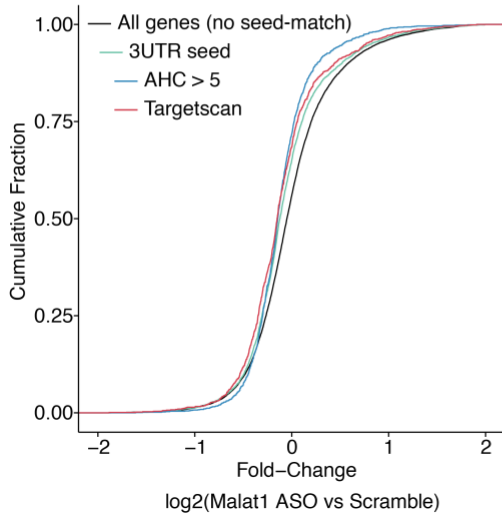
E
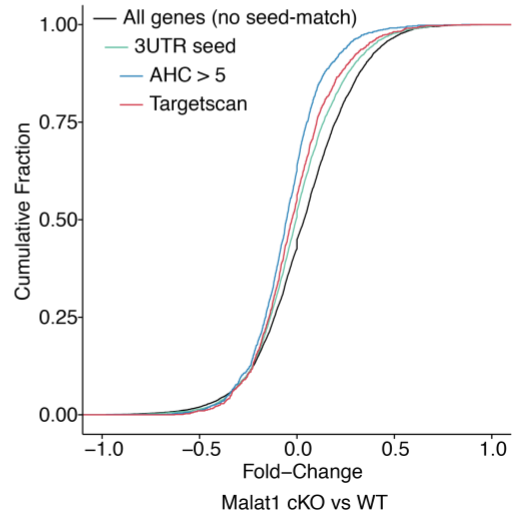
Figure 2: Generation of *Malat1* miR-15/16 seed-match scrambled mice

(A) Experimental outline and design of *Malat1* miR-15/16 seed-match scrambled mice.

Generation of Malat1 miR-15/16 seed-match scrambled mice

A

Table 1: Luciferase primers used

Reagent	Sequence
Malat1 forward	CAGTAATTCTAGGCGATCGCGGATTTGAGCCAGAAGAC
Malat1 reverse	GATATTTTATTGCGGCCAGCGATGCTTCAATTCCAACAAG

Table 2: Reagents used in mouse generation
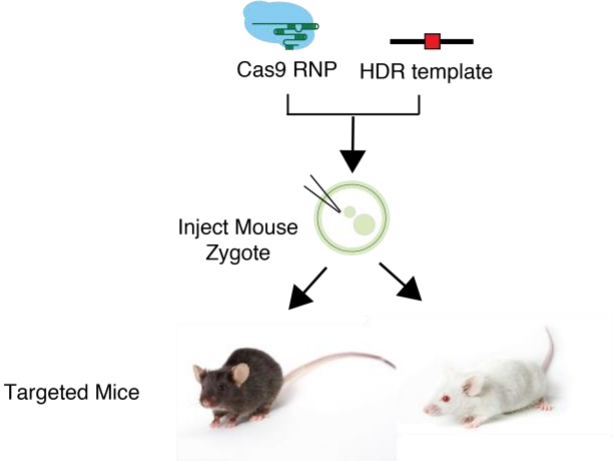
Reagent	Sequence
crRNA	ATCTGCTGCTATTAGAATGC
HDR template	ACAGACCACACAGAATGCAGGTGTCTTGACTTCAGGTCATGTCTGTTCTTTGG CAAGTAATATGTGCAGTACTGTTCCAATCTGTCCTGATTAGAATGCATTGTGAC GCGACTGGAGTATGATTAAAGAAAGTTGTGTTTCCCCAAGTGTTTGGAGTAGTG GTTGTTGGAGGAAAAGCCATGAGTAACAGGCAAGTGTTTGGAGTAGTGGTTGTT GGAGGAAAAGCCATGAGTAACAGGCTGAGTGTT

Chapter 4: miR-15/16 restrain the accumulation of regulatory T cells with

hallmarks of disfunction

Summary:

Using novel miR-15/16 compound conditional mutant mice, we show that miR-15/16 restrain the accumulation of regulatory T cells and are necessary for the expression of markers associated with functional activity.

Introduction

Regulatory T (Treg) cells are a subset of CD4$^+$ T lymphocytes, which express the transcription factor Foxp3 and are required for the suppression of autoimmunity and tolerance of non-pathological foreign antigens (e.g., allergens) (Sakaguchi et al., 2008). Treg cells engender their effects through the production of a broad range of immunosuppressive factors (e.g., IL-10, TGF-beta, CTLA-4, CD25, CD39/CD73 and granzyme A/B) and can target cells of both the adaptive and innate immune system; making them potent suppressors of inflammation. Highlighting the importance of Treg cells in maintaining tolerance, ablation of Treg cells can lead to type I diabetes as rapidly as 3 days (Feuerer et al., 2009). Due to their potency as suppressors of aberrant inflammation, there is excitement surrounding the therapeutic adoptive transfer of Treg cells to treat autoimmune diseases such as type 1 diabetes (Bluestone et al., 2015).

While the adoptive transfer of Treg cells has been demonstrated to be effective in numerous murine models, when introduced to an inflammatory environment, Treg cells can lose Foxp3 expression (Josefowicz et al., 2012; Zheng et al., 2010; Yue et al., 2016) and even take on a T effector (T$_{eff}$) cell phenotype (Zhou et al., 2009). Peripherally derived and induced Treg cells display reduced stability in the face of inflammation, especially those expressing low levels of the high affinity IL-2 receptor, CD25 (Zhou et al., 2009; Ohkura et al., 2012). CD25 is required for optimal Treg function (Chinen et al., 2016). Further linking the expression of CD25 to Treg stability, antigen-driven *in vivo* de-stabilization of induced Treg cells can be reversed by administration of IL-2 (Chen et al., 2011).

These findings regarding iTreg stability represents an especially grim possibility for adoptive transfer-based therapies particularly given the finding that, while peripherally circulating adoptively transferred Treg cells appear to be stable for at least one year, the fate of inflamed-tissue infiltrating transferred Treg cells remains to be determined (Bluestone et al., 2015). Support for reduced stability in the face of inflammation is corroborated by a previous study using Treg lineage-tracing reporter mice, which demonstrated that the highest percentages of these "ex-Treg" cells were found in non-lymphoid tissues where high levels of activation were occurring (DuPage et al., 2015).

miRNAs have been demonstrated to be critical regulators of Treg cell biology. Deletion of Dicer or Drosha, key components of miRNA biogenesis, in either CD4^{+} T cells or specifically among Foxp3^{+} Treg cells results in spontaneous inflammatory disease (Liston et al., 2008; Chong et al., 2008). To date, numerous specific miRNAs have been linked with Treg cell differentiation within the thymus and in the periphery, control of Foxp3 expression, and the regulation of suppression-related molecules among Treg cells (Hippen et al., 2018).

Previous work describing the effects of miR-15/16 on Treg cell biology has been surprisingly inconsistent. miR-15/16 have been demonstrated to be upregulated among induced mouse Treg cells (Kuchen et al., 2010; Singh et al., 2015a) while miR-15/16 are down-regulated in cord blood-derived Treg cells (Liu et al., 2014). Furthermore, correlational studies of rheumatoid arthritis patients revealed that miR-16 expression is elevated in Th17 cells while being decreased among Tregs suggesting that miR-16 may guide Th17 fate while inhibiting Treg fate (Wu et al., 2016). However, even within this

single study, the authors found that miR-16 expression was positively correlated with both RORγt and Foxp3 mRNA expression (Wu et al., 2016). Conversely, Liu et. al. found that over-expression of miR-15a or miR-16 was associated with reduced expression of Foxp3 and CTLA-4 (Liu et al., 2014). Counter to these findings, transfection of Dicer deficient T cells with miR-15b or miR-16 mimics enhanced iTreg differentiation while inhibition of miR-15b and miR-16 reduced iTreg frequency (Singh et al., 2015a). Further supporting a positive role for miR-15/16 in the regulation of iTreg differentiation, over-expression of miR-15b/16 in adoptively transferred naïve CD4$^+$ T cells led to increased frequencies of iTregs in the spleen, lungs, and mesenteric lymph nodes of recipient RAG deficient mice (Singh et al., 2015a).

While these studies differ in their approaches to understand the role of miR-15/16 in Treg biology, none use the approach of genetic ablation among CD4$^+$ T cells in intact animals. To this end, we examined our *miR-15/16$^{Δ/Δ}$* for effects on Treg biology in the steady state. Our findings reveal a role for miR-15/16 in the thymic differentiation of Tregs and the peripheral maintenance of Treg-specific functional markers. Deletion of miR-15/16 in CD4$^+$ T cells resulted in increased frequencies of Tregs. However, Tregs lacking miR-15/16 exhibited hallmarks of disfunction based on expression of Foxp3, CD25, CD127, and Nur77. Through the use of mixed bone marrow chimeras, we demonstrate that these effects are cell intrinsic and through the use of fixed TCR-transgenic animals, preliminary results suggest that these effects are independent of the TCR. Surprisingly, these effects on Tregs did not lead to autoimmunity, suggesting that either the increased frequencies of Tregs or their suppressive capacity are sufficient to protect *miR-15/16$^{Δ/Δ}$* animals.

Materials and Methods

Mice

miR-15/16$^{\Delta/\Delta}$ animals described in **Chapter 2** were crossed to mice containing the OTII ovalbumin residue 323-339-specific TCR transgenic animals (B6.Cg-Tg(TcraTcrb)425Cbn/J, Jackson Laboratory). For hematopoietic chimeras, B6-Ly5.1/Cr (CD45.1+; Charles River) mice were lethally irradiated (2x550 rad), reconstituted with $5x10^6$ bone marrow cells, and analyzed 8-10 weeks later. Male and female age and sex matched mice were used between 5 to 12 weeks of age. All mice were housed and bred in specific pathogen-free conditions in the Animal Barrier Facility at the University of California, San Francisco. Animal experiments were approved by the Institutional Animal Care and Use Committee of the University of California, San Francisco.

Flow Cytometry

Cells were harvested from thymus, spleen, and lymph nodes by mashing through 70µM filters. Splenic and blood RBCs were lysed with ACK buffer. Single cell suspensions were prepared in PBS 2% FCS and stained with reagents (Supplementary Table 1) for analysis on an LSRFortessa (Becton Dickenson). For transcription factor stains, cells were fixed and permeabilized using the Foxp3 Transcription Factor Staining Buffer Set (eBioscience). Data were analyzed with FlowJo.

Statistics and Data Analysis

Excel (Windows) and R were used for data analysis. Plots were generated using the Bioconductor package, plotGrouper (Gagnon, 2018). For all figures, bar graphs display

mean ± s.d. and each point represents an individual mouse unless otherwise stated.

*P<0.05, **P<0.01, ***P<0.001, and ****P<0.0001 for significance. All data were

assumed to be normally distributed unless otherwise stated.

Results

miR-15/16 restrict the accumulation of CD4⁺ Foxp3⁺ Tregs

During positive selection in the thymus, CD4$^+$ T cells with greater affinity for self-

antigen-MHC complexes may undergo differentiation to the Treg lineage. To assess the

role of miR-15/16 in Treg development, we performed flow cytometric analysis of

primary and secondary lymphatic organs for CD4$^+$ T cells expressing the Treg lineage

defining transcription factor, Foxp3. *miR-15/16$^{Δ/Δ}$* animals exhibited increased

frequencies and absolute numbers of Foxp3$^+$ T cells in the thymus, spleen and inguinal

lymph nodes (Figure 1A-C). Similar, yet less pronounced results were observed within

mixed bone marrow chimeric mice suggesting that these effects are cell intrinsic (Figure

1D).

Given the fact that thymic differentiation of Tregs has been linked with TCR

specificity for self (Ohkura et al., 2013), we wondered whether these effects could be

related to a shift in the TCR repertoire of miR-15/16 deficient CD4$^+$ T cells. To test this

hypothesis, we crossed *miR-15/16$^{Δ/Δ}$* animals to OTII TCR-transgenic animals in which

all T cells exhibit TCR specificity to the ovalbumin peptide residue 323-339. Since

ovalbumin is found within chicken egg whites and not mice and given that all CD4$^+$ T

cells within OTII animals would have identical levels of self-reactivity, this provides a

robust system to test for TCR-intrinsic phenotypes. Supporting a TCR specificity-

independent role for miR-15/16 in the restriction of Treg accumulation, miR-15/16 deficient OTII CD4$^+$ T cells trended towards increased Treg frequencies in the spleen (Figure 1E).

In order to determine whether this phenotype would become exacerbated with over time, $miR\text{-}15/16^{\Delta/\Delta}$ animals were aged 1.5 years. Phenotypic analysis of primary and secondary lymphoid organs determined that the frequency of Tregs within $miR\text{-}15/16^{\Delta/\Delta}$ animals was unchanged compared with $miR\text{-}15/16^{fl/fl}$ animals suggesting both that miR-15/16 deficient Treg accumulation stabilized over time (Figure 1F).

miR-15/16 are required for appropriate expression of Treg functional markers

Tregs utilize a broad range of effector molecules to exert their suppressive effects. Critical to the initiation and maintenance of expression of many of these is the Treg master transcription factor, Foxp3 (Williams and Rudensky, 2007). Surprisingly, while miR-15/16 deficiency lead to increased frequencies and absolute numbers of Foxp3$^+$ CD4$^+$ T cells, these cells exhibited a reduced expression level of Foxp3 across primary and secondary lymphoid organs (Figure 2A). Reduced Foxp3 expression among Tregs is associated with Treg instability and functional insufficiency.

In further investigating the phenotype of miR-15/16 deficient Tregs, we observed decreased expression of the high-affinity IL-2 receptor, CD25 on the surface of Tregs as well as the transcription factor, Nur77 (Figure 2B,C). Consistent with this being a cell-intrinsic effect, miR-15/16 deficient Tregs within mixed bone marrow chimeric mice also exhibited reduced CD25 surface expression (Figure 2D). Furthermore, OTII TCR-

transgenic miR-15/16 deficient Tregs had reduced surface CD25, demonstrating that this phenotype is TCR-specificity independent (Figure 2E).

Given the lack of autoimmunity within *miR-15/16$^{\Delta/\Delta}$* animals, we hypothesized that miR-15/16 deficient Tregs must either maintain sufficient effector function despite low Foxp3, CD25, and Nur77 expression or through a compensatory increase in their absolute number in the periphery. One interesting observation was that miR-15/16 deficient Tregs expressed high levels of the IL-7 receptor, CD127 (Figure 2F). These findings suggest that miR-15/16 Tregs may have reduced suppressive capacity, however, their elevated expression of CD127 may be sufficient to compensate for low CD25 expression.

Discussion

The experiments in this study demonstrate that miR-15/16 restrict the accumulation of Foxp3^{+} CD4^{+} Tregs. Furthermore, Tregs deficient in miR-15/16 exhibit reduced expression of markers associated with Treg function and stability. Interestingly, miR-15/16 deficient Tregs expressed high surface levels of the IL-7 receptor alpha chain, CD127. Given our findings in Chapter 2, it is likely that elevated expression of CD127 is due to the direct effects miR-15/16 on the *Il7r* 3'UTR.

Our findings related to Tregs and miR-15/16 are somewhat in opposition to those described by Singh et. al. (Singh et al., 2015a), however, while their study focused on induced Tregs, our findings that miR-15/16 restrict Treg accumulation in the thymus suggest that the effects we observe are related to natural Tregs. Natural Tregs exhibit distinct epigenetic signatures, suggesting that the drivers of their differentiation likely

differ from those of induced Tregs (Ohkura et al., 2012). Furthermore, the present study utilized T cell-specific deletion of miR-15/16 while the findings of Singh et. al. relied upon miR-15/16 over-expression. It is possible that over-expression of miR-15/16 could lead to the targeting of transcripts that typically are insensitive to endogenous levels of miR-15/16.

We demonstrate that while miR-15/16 deficient Tregs express reduced levels of Foxp3 and CD25. Tregs are dependent on CD25 for their suppressor activity *in vivo*, however expression of active STAT5 is sufficient to restore Treg function (Chinen et al., 2016). This presents the intriguing possibility that elevated CD127 expression among miR-15/16 deficient Tregs may provide sufficient STAT5 activation to maintain Treg function.

Another interesting area of inquiry will be with respect to Nur77. Prior work has demonstrated that Nur77 expression level is a good indicator of activation within T cells (Ashouri and Weiss, 2017). One possible explanation for reduced Nur77 expression among miR-15/16 deficient Tregs is that they may be experiencing reduced tonic signaling. This presents an interesting potential line of inquiry given that Tregs appear to require constant tonic signals to maintain their suppressive function and key Treg expression profiles (Vahl et al., 2014; Levine et al., 2014).

One distinction between peripherally induced and natural Tregs is methylation status of Foxp3 and other Treg associated markers including CD25. While natural Tregs generated within the thymus typically have robust demethylation at conserved non-coding sequence (CNS)1 and CNS2 within Foxp3 as well as CD25, peripheral Tregs exhibit demethylation specific to CNS1 (Ohkura et al., 2012). Due in part to

hypomethylation of CNS2, natural Tregs express Foxp3 more stably through Ets1, CREB, and Foxp3 itself while peripheral Tregs rely on Smad3 driven by TGF-B (Ohkura et al., 2013). Given that both Smad3 exhibits robust AGO2 occupancy at a miR-15/16 seed-match and is up-regulated in the absence of miR-15/16, it is possible that this could represent a mechanism by which miR-15/16 could restrict Treg development (unpublished data).

Future work will be needed to further dissect the role of miR-15/16 in Treg biology. Of particular interest will be the suppressive capacity of miR-15/16 deficient Tregs. This can be tested using both *in vitro* and *in vivo* suppression assays. Complicating these experiments, traditional sorting Tregs relies on identifying cells expressing high levels of CD25 and low levels of CD127 on their surface. This presents an obvious issue with miR-15/16 deficient Tregs since their expression of these markers is an unreliable means of their detection. To address this issue, I have generated miR-15/16 T cell deficient Foxp3-GFP reporter mice (Haribhai et al., 2007; Lin et al., 2007). This will enable the effective sorting of Tregs for quantitative assessment of their suppressive function.

Figure 1: miR-15/16 restrict the accumulation of CD4$^+$ Foxp3$^+$ Tregs

(**A**) Flow cytometry of CD4$^+$ T cells at baseline. **(B)** Quantification of frequencies of Foxp3$^+$ CD4$^+$ T cells at baseline (n ≥ 4 representative of ≥ 4 independent experiments, two-tailed t test). **(C)** Quantification of absolute numbers of Foxp3$^+$ CD4$^+$ T cells at baseline (n ≥ 4 representative of ≥ 4 independent experiments, two-tailed t test). **(D)** Quantification of frequencies of Foxp3$^+$ CD4$^+$ T cells at baseline in mixed bone marrow chimeras (n = 10 two independent experiments, two-tailed t test). **(E)** Quantification of frequencies of Foxp3$^+$ CD4$^+$ T cells at baseline in OTII TCR-transgenic animals (n ≥ 2, single experiment). **(F)** Quantification of frequencies of Foxp3$^+$ CD4$^+$ T cells at baseline in animals aged 1.5 years (n ≥ 2 1 experiment, two-tailed t test). *, P < 0.05; **, P < 0.01; ***, P < 0.001; ****, P < 0.0001.

miR-15/16 restrict the accumulation of CD4+ Foxp3+ Tregs
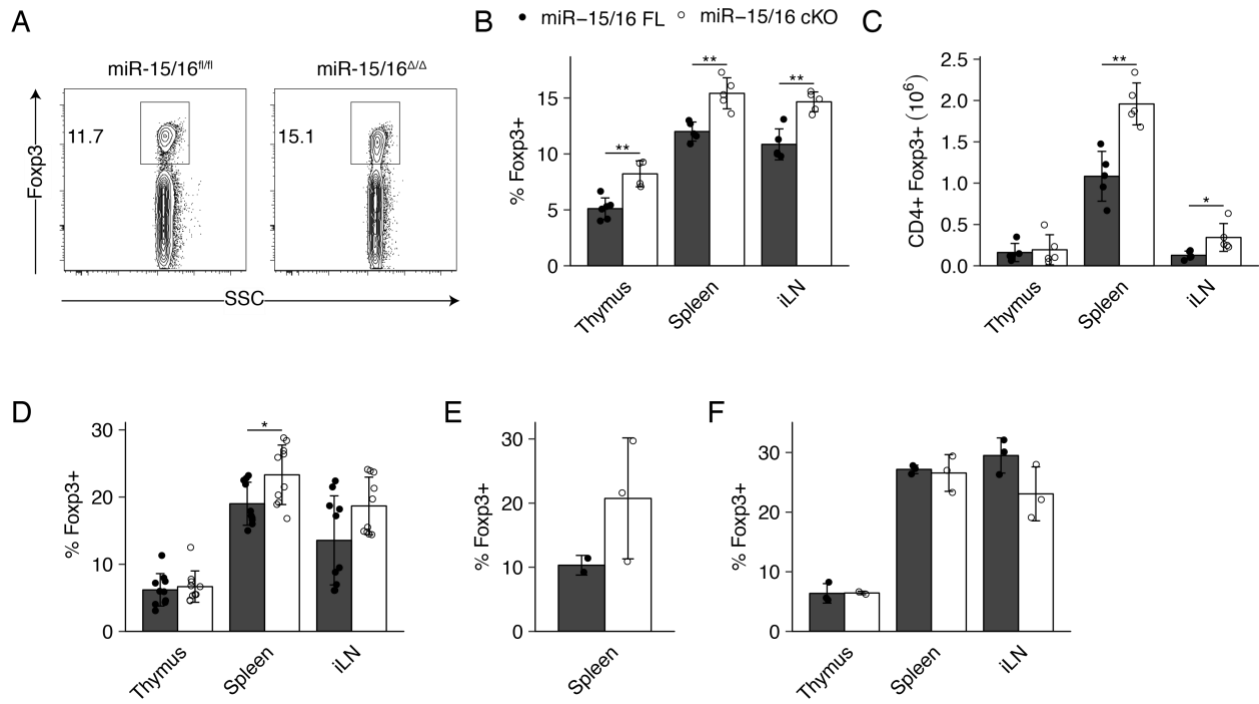
Figure 2: miR-15/16 are required for appropriate expression of Treg functional markers

(A-C) Flow cytometry (left) and quantification (right) of Treg functional marker expression among CD4$^+$ Foxp3$^+$ T cells (n $\geq$ 4 representative of $\geq$ 4 independent experiments, two-tailed t test). **(D)** Quantification of CD25 MFI among Foxp3$^+$ CD25$^+$ T cells among mixed bone marrow chimeric mice (n = 10 two independent experiments, two-tailed t test). **(E)** Quantification of CD25 MFI among Foxp3$^+$ CD25$^+$ T cells among OTII TCR transgenic mice (n $\geq$ 2, single experiment). **(F)** Flow cytometry (left) and quantification (right) of CD127 expression among CD4$^+$ Foxp3$^+$ T cells (n $\geq$ 4 representative of $\geq$ 4 independent experiments, two-tailed t test). *, P < 0.05; **, P < 0.01; ***, P < 0.001; ****, P < 0.0001.

miR-15/16 are required for appropriate expression of Treg functional markers
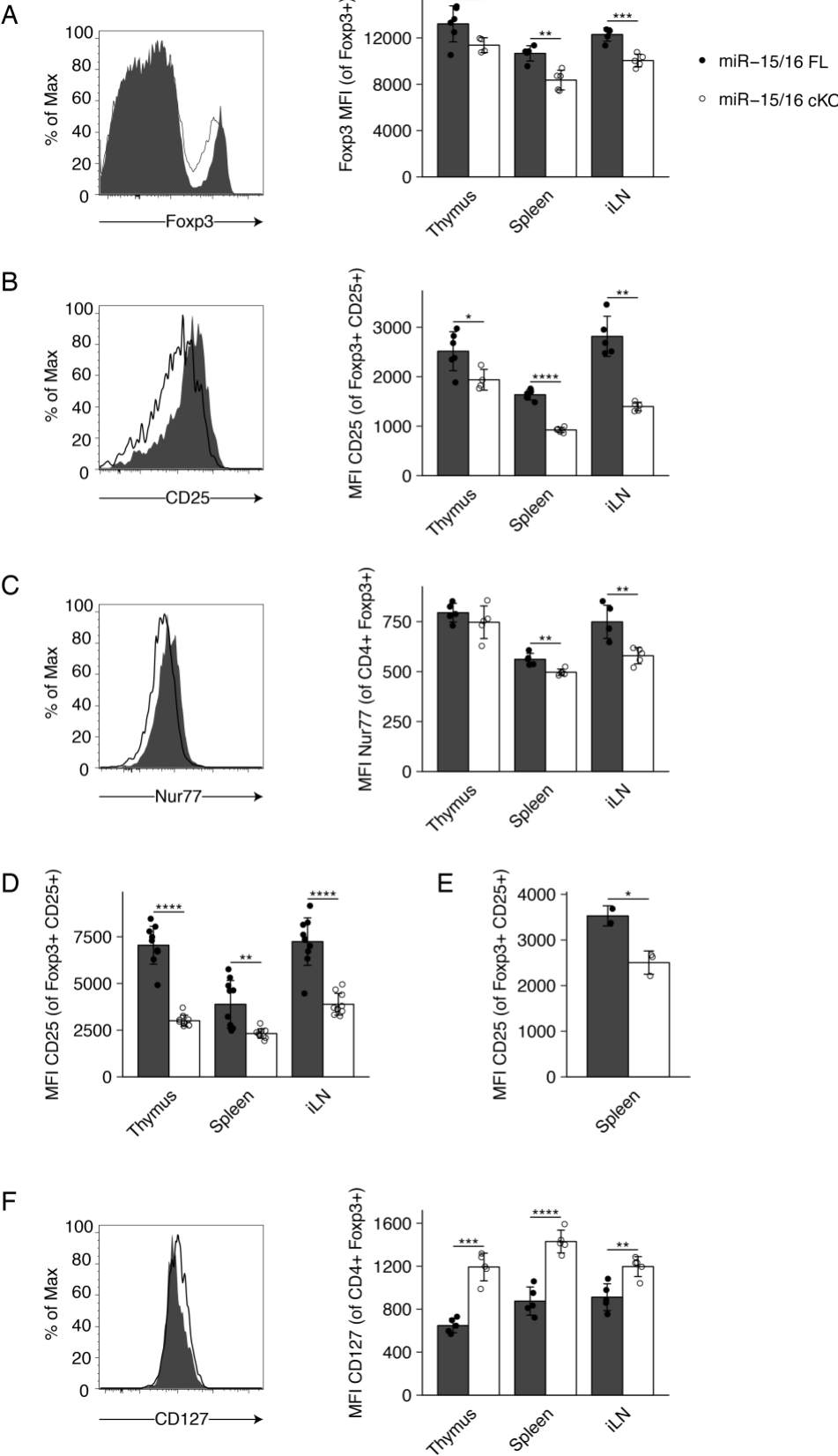
Chapter 5: plotGrouper

Summary:

A shiny app-based GUI wrapper for ggplot with built-in statistical analysis. Import data from file and use dropdown menus and checkboxes to specify the plotting variables, graph type, and look of your plots. Once created, plots can be saved independently or stored in a report that can be saved as a pdf. If new data are added to the file, the report can be refreshed to include new data. Statistical tests can be selected and added to the graphs. Analysis of flow cytometry data is especially integrated with plotGrouper. Count data can be transformed to return the absolute number of cells in a sample (this feature requires inclusion of the number of beads per sample and information about any dilution performed).

Introduction

Data are at the core of all scientific findings. Hypotheses are tested through carefully designed and controlled experiments. Key to the interpretation and publication of the results of an experiment is the visual representation and statistical analysis of said results. However, the current tools available for displaying and analyzing data suffer from a number of non-mutually exclusive problems. Free tools, such as R, require a significant amount of training to learn how to utilize. User-friendly solutions, such as GraphPad Prism, are often expensive. Additionally, the use of third-party software often requires users to copy and paste data introducing the possibility for error.

In order to address these issues, I have developed a shiny app-based R package, which requires no knowledge of R to use, is free of cost, and allows the direct import of data from a range of file formats. This package, titled "plotGrouper", was designed for generating figure-ready graphs from raw data files. Plots can be made using combinations of graphical objects including bar plots, violin plots, box and whisker plots, crossbar plots, density plots, line plots, display of individual data points, and error bars. Additionally significance formatted information can be optionally calculated and displayed above the appropriate comparisons. This tool simplifies the analysis of raw data and generates graphs that require minimal manipulation before publication.

Prerequisites

1. If you do not already have R installed, or your version is out of date, download the latest version (https://cran.r-project.org).

a. Optionally, install the latest version of RStudio Desktop

(https://www.rstudio.com/products/rstudio/#Desktop).

2. Download the package from Bioconductor.

if (!requireNamespace("BiocManager", quietly = TRUE))

install.packages("BiocManager")

BiocManager::install("plotGrouper")

a. Alternatively, install the development version of the package from Github

using `BbiocManager`:

BiocManager::install("jdgagnon/plotGrouper")

b. Or using `devtools`:

devtools::install_github("jdgagnon/plotGrouper")

3. If using RStudio, restarting the application will ensure that the updated packages

are loaded.

Usage

- Load the package into the R session.

library(plotGrouper)

- To initialize the shiny app, paste the following code in your R console and run it.

plotGrouper()

- Once the web app opens, you can load your dataset by using the 'Browse' button

- Your file should be organized according to Table 1.

- These columns can be titled anything you want but values in the columns are

important.

o As an example, click the 'iris' button to load the iris dataset.

- o   After the `iris` data loads, the selection windows will be automatically populated and a graph should be displayed.

- o   The `Raw Data` tab displays the structure of the data loaded.

    - ▪   The `Unique identifier` column should contain only unique values that identify each individual sample (e.g., `Sample` within `iris` `Raw Data`).

    - ▪   The `Comparisons` column should contain replicated values that identify each individual as belonging to a group (e.g., `Species` within `iris` `Raw Data`).

    - ▪   The `Variables` column(s) should created for each variable you wish to plot. The values in these columns must be numeric (e.g., `Sepal.Length`, `Sepal.Width`, `Petal.Length`, `Petal.Width` within `iris` `Raw Data`)

- •   If using flow cytometry data, the data table exported from FlowJo can be loaded directly with the addition of a column that specifies the group to which each sample belongs (i.e., if your comparison is going to be between wild-type and knockout samples, there must be a column in your data table that assigns each row as belonging to the wild-type or knockout group).

- •   After importing a data file, a `Sheet` column will be created and populated with the sheet name(s) from the file if it came from an excel spreadsheet or the file name if it came from a csv or tsv file.

    - o   The `Variables to plot` selection window is used to choose which variable(s) to plot (e.g., `Sepal.Width` from the `iris` data). If multiple are

selected, they will be grouped according to the `Independent variable` selected.

- o The `Comparisons` selection window is used to choose which column contains the information that identifies which condition each sample belongs to (e.g., the `Species` column within the `iris` data).

- o The `Independent variable` selection window is used to select how the plots should be grouped. If `variable` is selected (the default), the plots will be grouped by the values in `Variables to plot`.

- o Use the `Shapes` selector to change the shape of the points for each comparison variable.

- o Use the `Colors` selector to change the point colors for each comparison variable.

- o Use the `Fills` selector to change the fill color for the other geoms being plotted for each comparison variable.

- To prevent the `Shapes`, `Colors`, or `Fills` from reverting to their defaults, click the `Lock` checkboxes.

- Individual plots can be saved by clicking `Save` on the `Plot` tab or multiple plots may be arranged on a single page by clicking `Add plot to report`. Clicking this button will send the current plot to the `Report` tab and assign it a number in the `Report plot #` dropdown menu. To revisit a plot stored in the `Report` tab, select the plot you wish to restore and click `Load plot from report`. Changes can be made to this plot and then updated in the `Report` by clicking `Update plot in report`.

- The statistics calculated for the current plot being displayed in the `Plot` tab are stored in the `Statistics` tab. These can be saved by clicking the `Download` button on the `Statistics` tab.

- The `Plot Data` tab contains the reorganized subset of data being plotted.

- The `Raw Data` tab displays the data frame that was created upon import of the file along with the automatically created `Sheet` column.

Table 1: Data structure example

Sample	Species	Sepal length
Setosa_1	Setosa	5.1
Setosa_2	Setosa	4.9
Versicolor_1	Versicolor	7
Versicolor_2	Versicolor	6.4
Virginica_1	Virginica	6.3
Virginica_2	Virginica	5.8
Etc…	Etc…	Etc…

References

Agarwal, V., G.W. Bell, J.-W. Nam, and D.P. Bartel. 2015. Predicting effective microRNA target sites in mammalian mRNAs. *Elife*. 4:101. doi:10.7554/eLife.05005.

Araki, K., A.P. Turner, V.O. Shaffer, S. Gangappa, S.A. Keller, M.F. Bachmann, C.P. Larsen, and R. Ahmed. 2009. mTOR regulates memory CD8 T-cell differentiation. *Nature*. 460:108–112. doi:10.1038/nature08155.

Arun, G., S. Diermeier, M. Akerman, K.-C. Chang, J.E. Wilkinson, S. Hearn, Y. Kim, A.R. MacLeod, A.R. Krainer, L. Norton, E. Brogi, M. Egeblad, and D.L. Spector. 2016. Differentiation of mammary tumors and reduction in metastasis upon Malat1 lncRNA loss. *Genes & Development*. 30:34–51. doi:10.1101/gad.270959.115.

Ashouri, J.F., and A. Weiss. 2017. Endogenous Nur77 Is a Specific Indicator of Antigen Receptor Signaling in Human T and B Cells. *The Journal of Immunology*. 198:657–668. doi:10.4049/jimmunol.1601301.

Baars, P.A., S. Sierro, R. Arens, K. Tesselaar, B. Hooibrink, P. Klenerman, and R.A.W. van Lier. 2005. Properties of murine (CD8+)CD27- T cells. *Eur. J. Immunol.* 35:3131–3141. doi:10.1002/eji.200425770.

Ban, Y.H., S.-C. Oh, S.-H. Seo, S.-M. Kim, I.-P. Choi, P.D. Greenberg, J. Chang, T.-D. Kim, and S.-J. Ha. 2017. miR-150-Mediated Foxo1 Regulation Programs CD8+ T Cell Differentiation. *CellReports*. 20:2598–2611. doi:10.1016/j.celrep.2017.08.065.

Banerjee, A., S.M. Gordon, A.M. Intlekofer, M.A. Paley, E.C. Mooney, T. Lindsten, E.J. Wherry, and S.L. Reiner. 2010. Cutting edge: The transcription factor eomesodermin enables CD8+ T cells to compete for the memory cell niche. *The Journal of Immunology*. 185:4988–4992. doi:10.4049/jimmunol.1002042.

Bartel, D.P., and C.-Z. Chen. 2004. Micromanagers of gene expression: the potentially widespread influence of metazoan microRNAs. *Nature Reviews Genetics*. 5:396–400. doi:10.1038/nrg1328.

Baumjohann, D., and K.M. Ansel. 2013. MicroRNA-mediated regulation of T helper cell differentiation and plasticity. *Nat Rev Immunol*. 13:666–678. doi:10.1038/nri3494.

Bellare, P., and D. Ganem. 2009. Regulation of KSHV lytic switch protein expression by a virus-encoded microRNA: an evolutionary adaptation that fine-tunes lytic reactivation. *Cell Host and Microbe*. 6:570–575. doi:10.1016/j.chom.2009.11.008.

Blackburn, S.D., H. Shin, W.N. Haining, T. Zou, C.J. Workman, A. Polley, M.R. Betts, G.J. Freeman, D.A.A. Vignali, and E.J. Wherry. 2009. Coregulation of CD8+ T cell exhaustion by multiple inhibitory receptors during chronic viral infection. *Nature Immunology*. 10:29–37. doi:10.1038/ni.1679.

Blake, W.J., G. Balázsi, M.A. Kohanski, F.J. Isaacs, K.F. Murphy, Y. Kuang, C.R. Cantor, D.R. Walt, and J.J. Collins. 2006. Phenotypic consequences of promoter-mediated transcriptional noise. *Mol. Cell*. 24:853–865. doi:10.1016/j.molcel.2006.11.003.

Blattman, J.N., R. Antia, D.J.D. Sourdive, X. Wang, S.M. Kaech, K. Murali-Krishna, J.D. Altman, and R. Ahmed. 2002. Estimating the precursor frequency of naive antigen-specific CD8 T cells. *J. Exp. Med.* 195:657–664. doi:10.1084/jem.20001021.

Bluestone, J.A., J.H. Buckner, M. Fitch, S.E. Gitelman, S. Gupta, M.K. Hellerstein, K.C. Herold, A. Lares, M.R. Lee, K. Li, W. Liu, S.A. Long, L.M. Masiello, V. Nguyen, A.L. Putnam, M. Rieck, P.H. Sayre, and Q. Tang. 2015. Type 1 diabetes immunotherapy using polyclonal regulatory T cells. *Science Translational Medicine*. 7:315ra189–315ra189. doi:10.1126/scitranslmed.aad4134.

Brabletz, S., and T. Brabletz. 2010. The ZEB/miR-200 feedback loop--a motor of cellular plasticity in development and cancer? *EMBO Rep.* 11:670–677. doi:10.1038/embor.2010.117.

Bronevetsky, Y., A.V. Villarino, C.J. Eisley, R. Barbeau, A.J. Barczak, G.A. Heinz, E. Kremmer, V. Heissmeyer, M.T. McManus, D.J. Erle, A. Rao, and K.M. Ansel. 2013. T cell activation induces proteasomal degradation of Argonaute and rapid remodeling of the microRNA repertoire. *J. Exp. Med.* 210:417–432. doi:10.1084/jem.20111717.

Bronevetsky, Y., and K.M. Ansel. 2013. Regulation of miRNA biogenesis and turnover in the immune system. *Immunological Reviews*. 253:304–316. doi:10.1111/imr.12059.

Calin, G.A., C.D. Dumitru, M. Shimizu, R. Bichi, S. Zupo, E. Noch, H. Aldler, S. Rattan, M. Keating, K. Rai, L. Rassenti, T. Kipps, M. Negrini, F. Bullrich, and C.M. Croce. 2002. Frequent deletions and down-regulation of micro- RNA genes miR15 and miR16 at 13q14 in chronic lymphocytic leukemia. *Proceedings of the National Academy of Sciences.* 99:15524–15529. doi:10.1073/pnas.242606799.

Chang, J.T., E.J. Wherry, and A.W. Goldrath. 2014. Molecular regulation of effector and memory T cell differentiation. *Nature Immunology*. 15:1104–1115. doi:10.1038/ni.3031.

Chang, J.T., V.R. Palanivel, I. Kinjyo, F. Schambach, A.M. Intlekofer, A. Banerjee, S.A. Longworth, K.E. Vinup, P. Mrass, J. Oliaro, N. Killeen, J.S. Orange, S.M. Russell, W. Weninger, and S.L. Reiner. 2007. Asymmetric T lymphocyte division in the initiation of adaptive immune responses. *Science*. 315:1687–1691. doi:10.1126/science.1139393.

Cheadle, C., J. Fan, Y.S. Cho-Chung, T. Werner, J. Ray, L. Do, M. Gorospe, and K.G. Becker. 2005. Control of gene expression during T cell activation: alternate regulation of mRNA transcription and mRNA stability. *BMC Genomics*. 6:75. doi:10.1186/1471-2164-6-75.

Chen, Q., Y.C. Kim, A. Laurence, G.A. Punkosdy, and E.M. Shevach. 2011. IL-2 controls the stability of Foxp3 expression in TGF-beta-induced Foxp3+ T cells in vivo. *The Journal of Immunology*. 186:6329–6337. doi:10.4049/jimmunol.1100061.

Chen, Z., E. Stelekati, M. Kurachi, S. Yu, Z. Cai, S. Manne, O. Khan, X. Yang, and E.J. Wherry. 2017. miR-150 Regulates Memory CD8 T Cell Differentiation via c-Myb. *CellReports*. 20:2584–2597. doi:10.1016/j.celrep.2017.08.060.

Chi, S.W., J.B. Zang, A. Mele, and R.B. Darnell. 2009. Argonaute HITS-CLIP decodes microRNA-mRNA interaction maps. *Nature*. 460:479–486. doi:10.1038/nature08170.

Chinen, T., A.K. Kannan, A.G. Levine, X. Fan, U. Klein, Y. Zheng, G. Gasteiger, Y. Feng, J.D. Fontenot, and A.Y. Rudensky. 2016. An essential role for the IL-2 receptor in Treg cell function. *Nature Immunology*. 17:1322–1333. doi:10.1038/ni.3540.

Chong, M.M.W., J.P. Rasmussen, A.Y. Rudensky, A.Y. Rundensky, and D.R. Littman. 2008. The RNAseIII enzyme Drosha is critical in T cells for preventing lethal inflammatory disease. *J. Exp. Med.* 205:2005–2017. doi:10.1084/jem.20081219.

Cimmino, A., G.A. Calin, M. Fabbri, M.V. Iorio, M. Ferracin, M. Shimizu, S.E. Wojcik, R.I. Aqeilan, S. Zupo, M. Dono, L. Rassenti, H. Alder, S. Volinia, C.-G. Liu, T.J. Kipps, M. Negrini, and C.M. Croce. 2005. miR-15 and miR-16 induce apoptosis by targeting BCL2. *Proceedings of the National Academy of Sciences*. 102:13944–13949. doi:10.1073/pnas.0506654102.

Ciocca, M.L., B.E. Barnett, J.K. Burkhardt, J.T. Chang, and S.L. Reiner. 2012. Cutting edge: Asymmetric memory T cell division in response to rechallenge. *The Journal of Immunology*. 188:4145–4148. doi:10.4049/jimmunol.1200176.

Cui, W., Y. Liu, J.S. Weinstein, J. Craft, and S.M. Kaech. 2011. An interleukin-21-interleukin-10-STAT3 pathway is critical for functional maturation of memory CD8+ T cells. *Immunity*. 35:792–805. doi:10.1016/j.immuni.2011.09.017.

Dobin, A., C.A. Davis, F. Schlesinger, J. Drenkow, C. Zaleski, S. Jha, P. Batut, M. Chaisson, and T.R. Gingeras. 2013. STAR: ultrafast universal RNA-seq aligner. *Bioinformatics*. 29:15–21. doi:10.1093/bioinformatics/bts635.

Dorsett, Y., K.M. McBride, M. Jankovic, A. Gazumyan, T.-H. Thai, D.F. Robbiani, M. Di Virgilio, B.R. San-Martin, G. Heidkamp, T.A. Schwickert, T. Eisenreich, K. Rajewsky, and M.C. Nussenzweig. 2008. MicroRNA-155 Suppresses Activation-Induced Cytidine Deaminase-Mediated Myc-Igh Translocation. *Immunity*. 28:630–638. doi:10.1016/j.immuni.2008.04.002.

Dudda, J.C., B. Salaun, Y. Ji, D.C. Palmer, G.C. Monnot, E. Merck, C. Boudousquie, D.T. Utzschneider, T.M. Escobar, R. Perret, S.A. Muljo, M. Hebeisen, N. Rufer, D. Zehn, A. Donda, N.P. Restifo, W. Held, L. Gattinoni, and P. Romero. 2013. MicroRNA-155 is required for effector CD8+ T cell responses to virus infection and cancer. *Immunity*. 38:742–753. doi:10.1016/j.immuni.2012.12.006.

DuPage, M., G. Chopra, J. Quiros, W.L. Rosenthal, M.M. Morar, D. Holohan, R. Zhang, L. Turka, A. Marson, and J.A. Bluestone. 2015. The chromatin-modifying enzyme Ezh2 is critical for the maintenance of regulatory T cell identity after activation. *Immunity*. 42:227–238. doi:10.1016/j.immuni.2015.01.007.

Ebert, M.S., and P.A. Sharp. 2012. Roles for microRNAs in conferring robustness to biological processes. *CELL*. 149:515–524. doi:10.1016/j.cell.2012.04.005.

Enamorado, M., S. Iborra, E. Priego, F.J. Cueto, J.A. Quintana, S. Martínez-Cano, E. Mejías-Pérez, M. Esteban, I. Melero, A. Hidalgo, and D. Sancho. 2017. Enhanced anti-tumour immunity requires the interplay between resident and circulating memory CD8+ T cells. *Nat Commun*. 8:16073. doi:10.1038/ncomms16073.

Feuerer, M., Y. Shen, D.R. Littman, C. Benoist, and D. Mathis. 2009. How punctual ablation of regulatory T cells unleashes an autoimmune lesion within the pancreatic islets. *Immunity*. 31:654–664. doi:10.1016/j.immuni.2009.08.023.

Florent Carrette, C.D.S. 2012. IL-7 signaling and CD127 receptor regulation in the control of T cell homeostasis. *Seminars in Immunology*. 24:209–217. doi:10.1016/j.smim.2012.04.010.

Friedman, R.C., K.K.-H. Farh, C.B. Burge, and D.P. Bartel. 2009. Most mammalian mRNAs are conserved targets of microRNAs. *Genome Res.* 19:92–105. doi:10.1101/gr.082701.108.

Gagnon, J.D. 2018. plotGrouper: Shiny app GUI wrapper for ggplot with built-in statistical analysis. *Bioconductor*. 1–8.

Gagnon, J.D., R. Kageyama, H.M. Shehata, M.S. Fassett, D. Mar, A.J. Litterman, P. Odorizzi, D. Simeonov, M.E. Feeney, M.T. McManus, A. Marson, M. Matloubian, S. Sanjabi, and K.M. Ansel. 2018. miR-15/16 Restrain Memory T Cell Differentiation, Cell Cycle, and Survival. doi:10.2139/ssrn.3280244.

Gerlach, C., J.C. Rohr, L. Perié, N. van Rooij, J.W.J. van Heijst, A. Velds, J. Urbanus, S.H. Naik, H. Jacobs, J.B. Beltman, R.J. de Boer, and T.N.M. Schumacher. 2013. Heterogeneous differentiation patterns of individual CD8+ T cells. *Science*. 340:635–639. doi:10.1126/science.1235487.

Gerlach, C., J.W.J. van Heijst, E. Swart, D. Sie, N. Armstrong, R.M. Kerkhoven, D. Zehn, M.J. Bevan, K. Schepers, and T.N.M. Schumacher. 2010. One naive T cell, multiple fates in CD8+ T cell differentiation. *J. Exp. Med.* 207:1235–1246. doi:10.1084/jem.20091175.

Gracias, D.T., E. Stelekati, J.L. Hope, A.C. Boesteanu, T.A. Doering, J. Norton, Y.M. Mueller, J.A. Fraietta, E.J. Wherry, M. Turner, and P.D. Katsikis. 2013. The microRNA miR-155 controls CD8(+) T cell responses by regulating interferon signaling. *Nature Immunology*. 14:593–602. doi:10.1038/ni.2576.

Grusdat, M., D.R. McIlwain, H.C. Xu, V.I. Pozdeev, J. Knievel, S.Q. Crome, C. Robert-Tissot, R.J. Dress, A.A. Pandyra, D.E. Speiser, E. Lang, S.K. Maney, A.R. Elford, S.R. Hamilton, S. Scheu, K. Pfeffer, J. Bode, H.-W. Mittrücker, M. Lohoff, M. Huber, D. Häussinger, P.S. Ohashi, T.W. Mak, K.S. Lang, and P.A. Lang. 2014. IRF4 and BATF are critical for CD8^{+} T-cell function following infection with LCMV. *Cell Death & Differentiation*. 21:1050–1060. doi:10.1038/cdd.2014.19.

Guan, T., C.X. Dominguez, R.A. Amezquita, B.J. Laidlaw, J. Cheng, J. Henao-Mejia, A. Williams, R.A. Flavell, J. Lu, and S.M. Kaech. 2018. ZEB1, ZEB2, and the miR-200 family form a counterregulatory network to regulate CD8 +T cell fates. *J. Exp. Med.* 215:1153–1168. doi:10.1084/jem.20171352.

Hand, T.W., M. Morre, and S.M. Kaech. 2007. Expression of IL-7 receptor alpha is necessary but not sufficient for the formation of memory CD8 T cells during viral infection. *Proceedings of the National Academy of Sciences*. 104:11730–11735. doi:10.1073/pnas.0705007104.

Haribhai, D., W. Lin, L.M. Relland, N. Truong, C.B. Williams, and T.A. Chatila. 2007. Regulatory T cells dynamically control the primary immune response to foreign antigen. *J. Immunol.* 178:2961–2972. doi:10.4049/jimmunol.178.5.2961.

Herndler-Brandstetter, D., H. Ishigame, R. Shinnakasu, V. Plajer, C. Stecher, J. Zhao, M. Lietzenmayer, L. Kroehling, A. Takumi, K. Kometani, T. Inoue, Y. Kluger, S.M. Kaech, T. Kurosaki, T. Okada, and R.A. Flavell. 2018. KLRG1+ Effector CD8+ T Cells Lose KLRG1, Differentiate into All Memory T Cell Lineages, and Convey Enhanced Protective Immunity. *Immunity*. 48:716–729.e8. doi:10.1016/j.immuni.2018.03.015.

Hess Michelini, R., A.L. Doedens, A.W. Goldrath, and S.M. Hedrick. 2013. Differentiation of CD8 memory T cells depends on Foxo1. *J. Exp. Med.* 210:1189–1200. doi:10.1084/jem.20130392.

Hikono, H., J.E. Kohlmeier, S. Takamura, S.T. Wittmer, A.D. Roberts, and D.L. Woodland. 2007. Activation phenotype, rather than central– or effector–memory phenotype, predicts the recall efficacy of memory CD8+ T cells. *J. Exp. Med.* 204:1625–1636. doi:10.1084/jem.20070322.

Hintzen, R.Q., R. de Jong, S.M. Lens, M. Brouwer, P. Baars, and R.A. van Lier. 1993. Regulation of CD27 expression on subsets of mature T-lymphocytes. *J. Immunol.* 151:2426–2435.

Hippen, K.L., M. Loschi, J. Nicholls, K.P.A. MacDonald, and B.R. Blazar. 2018. Effects of MicroRNA on Regulatory T Cells and Implications for Adoptive Cellular Therapy to Ameliorate Graft-versus-Host Disease. *Front Immunol.* 9:57. doi:10.3389/fimmu.2018.00057.

Hope, J.L., C.J. Stairiker, P.I. Spantidea, D.T. Gracias, A.J. Carey, A.J. Fike, M. van Meurs, I. Brouwers-Haspels, L.C. Rijsbergen, J.A. Fraietta, Y.M. Mueller, R.C. Klop, E. Stelekati, E.J. Wherry, S.J. Erkeland, and P.D. Katsikis. 2017. The Transcription Factor T-Bet Is Regulated by MicroRNA-155 in Murine Anti-Viral CD8+ T Cells via SHIP-1. *Front Immunol.* 8:1696. doi:10.3389/fimmu.2017.01696.

Hu, G., and J. Chen. 2013. A genome-wide regulatory network identifies key transcription factors for memory CD8+ T-cell development. *Nat Commun.* 4:2830. doi:10.1038/ncomms3830.

Hu, J.K., T. Kagari, J.M. Clingan, and M. Matloubian. 2011. Expression of chemokine receptor CXCR3 on T cells affects the balance between effector and memory CD8 T-cell generation. *Proc. Natl. Acad. Sci. U.S.A.* 108:E118–27. doi:10.1073/pnas.1101881108.

Intlekofer, A.M., N. Takemoto, C. Kao, A. Banerjee, F. Schambach, J.K. Northrop, H. Shen, E.J. Wherry, and S.L. Reiner. 2007. Requirement for T-bet in the aberrant differentiation of unhelped memory CD8+ T cells. *J. Exp. Med.* 204:2015–2021. doi:10.1084/jem.20070841.

Ji, Y., C. Wrzesinski, Z. Yu, J. Hu, S. Gautam, N.V. Hawk, W.G. Telford, D.C. Palmer, Z. Franco, M. Sukumar, R. Roychoudhuri, D. Clever, C.A. Klebanoff, C.D. Surh, T.A. Waldmann, N.P. Restifo, and L. Gattinoni. 2015. miR-155 augments CD8+ T-cell antitumor activity in lymphoreplete hosts by enhancing responsiveness to homeostatic γc cytokines. *Proc. Natl. Acad. Sci. U.S.A.* 112:476–481. doi:10.1073/pnas.1422916112.

Josefowicz, S.Z., R.E. Niec, H.Y. Kim, P. Treuting, T. Chinen, Y. Zheng, D.T. Umetsu, and A.Y. Rudensky. 2012. Extrathymically generated regulatory T cells control mucosal TH2 inflammation. *Nature*. 482:395–399. doi:10.1038/nature10772.

Joshi, N.S., W. Cui, A. Chandele, H.K. Lee, D.R. Urso, J. Hagman, L. Gapin, and S.M. Kaech. 2007. Inflammation directs memory precursor and short-lived effector CD8(+) T cell fates via the graded expression of T-bet transcription factor. *Immunity*. 27:281–295. doi:10.1016/j.immuni.2007.07.010.

Kaech, S.M., and W. Cui. 2012. Transcriptional control of effector and memory CD8+ T cell differentiation. *Nat Rev Immunol*. 12:749–761. doi:10.1038/nri3307.

Kaech, S.M., J.T. Tan, E.J. Wherry, B.T. Konieczny, C.D. Surh, and R. Ahmed. 2003.
Selective expression of the interleukin 7 receptor identifies effector CD8 T cells that
give rise to long-lived memory cells. *Nature Immunology*. 4:1191–1198.
doi:10.1038/ni1009.

Kaech, S.M., S. Hemby, E. Kersh, and R. Ahmed. 2002. Molecular and functional
profiling of memory CD8 T cell differentiation. *CELL*. 111:837–851.
doi:10.1016/S0092-8674(02)01139-X.

Kakaradov, B., J. Arsenio, C.E. Widjaja, Z. He, S. Aigner, P.J. Metz, B. Yu, E.J.
Wehrens, J. Lopez, S.H. Kim, E.I. Zuniga, A.W. Goldrath, J.T. Chang, and G.W.
Yeo. 2017. Early transcriptional and epigenetic regulation of CD8+ T cell
differentiation revealed by single-cell RNA sequencing. *Nature Immunology*.
18:422–432. doi:10.1038/ni.3688.

Kallies, A., A. Xin, G.T. Belz, and S.L. Nutt. 2009. Blimp-1 transcription factor is required
for the differentiation of effector CD8(+) T cells and memory responses. *Immunity*.
31:283–295. doi:10.1016/j.immuni.2009.06.021.

Khan, A.A., L.A. Penny, Y. Yuzefpolskiy, S. Sarkar, and V. Kalia. 2013. MicroRNA-
17~92 regulates effector and memory CD8 T-cell fates by modulating proliferation in
response to infections. *Blood*. 121:4473–4483. doi:10.1182/blood-2012-06-435412.

Kim, M.V., W. Ouyang, W. Liao, M.Q. Zhang, and M.O. Li. 2013. The transcription factor
Foxo1 controls central-memory CD8+ T cell responses to infection. *Immunity*.
39:286–297. doi:10.1016/j.immuni.2013.07.013.

Klebanoff, C.A., L. Gattinoni, P. Torabi-Parizi, K. Kerstann, A.R. Cardones, S.E. Finkelstein, D.C. Palmer, P.A. Antony, S.T. Hwang, S.A. Rosenberg, T.A. Waldmann, and N.P. Restifo. 2005. Central memory self/tumor-reactive CD8+ T cells confer superior antitumor immunity compared with effector memory T cells. *Proceedings of the National Academy of Sciences*. 102:9571–9576. doi:10.1073/pnas.0503726102.

Klein Geltink, R.I., D. O'Sullivan, M. Corrado, A. Bremser, M.D. Buck, J.M. Buescher, E. Firat, X. Zhu, G. Niedermann, G. Caputa, B. Kelly, U. Warthorst, A. Rensing-Ehl, R.L. Kyle, L. Vandersarren, J.D. Curtis, A.E. Patterson, S. Lawless, K. Grzes, J. Qiu, D.E. Sanin, O. Kretz, T.B. Huber, S. Janssens, B.N. Lambrecht, A.S. Rambold, E.J. Pearce, and E.L. Pearce. 2017. Mitochondrial Priming by CD28. *CELL*. 171:385–397.e11. doi:10.1016/j.cell.2017.08.018.

Klein, U., M. Lia, M. Crespo, R. Siegel, Q. Shen, T. Mo, A. Ambesi-Impiombato, A. Califano, A. Migliazza, G. Bhagat, and R. Dalla-Favera. 2010. The DLEU2/miR-15a/16-1 cluster controls B cell proliferation and its deletion leads to chronic lymphocytic leukemia. *Cancer Cell*. 17:28–40. doi:10.1016/j.ccr.2009.11.019.

Knudson, K.M., C.J. Pritzl, V. Saxena, A. Altman, M.A. Daniels, and E. Teixeiro. 2017. NFκB-Pim-1-Eomesodermin axis is critical for maintaining CD8 T-cell memory quality. *Proc. Natl. Acad. Sci. U.S.A.* 114:E1659–E1667. doi:10.1073/pnas.1608448114.

Kuchen, S., W. Resch, A. Yamane, N. Kuo, Z. Li, T. Chakraborty, L. Wei, A. Laurence,

    T. Yasuda, S. Peng, J. Hu-Li, K. Lu, W. Dubois, Y. Kitamura, N. Charles, H.-W. Sun,

    S. Muljo, P.L. Schwartzberg, W.E. Paul, J. O'Shea, K. Rajewsky, and R. Casellas.

    2010. Regulation of microRNA expression and abundance during lymphopoiesis.

    Immunity. 32:828–839. doi:10.1016/j.immuni.2010.05.009.

Kurtulus, S., P. Tripathi, M.E. Moreno-Fernandez, A. Sholl, J.D. Katz, H.L. Grimes, and

    D.A. Hildeman. 2011. Bcl-2 allows effector and memory CD8+ T cells to tolerate

    higher expression of Bim. *The Journal of Immunology*. 186:5729–5737.

    doi:10.4049/jimmunol.1100102.

Leach, D.R., M.F. Krummel, and J.P. Allison. 1996. Enhancement of antitumor immunity

    by CTLA-4 blockade. *Science*. 271:1734–1736.

Levine, A.G., A. Arvey, W. Jin, and A.Y. Rudensky. 2014. Continuous requirement for

    the TCR in regulatory T cell function. *Nature Immunology*. 15:1070–1078.

    doi:10.1038/ni.3004.

Li, G., K.L. Miskimen, Z. Wang, X.Y. Xie, J. Brenzovich, J.J. Ryan, W. Tse, R. Moriggl,

    and K.D. Bunting. 2010. STAT5 requires the N-domain for suppression of miR15/16,

    induction of bcl-2, and survival signaling in myeloproliferative disease. *Blood*.

    115:1416–1424. doi:10.1182/blood-2009-07-234963.

Li, H., B. Handsaker, A. Wysoker, T. Fennell, J. Ruan, N. Homer, G. Marth, G. Abecasis, R. Durbin, 1000 Genome Project Data Processing Subgroup. 2009. The Sequence Alignment/Map format and SAMtools. *Bioinformatics*. 25:2078–2079. doi:10.1093/bioinformatics/btp352.

Lin, W., D. Haribhai, L.M. Relland, N. Truong, M.R. Carlson, C.B. Williams, and T.A. Chatila. 2007. Regulatory T cell development in the absence of functional Foxp3. *Nature Immunology*. 8:359–368. doi:10.1038/ni1445.

Lind, E.F., A.R. Elford, and P.S. Ohashi. 2013. Micro-RNA 155 is required for optimal CD8+ T cell responses to acute viral and intracellular bacterial challenges. *The Journal of Immunology*. 190:1210–1216. doi:10.4049/jimmunol.1202700.

Lindner, S.E., M. Lohmüller, B. Kotkamp, F. Schuler, Z. Knust, A. Villunger, and S. Herzog. 2017. The miR-15 family reinforces the transition from proliferation to differentiation in pre-B cells. *EMBO Rep.* 18:1604–1617. doi:10.15252/embr.201643735.

Liston, A., L.-F. Lu, D. O'Carroll, A. Tarakhovsky, and A.Y. Rudensky. 2008. Dicer-dependent microRNA pathway safeguards regulatory T cell function. *J. Exp. Med.* 205:1993–2004. doi:10.1084/jem.20081062.

Liu, Q., H. Fu, F. Sun, H. Zhang, Y. Tie, J. Zhu, R. Xing, Z. Sun, and X. Zheng. 2008. miR-16 family induces cell cycle arrest by regulating multiple cell cycle genes. *Nucleic Acids Res.* 36:5391–5404. doi:10.1093/nar/gkn522.

Liu, X., S.N. Robinson, T. Setoyama, S.S. Tung, L. D'Abundo, M.Y. Shah, E. Yvon, N. Shah, H. Yang, M. Konopleva, G. Garcia-Manero, I. McNiece, K. Rezvani, G.A. Calin, E.J. Shpall, and S. Parmar. 2014. FOXP3 is a direct target of miR15a/16 in umbilical cord blood regulatory T cells. *Bone Marrow Transplant.* 49:793–799. doi:10.1038/bmt.2014.57.

Loeb, G.B., A.A. Khan, D. Canner, J.B. Hiatt, J. Shendure, R.B. Darnell, C.S. Leslie, and A.Y. Rudensky. 2012a. Transcriptome-wide miR-155 binding map reveals widespread noncanonical microRNA targeting. *Mol. Cell.* 48:760–770. doi:10.1016/j.molcel.2012.10.002.

Loeb, G.B., A.A. Khan, D. Canner, J.B. Hiatt, J. Shendure, R.B. Darnell, C.S. Leslie, and A.Y. Rudensky. 2012b. Transcriptome-wide miR-155 binding map reveals widespread noncanonical microRNA targeting. *Mol. Cell.* 48:760–770. doi:10.1016/j.molcel.2012.10.002.

Love, M.I., W. Huber, and S. Anders. 2014. Moderated estimation of fold change and dispersion for RNA-seq data with DESeq2. *Genome Biol.* 15:31. doi:10.1186/s13059-014-0550-8.

Lu, L.-F., G. Gasteiger, I.-S. Yu, A. Chaudhry, J.-P. Hsin, Y. Lu, P.D. Bos, L.-L. Lin, C.L. Zawislak, S. Cho, J.C. Sun, C.S. Leslie, S.-W. Lin, and A.Y. Rudensky. 2015. A Single miRNA-mRNA Interaction Affects the Immune Response in a Context- and Cell-Type-Specific Manner. *Immunity.* 43:52–64. doi:10.1016/j.immuni.2015.04.022.

Ma, F., S. Xu, X. Liu, Q. Zhang, X. Xu, M. Liu, M. Hua, N. Li, H. Yao, and X. Cao. 2011. The microRNA miR-29 controls innate and adaptive immune responses to intracellular bacterial infection by targeting interferon-γ. *Nature Immunology*. 12:861–869. doi:10.1038/ni.2073.

Man, K., S.S. Gabriel, Y. Liao, R. Gloury, S. Preston, D.C. Henstridge, M. Pellegrini, D. Zehn, F. Berberich-Siebelt, M.A. Febbraio, W. Shi, and A. Kallies. 2017. Transcription Factor IRF4 Promotes CD8+ T Cell Exhaustion and Limits the Development of Memory-like T Cells during Chronic Infection. *Immunity*. 47:1129–1141.e5. doi:10.1016/j.immuni.2017.11.021.

Marcais, A., R. Blevins, J. Graumann, A. Feytout, G. Dharmalingam, T. Carroll, I.F. Amado, L. Bruno, K. Lee, T. Walzer, M. Mann, A.A. Freitas, M. Boothby, A.G. Fisher, and M. Merkenschlager. 2014. microRNA-mediated regulation of mTOR complex components facilitates discrimination between activation and anergy in CD4 T cells. *J. Exp. Med.* 211:2281–2295. doi:10.1084/jem.20132059.

Masson, F., M. Minnich, M. Olshansky, I. Bilic, A.M. Mount, A. Kallies, T.P. Speed, M. Busslinger, S.L. Nutt, and G.T. Belz. 2013. Id2-mediated inhibition of E2A represses memory CD8+ T cell differentiation. *The Journal of Immunology*. 190:4585–4594. doi:10.4049/jimmunol.1300099.

Matloubian, M., T. Somasundaram, S.R. Kolhekar, R. Selvakumar, and R. Ahmed. 1990. Genetic basis of viral persistence: single amino acid change in the viral glycoprotein affects ability of lymphocytic choriomeningitis virus to persist in adult mice. *J. Exp. Med.* 172:1043–1048. doi:10.1084/jem.172.4.1043.

McCausland, M.M., and S. Crotty. 2008. Quantitative PCR technique for detecting lymphocytic choriomeningitis virus in vivo. *J. Virol. Methods*. 147:167–176. doi:10.1016/j.jviromet.2007.08.025.

Moffett, H.F., A.N.R. Cartwright, H.-J. Kim, J. Godec, J. Pyrdol, T. Aijö, G.J. Martinez, A. Rao, J. Lu, T.R. Golub, H. Cantor, A.H. Sharpe, C.D. Novina, and K.W. Wucherpfennig. 2017. The microRNA miR-31 inhibits CD8+ T cell function in chronic viral infection. *Nature Immunology*. 18:791–799. doi:10.1038/ni.3755.

Mollo, S.B., J.T. Ingram, R.L. Kress, A.J. Zajac, and L.E. Harrington. 2014. Virus-specific CD4 and CD8 T cell responses in the absence of Th1-associated transcription factors. *Journal of Leukocyte Biology*. 95:705–713. doi:10.1189/jlb.0813429.

Muljo, S.A., K.M. Ansel, C. Kanellopoulou, D.M. Livingston, A. Rao, and K. Rajewsky. 2005. Aberrant T cell differentiation in the absence of Dicer. *J. Exp. Med.* 202:261–269. doi:10.1084/jem.20050678.

Nakagawa, S., J.Y. Ip, G. Shioi, V. Tripathi, X. Zong, T. Hirose, and K.V. Prasanth. 2012. Malat1 is not an essential component of nuclear speckles in mice. *RNA*. 18:1487–1499. doi:10.1261/rna.033217.112.

Nanjappa, S.G., J.H. Walent, M. Morre, and M. Suresh. 2008. Effects of IL-7 on memory CD8 T cell homeostasis are influenced by the timing of therapy in mice. *J. Clin. Invest.* 118:1027–1039. doi:10.1172/JCI32020.

Ofir, M., D. Hacohen, and D. Ginsberg. 2011. miR-15 and miR-16 Are Direct Transcriptional Targets of E2F1 that Limit E2F-Induced Proliferation by Targeting Cyclin E. *Mol Cancer Res*. 9:440–447. doi:10.1158/1541-7786.MCR-10-0344.

Ohkura, N., M. Hamaguchi, H. Morikawa, K. Sugimura, A. Tanaka, Y. Ito, M. Osaki, Y. Tanaka, R. Yamashita, N. Nakano, J. Huehn, H.J. Fehling, T. Sparwasser, K. Nakai, and S. Sakaguchi. 2012. T cell receptor stimulation-induced epigenetic changes and Foxp3 expression are independent and complementary events required for Treg cell development. *Immunity*. 37:785–799. doi:10.1016/j.immuni.2012.09.010.

Ohkura, N., Y. Kitagawa, and S. Sakaguchi. 2013. Development and maintenance of regulatory T cells. *Immunity*. 38:414–423. doi:10.1016/j.immuni.2013.03.002.

Olson, J.A., C. McDonald-Hyman, S.C. Jameson, and S.E. Hamilton. 2013. Effector-like CD8$^+$ T cells in the memory population mediate potent protective immunity. *Immunity*. 38:1250–1260. doi:10.1016/j.immuni.2013.05.009.

Park, C.Y., L.T. Jeker, K. Carver-Moore, A. Oh, H.J. Liu, R. Cameron, H. Richards, Z. Li, D. Adler, Y. Yoshinaga, M. Martinez, M. Nefadov, A.K. Abbas, A. Weiss, L.L. Lanier, P.J. de Jong, J.A. Bluestone, D. Srivastava, and M.T. McManus. 2012. A resource for the conditional ablation of microRNAs in the mouse. *CellReports*. 1:385–391. doi:10.1016/j.celrep.2012.02.008.

Pauken, K.E., M.A. Sammons, P.M. Odorizzi, S. Manne, J. Godec, O. Khan, A.M. Drake, Z. Chen, D.R. Sen, M. Kurachi, R.A. Barnitz, C. Bartman, B. Bengsch, A.C. Huang, J.M. Schenkel, G. Vahedi, W.N. Haining, S.L. Berger, and E.J. Wherry. 2016. Epigenetic stability of exhausted T cells limits durability of reinvigoration by PD-1 blockade. *Science*. 354:1160–1165. doi:10.1126/science.aaf2807.

Pearce, E.L., M.C. Walsh, P.J. Cejas, G.M. Harms, H. Shen, L.-S. Wang, R.G. Jones, and Y. Choi. 2009. Enhancing CD8 T-cell memory by modulating fatty acid metabolism. *Nature*. 460:103–107. doi:10.1038/nature08097.

Peschiaroli, A., A. Giacobbe, A. Formosa, E.K. Markert, L. Bongiorno-Borbone, A.J. Levine, E. Candi, A. D'Alessandro, L. Zolla, A. Finazzi Agrò, and G. Melino. 2013. miR-143 regulates hexokinase 2 expression in cancer cells. *Oncogene*. 32:797–802. doi:10.1038/onc.2012.100.

Plumlee, C.R., B.S. Sheridan, B.B. Cicek, and L. Lefrançois. 2013. Environmental cues dictate the fate of individual CD8+ T cells responding to infection. *Immunity*. 39:347–356. doi:10.1016/j.immuni.2013.07.014.

Pollizzi, K.N., I.-H. Sun, C.H. Patel, Y.-C. Lo, M.-H. Oh, A.T. Waickman, A.J. Tam, R.L. Blosser, J. Wen, G.M. Delgoffe, and J.D. Powell. 2016. Asymmetric inheritance of mTORC1 kinase activity during division dictates CD8(+) T cell differentiation. *Nature Immunology*. 17:704–711. doi:10.1038/ni.3438.

Pua, H.H., D.F. Steiner, S. Patel, J.R. Gonzalez, J.F. Ortiz-Carpena, R. Kageyama, N.-T. Chiou, A. Gallman, D. de Kouchkovsky, L.T. Jeker, M.T. McManus, D.J. Erle, and K.M. Ansel. 2016. MicroRNAs 24 and 27 Suppress Allergic Inflammation and Target a Network of Regulators of T Helper 2 Cell-Associated Cytokine Production. *Immunity*. 44:821–832. doi:10.1016/j.immuni.2016.01.003.

Raj, A., C.S. Peskin, D. Tranchina, D.Y. Vargas, and S. Tyagi. 2006. Stochastic mRNA synthesis in mammalian cells. *PLoS Biol.* 4:e309. doi:10.1371/journal.pbio.0040309.

Rao, R.R., Q. Li, K. Odunsi, and P.A. Shrikant. 2010. The mTOR kinase determines effector versus memory CD8+ T cell fate by regulating the expression of transcription factors T-bet and Eomesodermin. *Immunity*. 32:67–78. doi:10.1016/j.immuni.2009.10.010.

Reid, G., M.E. Pel, M.B. Kirschner, Y.Y. Cheng, N. Mugridge, J. Weiss, M. WILLIAMS, C. Wright, J.J.B. Edelman, M.P. Vallely, B.C. McCaughan, S. Klebe, H. Brahmbhatt, J.A. MacDiarmid, and N. van Zandwijk. 2013. Restoring expression of miR-16: a novel approach to therapy for malignant pleural mesothelioma. *Ann Oncol*. 24:3128–3135. doi:10.1093/annonc/mdt412.

Roychoudhuri, R., D. Clever, P. Li, Y. Wakabayashi, K.M. Quinn, C.A. Klebanoff, Y. Ji, M. Sukumar, R.L. Eil, Z. Yu, R. Spolski, D.C. Palmer, J.H. Pan, S.J. Patel, D.C. Macallan, G. Fabozzi, H.-Y. Shih, Y. Kanno, A. Muto, J. Zhu, L. Gattinoni, J.J. O'Shea, K. Okkenhaug, K. Igarashi, W.J. Leonard, and N.P. Restifo. 2016. BACH2 regulates CD8(+) T cell differentiation by controlling access of AP-1 factors to enhancers. *Nature Immunology*. 17:851–860. doi:10.1038/ni.3441.

Rutishauser, R.L., G.A. Martins, S. Kalachikov, A. Chandele, I.A. Parish, E. Meffre, J. Jacob, K. Calame, and S.M. Kaech. 2009. Transcriptional repressor Blimp-1 promotes CD8(+) T cell terminal differentiation and represses the acquisition of central memory T cell properties. *Immunity*. 31:296–308. doi:10.1016/j.immuni.2009.05.014.

Sakaguchi, S., T. Yamaguchi, T. Nomura, and M. Ono. 2008. Regulatory T Cells and Immune Tolerance. *CELL*. 133:775–787. doi:10.1016/j.cell.2008.05.009.

Sarkar, S., V. Kalia, W.N. Haining, B.T. Konieczny, S. Subramaniam, and R. Ahmed. 2008. Functional and genomic profiling of effector CD8 T cell subsets with distinct memory fates. *J. Exp. Med.* 205:625–640. doi:10.1084/jem.20071641.

Sawada, S., J.D. Scarborough, N. Killeen, and D.R. Littman. 1994. A lineage-specific transcriptional silencer regulates CD4 gene expression during T lymphocyte development. *CELL*. 77:917–929. doi:10.1016/0092-8674(94)90140-6.

Schmiedel, J.M., S.L. Klemm, Y. Zheng, A. Sahay, N. Blüthgen, D.S. Marks, and A. van Oudenaarden. 2015. Gene expression. MicroRNA control of protein expression noise. *Science*. 348:128–132. doi:10.1126/science.aaa1738.

Shehata, H.M., S. Khan, E. Chen, P.E. Fields, R.A. Flavell, and S. Sanjabi. 2018. Lack of Sprouty 1 and 2 enhances survival of effector CD8+ T cells and yields more protective memory cells. *Proc. Natl. Acad. Sci. U.S.A.* 115:E8939–E8947. doi:10.1073/pnas.1808320115.

Sheridan, B.S., Q.-M. Pham, Y.-T. Lee, L.S. Cauley, L. Puddington, and L. Lefrançois. 2014. Oral infection drives a distinct population of intestinal resident memory CD8(+) T cells with enhanced protective function. *Immunity*. 40:747–757. doi:10.1016/j.immuni.2014.03.007.

Shin, H., S.D. Blackburn, J.N. Blattman, and E.J. Wherry. 2007. Viral antigen and extensive division maintain virus-specific CD8 T cells during chronic infection. *J. Exp. Med.* 204:941–949. doi:10.1084/jem.20061937.

Singh, A., A. Jatzek, E.H. Plisch, R. Srinivasan, J. Svaren, and M. Suresh. 2010. Regulation of memory CD8 T-cell differentiation by cyclin-dependent kinase inhibitor p27Kip1. *Molecular and Cellular Biology*. 30:5145–5159. doi:10.1128/MCB.01045-09.

Singh, Y., O.A. Garden, F. Lang, and B.S. Cobb. 2015a. MicroRNA-15b/16 Enhances the Induction of Regulatory T Cells by Regulating the Expression of Rictor and mTOR. *The Journal of Immunology*. 195:5667–5677. doi:10.4049/jimmunol.1401875.

Singh, Y., O.A. Garden, F. Lang, and B.S. Cobb. 2015b. MicroRNA-15b/16 Enhances the Induction of Regulatory T Cells by Regulating the Expression of Rictor and mTOR. *The Journal of Immunology*. 195:5667–5677. doi:10.4049/jimmunol.1401875.

Slota, C., A. Shi, G. Chen, M. Bevans, and N.-P. Weng. 2015. Norepinephrine preferentially modulates memory CD8 T cell function inducing inflammatory cytokine production and reducing proliferation in response to activation. *Brain Behav. Immun.* 46:168–179. doi:10.1016/j.bbi.2015.01.015.

Steiner, D.F., M.F. Thomas, J.K. Hu, Z. Yang, J.E. Babiarz, C.D.C. Allen, M. Matloubian, R. Blelloch, and K.M. Ansel. 2011. MicroRNA-29 regulates T-box transcription factors and interferon-γ production in helper T cells. *Immunity*. 35:169–181. doi:10.1016/j.immuni.2011.07.009.

Stelekati, E., Z. Chen, S. Manne, M. Kurachi, M.-A. Ali, K. Lewy, Z. Cai, K. Nzingha, L.M. McLane, J.L. Hope, A.J. Fike, P.D. Katsikis, and E.J. Wherry. 2018. Long-Term Persistence of Exhausted CD8 T Cells in Chronic Infection Is Regulated by MicroRNA-155. *CellReports*. 23:2142–2156. doi:10.1016/j.celrep.2018.04.038.

Stemberger, C., K.M. Huster, M. Koffler, F. Anderl, M. Schiemann, H. Wagner, and D.H. Busch. 2007. A single naive CD8+ T cell precursor can develop into diverse effector and memory subsets. *Immunity*. 27:985–997. doi:10.1016/j.immuni.2007.10.012.

Teng, G., P. Hakimpour, P. Landgraf, A. Rice, T. Tuschl, R. Casellas, and F.N. Papavasiliou. 2008. MicroRNA-155 Is a Negative Regulator of Activation-Induced Cytidine Deaminase. *Immunity*. 28:621–629. doi:10.1016/j.immuni.2008.03.015.

Terawaki, S., S. Chikuma, S. Shibayama, T. Hayashi, T. Yoshida, T. Okazaki, and T. Honjo. 2011. IFN-α directly promotes programmed cell death-1 transcription and limits the duration of T cell-mediated immunity. *The Journal of Immunology*. 186:2772–2779. doi:10.4049/jimmunol.1003208.

Trifari, S., M.E. Pipkin, H.S. Bandukwala, T. Aijö, J. Bassein, R. Chen, G.J. Martinez, and A. Rao. 2013. MicroRNA-directed program of cytotoxic CD8+ T-cell differentiation. *Proc. Natl. Acad. Sci. U.S.A.* 110:18608–18613. doi:10.1073/pnas.1317191110.

Tsai, C.-Y., S.R. Allie, W. Zhang, and E.J. Usherwood. 2013. MicroRNA miR-155 affects antiviral effector and effector Memory CD8 T cell differentiation. *J. Virol.* 87:2348–2351. doi:10.1128/JVI.01742-12.

Vahl, J.C., C. Drees, K. Heger, S. Heink, J.C. Fischer, J. Nedjic, N. Ohkura, H. Morikawa, H. Poeck, S. Schallenberg, D. Rieß, M.Y. Hein, T. Buch, B. Polic, A. Schönle, R. Zeiser, A. Schmitt-Gräff, K. Kretschmer, L. Klein, T. Korn, S. Sakaguchi, and M. Schmidt-Supprian. 2014. Continuous T cell receptor signals maintain a functional regulatory T cell pool. *Immunity*. 41:722–736. doi:10.1016/j.immuni.2014.10.012.

Wells, A.C., K.A. Daniels, C.C. Angelou, E. Fagerberg, A.S. Burnside, M. Markstein, D. Alfandari, R.M. Welsh, E.L. Pobezinskaya, and L.A. Pobezinsky. 2017. Modulation of let-7 miRNAs controls the differentiation of effector CD8 T cells. *Elife*. 6:403. doi:10.7554/eLife.26398.

Wherry, E.J. 2011. T cell exhaustion. *Nature Immunology*. 12:492–499. doi:10.1038/ni.2035.

Wherry, E.J., and M. Kurachi. 2015. Molecular and cellular insights into T cell exhaustion. *Nat Rev Immunol*. 15:486–499. doi:10.1038/nri3862.

Wherry, E.J., V. Teichgräber, T.C. Becker, D. Masopust, S.M. Kaech, R. Antia, U.H. von Andrian, and R. Ahmed. 2003. Lineage relationship and protective immunity of memory CD8 T cell subsets. *Nature Immunology*. 4:225–234. doi:10.1038/ni889.

Williams, L.M., and A.Y. Rudensky. 2007. Maintenance of the Foxp3-dependent developmental program in mature regulatory T cells requires continued expression of Foxp3. *Nature Immunology*. 8:277–284. doi:10.1038/ni1437.

Williams, M.A., and M.J. Bevan. 2007. Effector and memory CTL differentiation. *Annu. Rev. Immunol.* 25:171–192. doi:10.1146/annurev.immunol.25.022106.141548.

Wu, H., J.R. Neilson, P. Kumar, M. Manocha, P. Shankar, P.A. Sharp, and N. Manjunath. 2007. miRNA profiling of naïve, effector and memory CD8 T cells. *PLoS ONE*. 2:e1020. doi:10.1371/journal.pone.0001020.

Wu, T., A. Wieland, K. Araki, C.W. Davis, L. Ye, J.S. Hale, and R. Ahmed. 2012. Temporal expression of microRNA cluster miR-17-92 regulates effector and memory CD8+ T-cell differentiation. *Proc. Natl. Acad. Sci. U.S.A.* 109:9965–9970. doi:10.1073/pnas.1207327109.

Wu, Y.-H., W. Liu, B. Xue, L. Zhang, X.-Y. Liu, B. Liu, Y. Wang, Y. Cai, and R. Duan. 2016. Upregulated Expression of microRNA-16 Correlates with Th17/Treg Cell Imbalance in Patients with Rheumatoid Arthritis. *DNA Cell Biol.* 35:853–860. doi:10.1089/dna.2016.3349.

Xi, Y., J. Li, L. Zan, J. Wang, G. Wang, and Y. Ning. 2013. Micro-RNA-16 expression in paraffin-embedded specimen correlates with overall survival of T-lymphoblastic lymphoma/leukemia. *Hum. Pathol.* 44:1011–1016. doi:10.1016/j.humpath.2012.08.023.

Xiao, C., L. Srinivasan, D.P. Calado, H.C. Patterson, B. Zhang, J. Wang, J.M. Henderson, J.L. Kutok, and K. Rajewsky. 2008. Lymphoproliferative disease and autoimmunity in mice with increased miR-17-92 expression in lymphocytes. *Nature Immunology*. 9:405–414. doi:10.1038/ni1575.

Yang, C.Y., J.A. Best, J. Knell, E. Yang, A.D. Sheridan, A.K. Jesionek, H.S. Li, R.R. Rivera, K.C. Lind, L.M. D'Cruz, S.S. Watowich, C. Murre, and A.W. Goldrath. 2011. The transcriptional regulators Id2 and Id3 control the formation of distinct memory CD8+ T cell subsets. *Nature Immunology*. 12:1221–1229. doi:10.1038/ni.2158.

Yang, J., R. Liu, Y. Deng, J. Qian, Z. Lu, Y. Wang, D. Zhang, F. Luo, and Y. Chu. 2017. MiR-15a/16 deficiency enhances anti-tumor immunity of glioma-infiltrating CD8+ T cells through targeting mTOR. *Int. J. Cancer*. 141:2082–2092. doi:10.1002/ijc.30912.

Yoon, H., T.S. Kim, and T.J. Braciale. 2010. The cell cycle time of CD8+ T cells responding in vivo is controlled by the type of antigenic stimulus. *PLoS ONE*. 5:e15423. doi:10.1371/journal.pone.0015423.

Youngblood, B., J.S. Hale, H.T. Kissick, E. Ahn, X. Xu, A. Wieland, K. Araki, E.E. West, H.E. Ghoneim, Y. Fan, P. Dogra, C.W. Davis, B.T. Konieczny, R. Antia, X. Cheng, and R. Ahmed. 2017. Effector CD8 T cells dedifferentiate into long-lived memory cells. *Nature*. 552:404–409. doi:10.1038/nature25144.

Yue, X., S. Trifari, T. Aijö, A. Tsagaratou, W.A. Pastor, J.A. Zepeda-Martínez, C.-W.J. Lio, X. Li, Y. Huang, P. Vijayanand, H. Lähdesmäki, and A. Rao. 2016. Control of Foxp3 stability through modulation of TET activity. *J. Exp. Med.* 213:377–397. doi:10.1084/jem.20151438.

Zhang, T., Z. Zhang, F. Li, Y. Ping, G. Qin, C. Zhang, and Y. Zhang. 2018. miR-143 Regulates Memory T Cell Differentiation by Reprogramming T Cell Metabolism. *The Journal of Immunology*. 201:2165–2175. doi:10.4049/jimmunol.1800230.

Zheng, Y., S. Josefowicz, A. Chaudhry, X.P. Peng, K. Forbush, and A.Y. Rudensky. 2010. Role of conserved non-coding DNA elements in the Foxp3 gene in regulatory T-cell fate. *Nature*. 463:808–812. doi:10.1038/nature08750.

Zhou, X., S. Yu, D.-M. Zhao, J.T. Harty, V.P. Badovinac, and H.-H. Xue. 2010. Differentiation and persistence of memory CD8(+) T cells depend on T cell factor 1. *Immunity*. 33:229–240. doi:10.1016/j.immuni.2010.08.002.
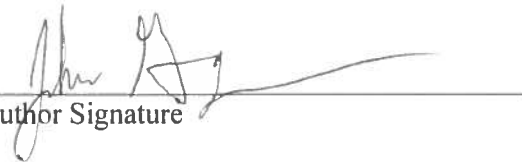
Zhou, X., S.L. Bailey-Bucktrout, L.T. Jeker, C. Penaranda, M. Martinez-Llordella, M. Ashby, M. Nakayama, W. Rosenthal, and J.A. Bluestone. 2009. Instability of the transcription factor Foxp3 leads to the generation of pathogenic memory T cells in vivo. *Nature Immunology*. 10:1000–1007. doi:10.1038/ni.1774.

Publishing Agreement

It is the policy of the University to encourage the distribution of all theses, dissertations, and manuscripts. Copies of all UCSF theses, dissertations, and manuscripts will be routed to the library via the Graduate Division. The library will make all theses, dissertations, and manuscripts accessible to the public and will preserve these to the best of their abilities, in perpetuity.

Please sign the following statement:

I hereby grant permission to the Graduate Division of the University of California, San Francisco to release copies of my thesis, dissertation, or manuscript to the Campus Library to provide access and preservation, in whole or in part, in perpetuity.

_____
Author Signature

_____ 12/12/2018 _____
Date